Indoor airflow patterns, dispersion of human exhalation flow and risk of airborne cross-infection between people in a room

Inés Olmedo Cortés

UNIVERSIDAD Ð CÓRDOBA

AALBORG UNIVERSITY
Department of Civil Engineering

TÍTULO: *Indoor airflow patterns, dispersion of human exhalation flow and risk of airborne cross-infection between people in a room*

AUTOR: *Inés Olmedo Cortés*

Aalborg University
Department of Civil Engineering

DCE Thesis No. 33

Indoor airflow patterns, dispersion of human exhalation flow and risk of airborne cross-infection between people in a room

by

Inés Olmedo Cortés

December 2011

Scientific Publications at the Department of Civil Engineering

Technical Reports are published for timely dissemination of research results and scientific work carried out at the Department of Civil Engineering (DCE) at Aalborg University. This medium allows publication of more detailed explanations and results than typically allowed in scientific journals.

Technical Memoranda are produced to enable the preliminary dissemination of scientific work by the personnel of the DCE where such release is deemed to be appropriate. Documents of this kind may be incomplete or temporary versions of papers—or part of continuing work. This should be kept in mind when references are given to publications of this kind.

Contract Reports are produced to report scientific work carried out under contract. Publications of this kind contain confidential matter and are reserved for the sponsors and the DCE. Therefore, Contract Reports are generally not available for public circulation.

Lecture Notes contain material produced by the lecturers at the DCE for educational purposes. This may be scientific notes, lecture books, example problems or manuals for laboratory work, or computer programs developed at the DCE.

Theses are monograms or collections of papers published to report the scientific work carried out at the DCE to obtain a degree as either PhD or Doctor of Technology. The thesis is publicly available after the defence of the degree.

Latest News is published to enable rapid communication of information about scientific work carried out at the DCE. This includes the status of research projects, developments in the laboratories, information about collaborative work and recent research results.

Preface

This thesis was written as a part of a PhD study during the past three years in a Joint-Degree Cooperation between the Department of Chemical Physics and Applied Thermodynamics, Córdoba University, Spain and the Department of Civil Engineering, Aalborg University, Denmark. The thesis is presented as a collection of the following seven peer-reviewed articles published in journals and conferences and the extended summary of those.

Paper I   Olmedo, I., Nielsen, P.V., Ruiz de Adana, M., Grzelecki, P. and Jensen, R.L. (2010) Study of the human breathing flow profile in a room with three different ventilation strategies. Proceedings of the 16th ASHRAE IAQ Conference *"Airborne Infection Control - Ventilation, IAQ & Energy", Kuala Lumpur/Malaysia 10-12 November 2010.*

Paper II   Nielsen, P.V., Olmedo, I., Ruiz de Adana, M., Grzelecki, P. and Jensen, R.L. (2010) Airborne Cross-Infection Risk between Two People Standing in Surroundings with a Vertical Temperature Gradient. *HVAC&Research* (RSCH-00040-2011.R1).

Paper III   Olmedo, I., Nielsen, P.V., Ruiz de Adana, M. and Jensen, R.L. (2010) Airflow pattern generated by three air diffusers: Experimental and visual analysis. Proceedings of the *6th Mediterranean Congress of Climatization, Madrid/Spain 2-3 June 2011.*

Paper IV   Olmedo, I., Nielsen, P.V., Ruiz de Adana, M., Grzelecki, P. and Jensen, R.L. (2010) Experimental study about how the thermal plume affects the air quality a person breathes. Proceedings of the *12th International Conference on Air Distribution, Trondheim/Norway 19-22 June 2011.*

Paper V   Olmedo, I., Nielsen, P.V., Ruiz de Adana, M., Grzelecki, P. and Jensen, R.L. (2011) Distribution of exhaled contaminants and personal exposure in a room using three different air distribution strategies. *Indoor Air doi: 10.1111/j.1600-0668.2011.00736.x.*

Paper VI   Olmedo, I., Nielsen, P.V., Ruiz de Adana, M. and Jensen, R.L. (2011) Risk of airborne cross-infection in a room with vertical low-velocity ventilation. *Submitted for Indoor Air.*

Paper VII   Olmedo, I. and Nielsen, P.V. (2010) Analysis of the IEA 2D test. 2D, 3D, steady or unsteady airflow? Technical report. Series number 106, *Department of Civil Engineering, Aalborg University.*

Summary in English

In recent years, an interest in understanding the mechanisms of cross-infection between people in the same room has increased significantly. The SARS (*Severe Acute Respiratory Syndrome*) outbreak occurred in Asia in 2003 reopened the study of the airborne disease transmission as one of the most prevalent transmission routes.

Airborne cross-infection of diseases is caused by the transmission of pathogens, such as viruses or bacteria, between people and across environments. When a person is breathing, talking, sneezing or coughing, small particles, which may carry biological contaminants, are spread in the air. These tiny particles or droplet nuclei can follow the air flow pattern in the room and produce high contaminant concentration in different areas of the indoor environment. This fact can provoke a high exposure to exhaled contaminants and a risk of cross-infection to a susceptible person situated in the same room.

Abundant evidence shows that the air flow distribution systems play a crucial role in the dispersion of these human exhaled contaminants. However, there are many parameters that influence the cross-infection risk between people situated close to each other in a ventilated room, such as: relative position and separation distance between people, difference in height between them, level of activity, breathing function or process (breathing frequency, exhalation through the mouth or through the nose, coughing, sneezing) or air velocity and turbulence level in the micro-environment around the persons.

This thesis analyzes some of these parameters in the influence of cross-infection risk between two people in a room, which are simulated by two breathing thermal manikins. One of the manikins is considered the source of contaminants, which is exhaling contaminated air through the mouth. The influence of different ventilation strategies in the personal micro-environment, the direction of the human exhalation flow and the dispersion of exhaled contaminants has also been studied.

Several experimental tests in a full-scale test room have been carried out in order to study the cross-infection risk between two people in a room. Different ventilation strategies and different separation distances, and relative positions, between the manikins produce different levels of contaminant exposure to the susceptible person (target manikin). These results have been discussed and carefully analyzed within this thesis.

Dansk Resumé

Der har i de seneste år været en stigende interesse for at undersøge og forstå mekanismerne i krydsinfektion imellem folk, som opholder sig i det samme lokale. SARS-hændelsen (Severe Acute Respiratory Syndrome) som fandt sted i Asien i 2003 betød, at studier af luftbårne transmissionsruter for sygdomme blev et meget aktivt forskningsområde.

Luftbåren krydsinfektion of sygdomme foregår ved transmission af patogene som virus eller bakterier imellem personer i indemiljøet. Når en person ånder, taler, nyser eller hoster, vil små biologisk forurenede partikler spredes i luften. Disse små partikler (droplet nuclei) følger luftstrømningsmønsteret i lokalet, og de kan danne høje koncentrationer i forskellige områder af indemiljøet. Dette kan betyde, at der kan opstå en høj eksponering for udåndet forurening og derfor en risiko for krydsinfektion af en påvirkelig person, som befinder sig i samme rum.

Mange hændelser viser, at luftfordelingssystemerne spiller en væsentlig rolle i fordelingen af disse udåndede humane forureninger. Der er imidlertid mange parametre, som har indflydelse på risikoen for krydsinfektion imellem folk, som befinder sig tæt ved hinanden i et ventileret lokale, som for eksempel relativ position og afstand, forskel i højde, aktivitetsniveau, åndingsproces (åndingsfrekvens, udånding gennem mund eller gennem næse, hosten eller nysen) samt lufthastighed og turbulensniveau i mikromiljøet rundt om personer.

Afhandlingen analyserer nogle af disse parametres indflydelse på risikoen for krydsinfektion imellem to personer i et lokale, idet man betragter en af personerne som en kilde til smitte. Den syge person udånder forurenet luft igennem munden. De forskellige luftfordelingsstrategiers indflydelse på det personlige mikromiljø, retningen af en persons udånding og fordelingen af den udåndede forurening er undersøgt.

Der er udført adskillige forsøg for at undersøge risikoen for krydsinfektion i et fuldskala forsøgslokale, hvor to personer er simuleret ved hjælp af to termiske manikiner med åndingsfunktion. Forskellige ventilationsstrategier og forskellige afstande imellem manikinerne samt forskellige relative positioner giver en person (Target manikin) forskellig forureningspåvirkning. Resultaterne er diskuteret og analyseret i denne afhandling.

Resumen en español

En los últimos años ha surgido un especial interés en entender los mecanismos de transmisión de infecciones cruzadas entre personas. El *Síndrome Respiratorio Agudo Severo* (SARS, por sus siglas en ingles) que tuvo lugar en Asia en el año 2003 reabrió el estudio de la transmisión de diferentes enfermedades vía aérea como una de las rutas de transmisión más activas.

Las infecciones cruzadas entre personas son causadas por la transmisión de patógenos, como virus o bacterias, entre personas en ambientes interiores. Cuando una persona respira, habla, estornuda o tose, pequeñas partículas, denominadas "droplet nuclei", que pueden contener contaminantes biológicos, son dispersadas en el aire. Estas pequeñas partículas pueden seguir las corrientes de flujos de aire dentro de una habitación y provocar altas concentraciones de contaminantes en diferentes áreas dentro de un recinto interior. Este hecho puede provocar una alta exposición a contaminantes exhalados y un riesgo de infección cruzada a personas susceptibles de ser contagiadas situadas en la misma habitación.

Existen numerosas evidencias de que los sistemas de ventilación y distribución de aire juegan un papel crucial en la dispersión de los contaminantes exhalados por personas en recintos interiores. Sin embargo, existen muchos parámetros que influencian el riesgo de infección cruzada entre personas en una habitación climatizada, como son: la posición relativa entre las personas, la distancia de separación entre ellas, su diferencia de alturas, su nivel de actividad, las funciones respiratorias de las personas (si exhalan el aire por la nariz o por la boca, si se produce un estornudo, etc.) o la velocidad y nivel de turbulencia del aire en el micro-ambiente alrededor de las personas.

El objetivo principal de esta tesis es analizar la relación de alguno de los parámetros detallados anteriormente con el riesgo de infección cruzada que se puede generar entre personas dentro de una habitación. La influencia de diferentes estrategias de climatización sobre el micro-ambiente de las personas, sobre la dirección de la exhalación y sobre la dispersión de contaminantes exhalados en el aire ha sido también estudiada.

Se han realizado numerosos estudios experimentales considerando dos personas dentro de una misma habitación climatizada mediante diferentes sistemas. La simulación de la personas se ha llevado a cabo mediante maniquíes térmicos que incluían funciones respiratorias. La exhalación de uno de ellos era considerada la fuente biológica de contaminantes mientras que el otro era la persona susceptible de ser contagiada a través del aire. Los estudios experimentales incluyen diferentes posiciones relativas entre personas y distintas distancias de separación.

Los resultados muestran una significativa influencia de la distancia de separación y la posición relativa entre las personas en la transmisión de patógenos por el aire y el riesgo de infección cruzada entre personas. Algunos de los sistemas de ventilación de aire considerados hasta ahora como adecuados en la prevención de este tipo de contagios a través del aire, como es el sistema de ventilación vertical a baja velocidad, no han mostrado especial protección contra las infecciones cruzadas en los ensayos experimentales. La exposición frente a contaminantes exhalados varía significativamente entre los distintos casos y los resultados han sido analizados minuciosamente a lo largo de esta tesis. Los resultados obtenidos dejan patente la influencia de las condiciones interiores de aire generada por los distintos sistemas de climatización en la transmisión de patógenos a través del aire en recintos interiores, en la calidad de aire que proporcionan a las personas y por lo tanto en el riesgo de infecciones cruzadas que se puede generar.

Nomenclature

a_0 area of the manikin´s mouth, m^2

A_0 opening area of a jet, m^2

Ar Archimedes number

c tracer gas concentration, ppm

c_0 peak concentration at the manikin´s mouth, ppm

c_R tracer gas concentration in the return, ppm

c_s tracer gas concentration surrounding the manikin, ppm

c_x tracer gas concentration at a horizontal distance from the mouth, ppm

c_{chest} tracer gas concentration at the chest, ppm

c_{exp} tracer gas concentration in the inhalation, ppm

c_{10} tracer gas concentration 0.10 m above the head, ppm

g gravitational acceleration (m^2/s)

H height of the test room, m

K_c characteristic concentration constant

K_{exp} characteristic velocity constant

K_v centre velocity decay constant for a jet

n_1 characteristic velocity exponent

n_2 characteristic concentration exponent

T absolute air temperature, K

T_0 exhaled air temperature, K

T_{amb} air temperature at the height of the manikin´s mouth, K

T_{in} supply air temperature, K

T_{out} return air temperature, K

u_0 initial velocity of a jet and peak velocity in the manikin´s mouth, m/s

u_x peak velocity at a horizontal distance from the manikin´s mouth, m/s

x horizontal distance, m

z vertical distance, m

β volume expansion coefficient

ΔT temperature difference between the exhalation flow, T_0, and the ambience in the room, T_{amb}

Contents

List of figures

List of tables

CHAPTER 1
Introduction

In this chapter the problem of cross-infection risk between people in indoor environments is presented. The route map of the thesis is outlined and the relationship of the represented publications to the subject matter of the study is pointed out. The main focus of the thesis has been on improving the understanding of how different ventilation systems can prevent us from a high exposure to exhaled contaminants and therefore a possible cross-infection risk in indoor environments. The results are based on experimental tests carried out in a full-scale test room. A description of different ventilation strategies, the human generation of exhaled contaminants, the routes of disease transmission and several parameters that influence the airflow patterns and the indoor environment conditions are presented.

1.1   Ventilation strategies in indoor environments

Since human beings are spending most of their time inside buildings, different ventilation strategies have been developed. The simplest one is the use of natural ventilation, which consists of renovating the indoor air of a building making fresh air pass through opened windows or doors. It does not require any device to move the air and therefore no energy is consumed. However, the characteristics and quality of the air are difficult to control since they depend on the outdoor and indoor ambient conditions. To avoid this problem and control the indoor conditions and air quality during the whole year and under different environmental conditions the HVAC (*Heating, Ventilation and Air Conditioning*) systems were developed.

The HVAC systems are supposed to create the right conditions of air temperature, velocity, humidity and quality in order to provide a comfortable and healthy indoor environment for people. The ventilation systems are also used to remove airborne particles or contamination generated inside a room, as for example aerosols or VOCs (*Volatile Organic Compounds*). To proportionate the desirable indoor conditions the air is cooled, heated and renovated in a central unit. After that, this air is directed through ducts and supplied to the indoor spaces or rooms through supply openings which can significantly vary the indoor air conditions and thermal environment in the area occupied by people. The way in which the air is supplied to the room, especially its velocity and momentum flow, together with the layout of the return openings, creates different airflow patterns, temperature distributions and indoor environments, and allows us to classify different air distribution systems. Short descriptions of the most used ones are presented in the

following sections.

1.1.1 Displacement ventilation

Displacement ventilation is a high efficiency air distribution system where the ventilation is driven by buoyancy force. The diffuser delivers cool air near the floor at a low velocity and temperature. The cool air initially drops as it leaves the diffuser and spreads across the room. At the same time, warm air in the room rises. Wherever there is a heat source in the room, e.g. a person, it creates a thermal plume, inducing cold air from the floor to the warm upper part of the room. The natural convective upward flow generated makes it appropriate to place the return openings in the upper part in order to allow the warmed air to leave the room. In the space between the cool air close to the floor and the warm air in the upper part of the room the air is thermally stratified. Figure 1.1 illustrates, with a short summary of its more common characteristics, the air distribution generated by this ventilation strategy in a room where a person is placed.
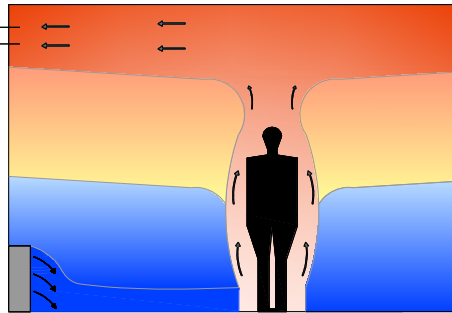
- ✓ Energy efficient
- ✓ Vertical temperature stratification
- ✓ Thermal comfort if the gradient is less than 3K/m
- ✓ Lack of draft, low air velocity

Figure 1.1 Picture of the displacement ventilation airflow pattern generated in a room occupied with one person and the most common characteristics of this ventilation system

This kind of system is very efficient in removing particles from the low part of the room, since the upward flow generated drives the contaminants to the upper part. In this way, this system generates a low clean air zone and a contaminated upper part in the room. However, a lock-up phenomenon of contaminants exhaled by a person has been reported by several authors (Brohus and Nielsen, 1996; Bjørn and Nielsen, 2002; Nielsen et al., 2009; Qian et al., 2006). The air exhaled by a person can remain stuck in a stratified layer in the surrounding of the person and produce high concentration of exhaled contaminants (Olmedo et al., 2011).

1.1.2 Mixing ventilation

The air movement in mixing ventilation is driven by the momentum flow generated by the supply opening. These supply devices are installed on the ceiling or in a wall at a certain height and generate a turbulent jet in front of them. This jet will entrain the air in the room generating a mixing process with the air into the room, see figure 1.2. The penetration distance of the jet will condition the maximum velocity in the occupied zone. The mixing

process creates a uniform temperature and contaminants distribution in the room (Jiang et al., 1992). In the occupied zone, the penetration distance of the jet will condition the maximum velocity and the contaminant concentration may be low due to the dilution process generated by this ventilation strategy (Jensen et al., 2001).

Figure 1.2(b) shows the general airflow patter generated by a ceiling mounted ceiling diffuser in a room occupied by one person.
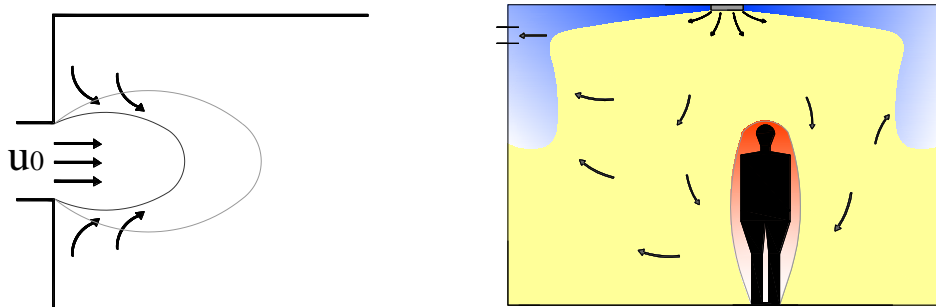
Figure 1.2 a) Airflow pattern close to a wall opening, where u_0 is the initial velocity of the jet, b) Picture of the mixing ventilation airflow pattern generated in a room occupied by a person

1.1.3 Unidirectional low-velocity flow ventilation

This ventilation system supplies air at a low velocity from a rather large inlet surface in a vertical or horizontal direction. When the air is supplied from the ceiling to the floor (vertical direction), a downward "laminar" flow is created into the room, see figure 1.3.
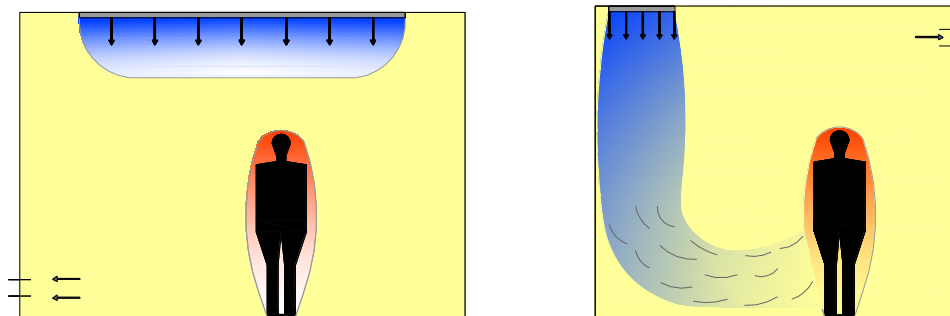
Figure 1.3 Picture of a downward airflow pattern generated in a room occupied with one person a) Front view, b) Lateral view

This system was developed for industrial clean rooms. It is considered one of the most efficient systems to control the dispersion of contaminants due to the large volume flow of clean air that can applied without generating draught (Chow and Yang, 2004; Nielsen 2007). For that reason, it is supposed to be very effective removing pollutants from a room and it is recommended in some design guidelines for prevention of airborne disease (CDC 2004; CDC 2005). The unidirectional downward flow (piston flow) that they can create

drives the pollutants to the low part of the room where they are removed. However, the convective air movement generated by heat loads can create a mixing flow pattern in the room (Nielsen et al., 2007). If people are placed below the diffuser they can disturb the expected unidirectional "laminar" flow and generate a mixing process with the air. Placement of heat loads such as people, exhaust openings and obstacles in the room significantly influence the airflow pattern generated in the room (Qian et al., 2008).

1.2 Influence of people in the airflow patterns

The airflow pattern generated inside a room is not only created by the ventilation strategy but it is also influenced by the room geometry, obstacles and thermal loads, such as people, which occupy a room.

As people are the main occupants of buildings the indoor environment has to fulfil several conditions of thermal comfort and air quality to provide a comfortable and healthy environment to people (ISO 7730:2005). However, occupants in a room are considered one of the most important heat loads and biological sources of contaminants. The following sections give a short description of the human metabolism and breathing functions that directly influence the indoor air conditions.

1.2.1 People as a heat load

The first aspect to consider about a person is that it is one of the most important thermal loads inside a building. Even when inactive, an adult will lose heat at a rate of about 90 watts as a result of his basal metabolism. Figure 1.4 shows a simplified model of the process by which the human body gives off heat.
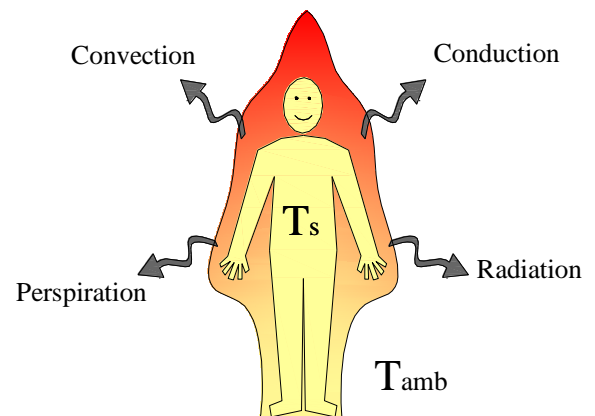
Figure 1.4 Model of the heat and the thermal plume generated by the metabolism of a person. T_s is the superficial temperature of the person and T_{amb} the ambient temperature

The heat transmission from a person to the environment is due to:

- ✓ Convective forces which are due to the temperature difference between the surface of a person and the ambience and varies depending on the clothes degree (ref), and the ambient.
- ✓ Radiation, which is generated by all warm surfaces as an emission of radiate waves.
- ✓ Conduction, the heat released by a person is carried out through the stationary air that is adjacent to the surface of a person.
- ✓ Perspiration. This is a cooling mechanism that evaporates liquid surface (sweat) when the human body is surrounded by a higher temperature.

When a person is placed in a room which is being conditioned, the temperature of the human body generates a convective upward flow due to the temperature difference with the ambient temperature, which is known as thermal plume (Clark and Edholm, 1985; Craven and Settles, 2006). This thermal plume can condition the airflow pattern and the temperature distribution expected in the same room without any occupant.

1.2.2 People as a source of biological contaminants

Human beings can be considered one of the main sources of diseases since they are transmitted most of the times by a human to human contact. The normal human pulmonary functions such as breathing, coughing, talking or sneezing produce atomized fluids containing pathogens, i.e. viruses, bacteria or fungi. The spreading of infectious respiratory diseases in indoor environments is a consequence of a direct or indirect contact with these droplets.

The normal breathing function consists of an inhalation period, during which the air comes into the respiratory system until it reaches the lungs. Once there, the oxygen of the air passes to the human blood through millions of small membranes called alveoli. After that, the second part of the respiration, which is called exhalation, takes part. The air empty of oxygen leaves the human respiratory system to leave the way to another inhalation. This process is repeated by a person between 10-20 times per minute depending on the size, age and gender, among other factors of the person, and the variation of its air flow rate over the time is a sinusoidal function (Gupta et al., 2010).
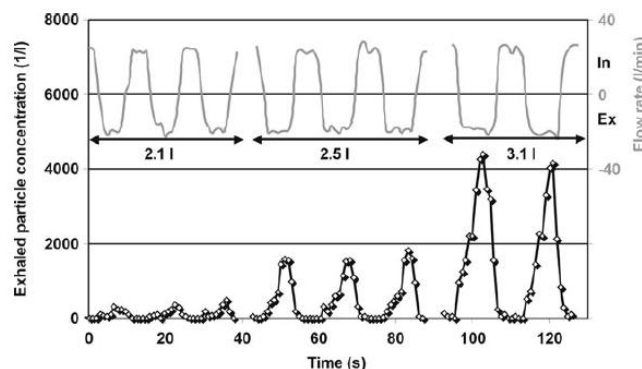
Figure 1.5 Relation between the number of particles expelled and the exhalation flow rate during a normal exhalation (Schwartz et al., 2010)

During the exhalation process human aerosol containing possible biological contaminants are spread in the air. Depending on the breathing function, the number of particles generated changes. A larger flow rate generates a larger number of exhaled particles, see figure 1.5.

Human sneeze and cough can be considered one of the most important sources for spreading respiratory infectious diseases. Much research has been done considering the human cough as a source of communicable diseases (Badeau et al., 2002; Zhu et al., 2006a). The droplet generation of a cough is significantly high and its initial high speed makes the exhaled particles flow long distances unaffected by the indoor airflow (Zhu et al., 2006b; Zhu and Kato, 2006; Chao et al., 2009; Zhao et al., 2005).

Figure 1.6 shows the particles expelled by a human cough and the flow rate variation in time. Gupta et al., 2009 characterized the human cough flow rate and direction with 25 human subjects. They also provided very useful information about the human mouth opening size during a normal cough.
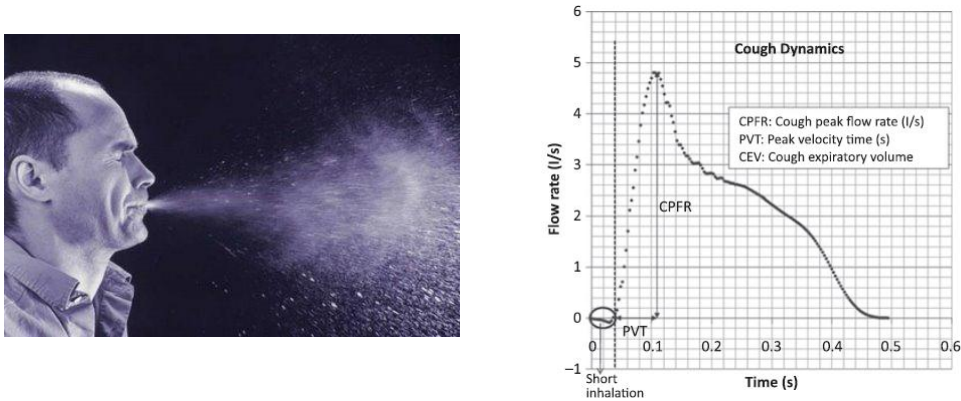
Figure 1.6 a) Flash picture of a human sneeze, b) Cough flow rate variation in time (Gupta et al., 2009)

The content and especially the size of the human exhaled particles determine the route of transmission of disease. The following section describes the transmission routes of diseases that are related with human exhaled particles.

1.3 Transmission routes of diseases

The daily contact with other humans makes us susceptible to pathogens, bacteria and viruses that affect our health. The routes of transmission of diseases are different and are described briefly in the following sections.

1.3.1 Direct contact with people

This route of disease transmission is not directly connected with exhaled particles by a person. It occurs when there is physical contact between a susceptible person and an infected person or contaminated object or surface.

Many illnesses spread through contact transmission, e.g.: chicken pox, common cold, conjunctivitis, Hepatitis A and B, herpes simplex, influenza, measles or mononucleosis. The way of preventing this way of transmission is by the use of physical barriers, such as gloves and the cleaning of contaminated, frequently touched surfaces, as well as washing hands.

A possible direct transmission route is also possible through vectors such as mosquitos, which can transport human fluids (blood) from one person to another.

1.3.2 Large droplet contact

Expiratory droplets expelled during coughing, sneezing, laughing or talking are pathogen carriers that can provoke a cross-infection risk between people in two ways. Firstly, by a direct contact of a person with a contaminated large droplet exhaled and spread in the air by an infected person. This route of transmission is quite common in hospitals wards or clinical sites, where the exposure to aerosol exhaled by infectious people is high (Chen et al., 2010). The common way to prevent this route of transmission is the use of masks and other physical barriers (Tang et al., 2009). The second way in which large expelled droplets can provoke a risk of infection to a healthy person is by indirect contact, provoking the contamination of a surface or object. Larger droplets fall down due to gravitational effect and can be deposited in different surfaces Qian and Li, 2010; Wan and Chao 2007; Xie et al., 2007; Chao et al., 2008). Once there, the bacterial cells or viruses contained in the droplets can remain for long periods. The possible cross-infection is caused when a person comes in contact with the contaminated large droplets deposited. The critical size of which is considered a large droplet is a function of many different parameters such as the ambient humidity. According to the Wells evaporation curve, see figure 1.7, which relates the droplet size with the time to fall down, larger droplets are considered to be droplets larger than 100µm, which fall down quickly due to gravitational effect. However, a recent study by Xie et al., 2007 determines the size of the large droplets between 60 and 100 µm and Chao et al., 2008 also determined that large droplets larger than 87.5 µm settle down due to the gravitational effect.
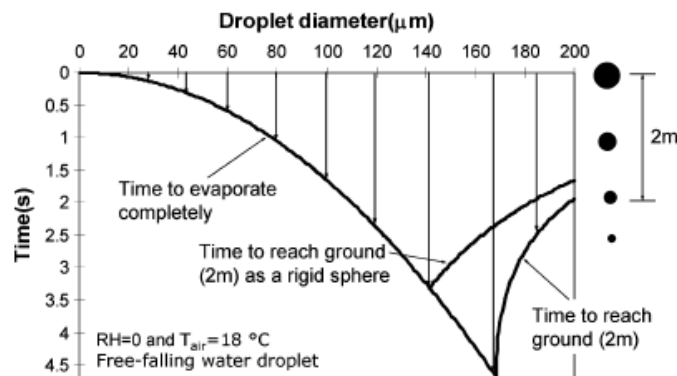
Figure 1.7 The Wells evaporation falling curve of droplets (Wells 1934)

1.3.3 Airborne transmission

Airborne transmission of infections is considered one of the major infectious routes of different diseases such as influenza, tuberculosis or measles. While contaminated exhaled large droplets fall due to gravitational effect, small droplets or droplet nuclei carrying biological contaminants remain in the air and follow the air stream dispersing in the air (Chao et al., 2008; Wan et al., 2009; Chen and Zhao 2010), see figure 1.8(a). Consequently, the exhaled air may be effective in the transportation of organisms, such as viruses that may be carried in these very fine droplets see Nicas et al. (2005) and Morawska (2006). When these particles reach the inhalation region of a person, they are inhaled and conduced to the lungs. However, the human respiratory system has several protective mechanisms such as the mucous in the nasal cavity or tiny hairs called cilia in the trachea. These systems avoid the particles to reach the lungs and prevent a blood infectious. The success of these human protective systems partly depends on the size of the particles. Yang et al., 2011 studied the relation between the size of the particles and the reach of these particles inside the human respiratory system, see figure 1.8(b). Most of the larger particles, close to 100 µm, are filtered in the nasal cavity, while very fine and small particles can easily reach the lungs. This fact makes the tiny exhaled contaminant particles one of the most active, invisible and dangerous airborne route of transmission of diseases.
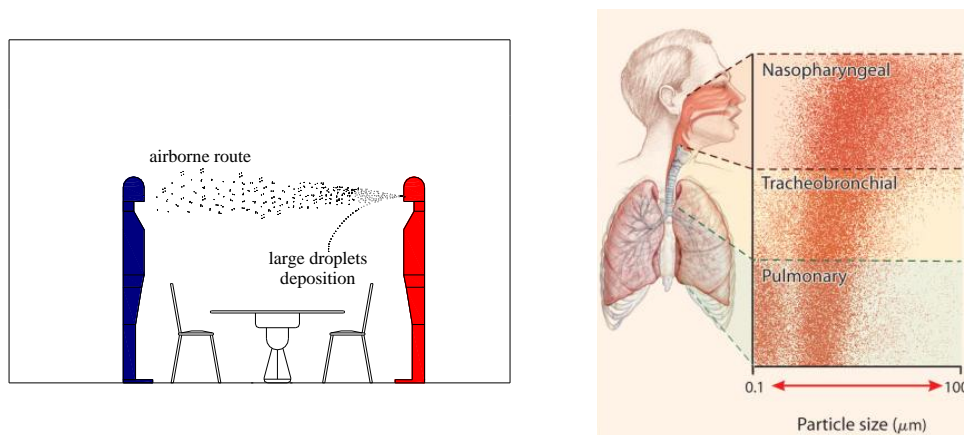
Figure 1.8 a) Dispersion of exhaled particles in a room with two people, in red the person exhaling the contaminants and in blue the susceptible person of being infected, b) Relation between the particles size and the region of the human respiratory system that the particles can reach (Yang et al., 2011)

In order to understand the origin of these fine contaminated exhaled particles, much research has been made. It is know that the exhaled contaminated aerosol contain a large amount of water (Effros et al., 2002), which is partly evaporated when the aerosols are dispersed in the air (Wells 1934). Then the large droplets generated by normal human breathing (Schwarz et al., 2010), coughing or sneezing can become "droplet nuclei" in less than a second (Wan and Chao 2007) and be dispersed in the air. These droplet nuclei can also be produced by human respiratory activities (breathing, coughing, sneezing or talking) (Chao et al., 2009; Morawska et al., 2009) and be spread in the air generating a high concentration values of contaminants in some areas of a room and increasing the risk of cross-infection   between   people.

Inés Olmedo

1.4 The importance of ventilation systems in preventing airborne cross-infections

Several sources of evidence point out to the airborne route as one of the most efficient routes of transmission of diseases (Roy et al., 2004; Yu et al., 2004). The SARS (*Severe Acute Respiratory Syndrome*) occurred in 2003 in China, reopened previous evaluations about the airborne route of communicable respiratory diseases. Some researchers conclude that the airborne dispersion of contaminants may play a significant role in the dispersion of respiratory diseases (Li et al., 2005; Li et al., 2004). After that, much research has been done about the parameters that influence the airborne transmission route and it has been proved that the ventilation systems and airflow patterns are a key factor in the spread of contaminants in the air (Li et al., 2007). Qian and Li, 2010 demonstrated that the placement of the exhaust openings in an isolation room can also have a significant influence on the efficiency of a system in removing large droplets and droplet nuclei. Some authors have reported that this efficiency depends also on the position of the air inlet and outlet, the presence of elements that can influence the ambient, such as furniture, or the air inlet velocity (Woloszyn et al., 2004; Liu et al., 2009; Cheong et al., 2003).

Generally speaking, different ventilation strategies influence the dispersion of contaminants in indoor environments in different ways. While a mixing ventilation system creates a homogeneous distribution of the contaminants, a displacement ventilation system creates different areas, a clean lower zone and a contaminated upper zone. However, the problem of the displacement ventilation system is when the pollutants are injected into the thermally stratified zone (Li et al 2011; Olmedo et al, 2011; Nielsen et al., 2011). Then the contaminants are trapped in a stratified layer and can provoke high contaminant concentration at the height of the breathing. The risk of cross-infection generated in a ventilated space will depend on the level of exhaled contaminants in the breathing area of a susceptible person.

The four following chapters of this thesis establish a relation between the airflow patterns generated by different ventilation strategies and the human exhaled contaminant concentration in a room.

1.5 Layout of the thesis

The thesis has been written in the following chronological order:

Chapter 1   The overview on the problem of cross-infection between people in indoor environments is given in this chapter. It also presents the summary of the papers which are considered within this work.

Chapter 2   Describes the experimental methodology carried out during the experiments. It includes the whole description of the laboratory facilities, measurements devices and manikins.

Chapter 3   Shows and describes the ventilation strategies used during the experiments and the airflow pattern generated by each of the ventilation systems in a room.

Chapter 4   Deals with the relation between the ventilation strategy used in a room and the dispersion of the contaminated exhalation flow of one manikin.

Chapter 5   Addresses experimental results about the risk of cross-infection between two people in a room with different ventilation strategies. It also presents the influence of

the different parameters in this cross-infection risk which can be: separation distance between the manikins or relative positions.

Chapter 6   Provides an abstract of the results achieved in this study.

Paper I   Discusses the characteristics of the human exhalation flow through the mouth with three different ventilation strategies: displacement, mixing and natural ventilation.

Paper II Addresses the analysis of the dispersion of exhaled contaminants and the cross-infection risk between two people in a room provided with displacement ventilation.

Paper III   Describes the airflow pattern and velocity profile generated by three different diffusers: semi-circular wall mounted displacement diffuser, four ways ceiling diffuser and ceiling mounted textile diffuser.

Paper IV   Shows the experimental results of how a thermal plume of a person can affects its personal microenvironment and therefore the air quality that person breathes.

Paper V   Discusses the influence of three ventilation strategies on the risk of cross-infection between two people in a room. Key factors that directly affect the risk of exposure to exhaled contaminants, such as: separation distance or relative position between the manikins, are addressed in the paper.

Paper VI   Studies the risk of cross-infection generated between two people in a room with a low-impulse vertical ventilation system. Compares the results with the ones obtained by other ventilation systems (Paper V) and gives a complete overview of the influence of the ventilation systems on the airborne transmission of diseases.

Paper VII   Describes a CFD simulation of the IEA 2D test considering it as a three dimensional and unsteady problem.

CHAPTER 2
Materials and method

The results of this thesis are mostly based on experimental tests carried out in a full-scale laboratory at Alborg University. One or two breathing thermal manikins have been used to simulate people in a room and the risk of cross-infection between them. The measurements have been carried out under different ventilation strategies in the room: non-mechanical ventilation, mixing ventilation, displacement ventilation and low-impulse vertical ventilation. This chapter shortly describes the methodology and the laboratory facilities used during the experimental work.

2.1. Experimental materials and facilities

2.1.1 Test room and measurements facilities

All the experimental test are carried out in a full-scale room, 4.10 m (length), 3.20 m (width) and 2.70 m (height) in the laboratory of the Civil Engineering Department at Aalborg University. The four different air distribution strategies used are: non-mechanical ventilation (NV), mixing ventilation (MV), displacement ventilation (DV) and low-impulse vertical ventilation, which generates downward flow (DWF) and upward flow areas (UWF) in the room. For the mixing ventilation case, a four-way square diffuser is mounted in the centre of the ceiling to produce a well-mixed flow field. For the displacement ventilation case, a wall-mounted semicircular diffuser is placed in the middle of the left wall. Two rectangular return openings, 0.30 m (length) and 0.10 m (width) each, are located in the left wall below the ceiling and used in both cases: the mixing and the displacement ventilation cases. For the vertical ventilation system two textile diffusers are placed next to each other in the ceiling of the room. One circular return opening, 0.12 m diameter, is placed in the back wall of the room at 2.6 m from the floor in this case, see figure 2.1.

The air change rate set in all the experiments is 5.6 h^{-1}, which corresponds to a volume flow rate (q_0) of 296 m^3/s. The ventilation system provides cold air supply at 16 ℃.
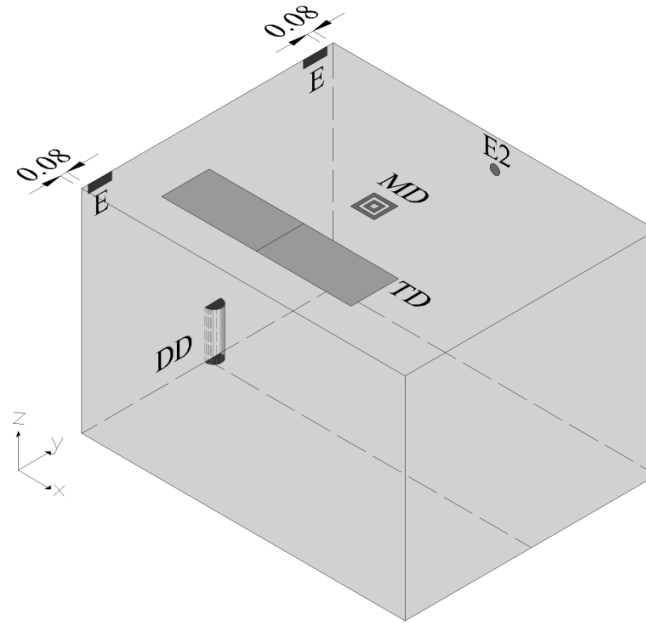
Figure 2.1 Sketch of the test room. Semi-circular displacement diffuser (DD), square mixing diffuser (MD), textile diffusers (TD), return openings for the mixing ventilation and displacement ventilation cases (E), return opening for the vertical ventilation with the textile diffusers (E2)

The test chamber is provided with hot sphere anemometers (Dantec 54R10), which are used to measure air velocity. The air temperature in the test room is measured during all the tests with thermocouples type K and a Squirrel 1000 data logger manufactured by Eltek. A tracer gas, N_2O, is used to simulate exhaled contaminants by one of the manikins in the room. The dispersion of this contaminant is studied and its concentration is measured at several locations with a Multi gas Monitor type 1412 and two Multipoint Sampler and Doser type 1303, both manufactured by Brüel & Kjaer. The accuracy and frequency of each measurement as well as the calibration process of each sensor is explained in Appendix A.

A smoke machine, manufactured by Safex, is also used to visualize the different air flow patterns in the room. An air current test kit used to create smoke to detect the direction of slight air currents in rooms is also used for some of the experiments, e.g.: to visualize the direction of the breathing of the manikins and the flow direction below the diffuser or above the manikins.

2.1.2 Description of the diffusers

The mixing diffuser used to generate a mixing ventilation airflow pattern in the room is a four-way ceiling mounted diffuser; model DSQ 225, manufactured by Madel. Figure 2.2 shows   its   dimension.

	E	A	C	B
Size (mm)	332	292	212	223
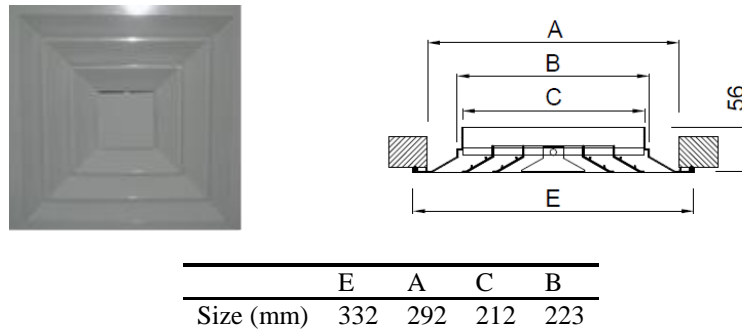
Figure 2.2 Description and size of the four-way ceiling mounted mixing diffuser

For the displacement ventilation cases a semi-circular wall-mounted displacement diffuser is used. The size and dimensions of this diffuser are shown in figure 2.3. The main characteristic is its large supply area that supplies the air into the room at a low velocity.

a)   b)
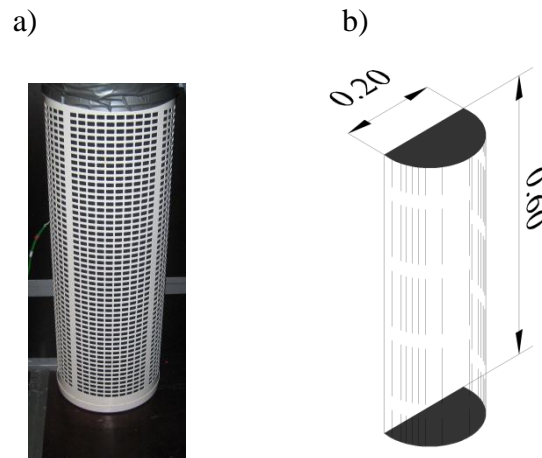
Figure 2.3 Semicircular wall-mounted displacement diffuser a) Picture, b) Size

The low impulse vertical ventilation system consists of two identcal textile diffuser placed one next to each other on the ceiling of the room, see figure 2.1. Each diffuser is sized 0.6 m x 1.2 m.

2.1.3 Manikin model of a person

One or two thermal manikins with breathing function are used during the experiments. The manikins are 1.68 m, average-sized women and the total surface area without clothes is about 1.40 m^2. The manikins have a human body shape in order to be able to accurately simulate the thermal plume generated by a person, see Zukowska et al. (2008). For details

of body shape see figure 2.4. One of the manikins is considered the source, which exhales biological contaminants simulated by the tracer gas N_2O. The target manikin is the one exposed to the exhaled contaminants by the source. With regard to the mouth openings there are slight differences for the two manikins. For the source manikin the mouth has a 123 mm^2 opening and a semi-ellipsoid form and for the target manikin, the mouth consists of a circular opening of diameter of 12 mm. Both manikins exhale the air through the mouth and inhale through the nose. The nose consists of two circular nostrils, with a 6 mm radius each, situated 10 mm above the mouth and facing downwards at a direction of 45º below horizontal plane.

a)　　　　　　　　　　　　b)
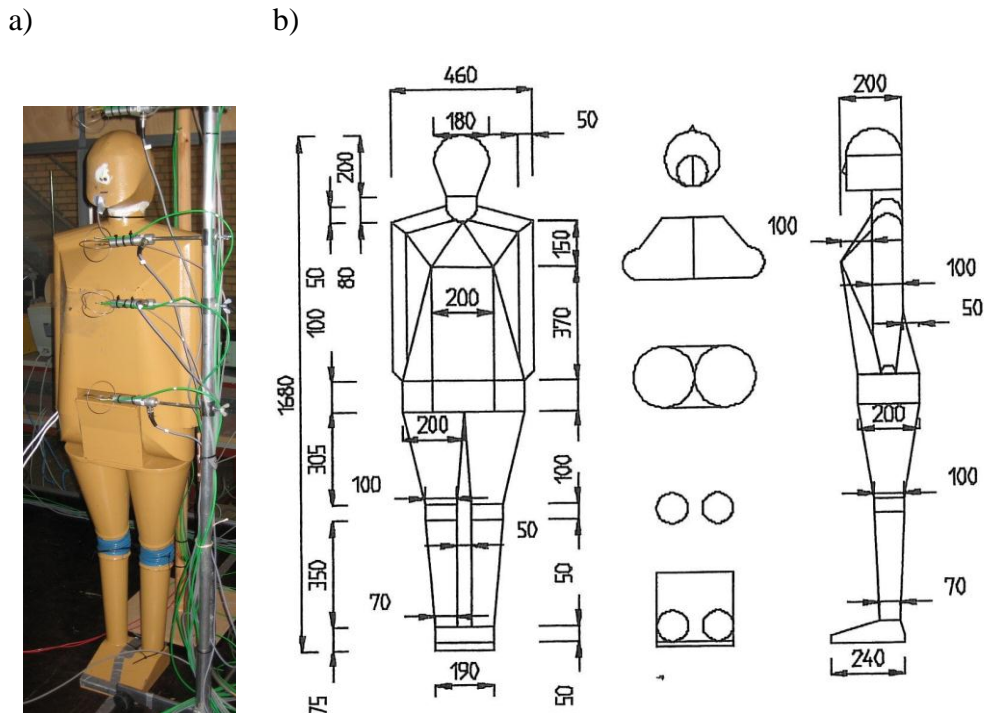
Figure 2.4 a) Picture of the source manikin, b) Detailed description of the manikins´ size (Bjørn, 1999)

2.1.4 Simulation of the human breathing

In order to simulate the human breathing two artificial lungs, one for each of the manikins, are used. They can be set to provide a given simulation of the breathing flow with the suitable pulmonary ventilation rate, frequency, gas concentration (in the source manikin) and temperature of the exhaled air. Figure 2.5 shows the two artificial lungs used for the manikins.

The temperature of the exhaled air is kept at 34±0.5 ºC using two small heaters mounted in the supply air tubes, which simulate human exhaled air saturated with water vapour at 31

ºC, see Bjørn (1999). This temperature is corrected in order to compensate for relative humidity in human exhalation.
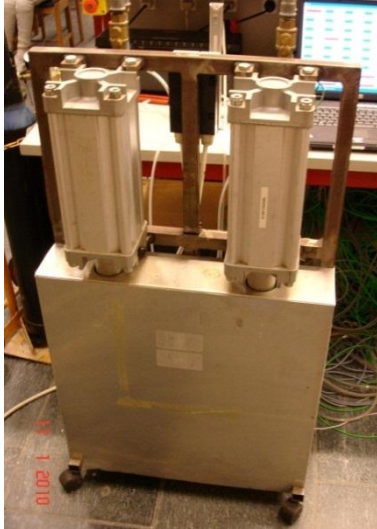
a)   b)

Figure 2.5 Picture of the artificial lungs a) for the source manikin, b) for the target manikin

During the tests, one of the manikins is used as the source manikin. A tracer gas, N_2O, is added to its exhalation in order to simulate small droplet nuclei exhaled by a person that can follow the air stream (Tang et al., 2011). N_2O is commonly known as the "laughing gas". It is an invisible and odourless gas which has a density similar to air. N_2O is mixed into the supply air in front of the air heater in order to simulate the exhalation of contaminated air from the source manikin. The other manikin is considered the exposed or the target one. Table 2.1 shows the pulmonary ventilation rate simulated for the two manikins for all the tests carried out with the different ventilation strategies.

Table 2.1 Breathing functions of the two manikins for the different ventilation strategies: non-mechanical ventilation (NV), mixing ventilation (MV), displacement ventilation (DV) and low-impulse vertical ventilation placing the manikins in the downward flow area (DWF) and in the upward flow area (UWF)

Ventilation strategy	Source manikin		Target manikin	
	Volume rate (l/exhalation)	Breathing frequency (breaths/minute)	Volume rate (l/exhalation)	Breathing frequency (breaths/minute)
NV MV DV	0.57	19.9	0.66	15.0
DWF UWF	0.75	14.6	0.66	10.0

2.2. Experimental method

2.2.1 Experimental set-up

For all the experimental tests the measurements are taken under steady state conditions. The laboratory where the test room is placed is maintained at a stable temperature similar to the temperature in the test room, in order to minimize the heat fluxes between the test room and the laboratory. Before starting each experiment, the steady state conditions are obtained by using at least five hours to stabilize the temperature in the room. Once the thermal conditions are stable, which means that the temperature in the room is stable at a certain value ± 0.5 °C, the experimental tests were carried out.

The anemometers, thermocouples and concentration tubes are fixed along vertical or horizontal poles placed at different positions in the room.

For the tests to study the airflow patterns in the room, the smoke machine was placed into a wooden box connected to the ventilation ducts.

During the tests where the manikins are used the direction of the exhaled air is to be set horizontally from the mouth using smoke visualisation at the beginning of each experiment.

Each experiment lasts between four and five hours, in order to have enough data to generate reliable average values of velocity, tracer gas concentration and temperature in the room.

2.2.1 Data process

Temperature, velocity and concentration data is measured and recorded. After each experiment the data is post-processed with the corresponding software.

The accuracy of the temperature measurements considering the uncertainties of the probe, wire length and the data acquisition equipment is ±0.5ºC of the reading. The frequency of the temperature measurements is 30 s.

Velocities are measured with Dantec 54R10 hot sphere anemometers, which are calibrated in a wind tunnel measuring the voltage and the real velocity value using pressure difference values, see Appendix A. The measurements are made with a precision of ±5% at a frequency of 100 ms.

The concentration equipment consists of twelve channels which measure the gas concentration in a sample of air. Measurements are taken for a period of 10 s for each channel consecutively. The accuracy of the concentration measurements is ±1%.

The average values during the experiments are used to obtain the thermal, velocity and contaminant concentration conditions in the room for each test.

Instead of the average values, the maximum concentration and velocity values are used to characterize the human breathing exhalation flow, see chapter 4.

CHAPTER 3
Airflow patterns generated in the room

Air diffusers perform in different ways and generate different airflow patterns, temperature and contaminant distributions in a room. Brief descriptions of the airflow pattern generated by three different terminal units: mixing, displacement and a low impulse diffuser are already presented. Smoke visualizations of the airflow and velocity measurements, for each of the terminal units, are also included in order to characterize the diffusers and gain knowledge about the air diffusion that generate in the room. The experimental tests with the wall-mounted displacement diffuser, the ceiling-mounted mixing diffuser and the low impulse textile diffuser were carried out in a full-scale test room at Aalborg University.

3.1 Importance of the air supply conditions

The air movement in a room is controlled or significantly influenced by the air momentum flow produced by the supply opening. Different supply openings generate different airflow patterns and thermal conditions in the room. Therefore, it is important to study the behavior of different diffusers to predict the indoor air conditions in an accurate way.

The correct description of air supply diffusers also plays a crucial role in the CFD predictions of the airflow pattern in a room. Different studies (Lee, 2007; Srebric, 2008) have demonstrated the importance of the diffuser characteristics and the CFD boundary conditions in the air distribution in a room. In the last years several authors have developed studies regarding different methods of diffuser simulation. The prescribed velocity method (Nielsen, 1997a), the box method (Nielsen, 1997b) and the momentum method (Chen and Moser, 1991) are practical methods for an accurate description of the terminal units in CFD. All of them require some previous experimental measurements to characterize the airflow provided by the diffuser and have been validated by several authors (Koskela, 2004; Huo et al 2000; Einberg et al., 2005; Srebric and Chen 2002).

The main purpose of this chapter is to provide some useful data about the airflow pattern generated by different diffusers, their symmetry or asymmetry, impact on the room conditions and developed regions of the jets. The results will provide knowledge about the airflow patterns generated in a room when the airflow is not influenced by any heat loads and it will provide also valuable information for the validation of CFD simulation methods.

3.2 Materials and methods

Three experimental tests were carried out in a full-scale test room with the internal dimensions of 4.1 m (length), 3.2 m (width) and 2.7 m (height). Figure 3.1(a) shows a sketch of the room with the three diffusers used: a four-way mixing diffuser, a wall-mounted semicircular displacement diffuser and a ceiling-mounted textile diffuser. Only one diffuser was used in each test. In order to create non-isothermal conditions in the room a radiator was also placed in the room. The heat load released was 394 W for all the tests. The position of the diffusers and the radiator in the room is illustrated in figure 3.1(b).

For the tests with the displacement and mixing diffusers two exhaust openings sized 0.3 x 0.1 m and placed in the left wall close to the ceiling were used. For the test with the textile diffuser, a circular exhaust opening (12 cm diameter) is used and placed in the back wall of the room, see figure 3.1. The air exchange rate was set to 5.6 h^{-1}. The details of the size and geometry of the diffusers can be found in chapter 2.

a)   b)
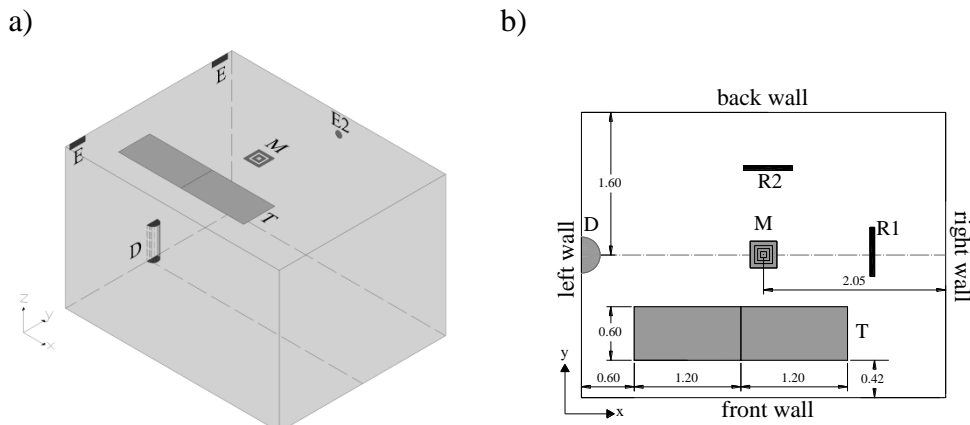
Figure 3.1 a) Sketch of the test room and location of the diffusers and exhaust (D, displacement diffuser; M, mixing diffuser; T, textile diffuser; E, exhaust openings for the mixing and displacement ventilation tests; E2, exhaust opening used with the textile diffuser), b) Placement of the diffusers and radiator in the room (R1, position of the radiator for the tests with the mixing and displacement diffuser; R2, position of the radiator for the test with the textile diffuser)

3.3 Airflow pattern for the mixing diffuser

The flow generated by a mixing ventilation diffuser is mainly controlled by its momentum flow. This section analyses the flow generated by a four-way ceiling mounted diffuser and describes the characteristic equation of the jet generated.

3.3.1 Turbulent isothermal free jets

The air supplied by a mixing diffuser generates a turbulent jet. This jet flows entraining the air in the room and generates a strong mixing process. The velocity of an air jet decreases with the distance to the diffuser. It is possible to describe a line of maximum velocity, which is also called centreline of the jet. Figure 3.2 shows the four regions in which a turbulent jet can be divided:

- ✓ Initial region or velocity core is a short zone. The maximum velocity of the jet remains practically unchanged.
- ✓ Transition region. Its length depends upon the diffuser type. The centreline of the jet is predictable and it is possible to find a relation between the maximum velocity and the distance from the diffuser.
- ✓ Main region: A fully turbulent flow has been established. It is possible to determine the velocity at the centreline of the jet with its characteristic equation.
- ✓ Terminal region: A region far from the diffuser. The initial velocity core is mixed with the surrounding air.
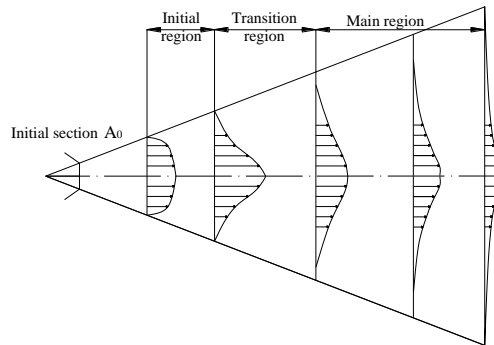
Figure 3.2 Picture of an isothermal jet

The centreline velocity decay of a three dimensional jet can be described by equation (3.1).

$$\frac{u_x}{u_o} = K_v \cdot \left(\frac{x}{\sqrt{A_o}} \right)^{n_1} \qquad (3.1)$$

where u_x is the velocity in the centreline, u_0 is the velocity at the discharge, x the distance to the diffuser, A_0 the free area of the diffuser, K_v the centreline velocity decay constant and n_1 the negative exponent of the velocity decay, which is close to -1.0.

Equation (3.1) can be illustrated and written in its logarithmic form, where the dimensionless velocity u_x/u_0 is represented as a function of the dimensionless distance $x/\sqrt{A_0}$ and where the exponent n_1 corresponds to the slope of the straight line of the graph, see figure 3.3 and equation (3.2).
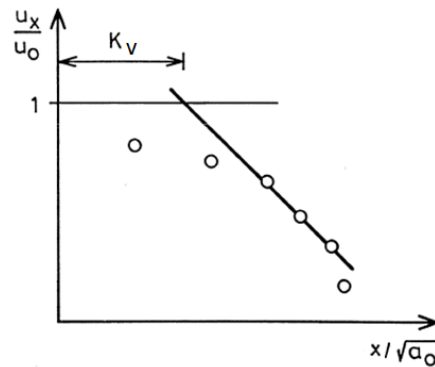
Figure 3.3 Dimensionless velocity versus dimensionless distance for a free jet (Reproduced from Nielsen, 1995)

$$\log\left(\frac{u_x}{u_0}\right) = \log\ K_v - n_1\ \log\left(\frac{x}{\sqrt{A_o}}\right) \qquad (3.2)$$

A plane wall and free jet will have a slope of -0.5 while a three dimensional wall and free jets will have a slope of -1.0 (Nielsen, 1995).

3.3.2 Airflow and velocity decay

In order to find the velocity profile close to the diffuser at different heights, five hot-sphere anemometers are placed at 0.03 m from the centre of each side of the diffuser. The anemometers are placed at the heights of: 2.65 m, 2.61 m, 2.57 m, 2.53 m and 2.49 m, corresponding with the measurements obtained for L1, L2, L3, L4 and L5 respectively, see figure 3.4(a).
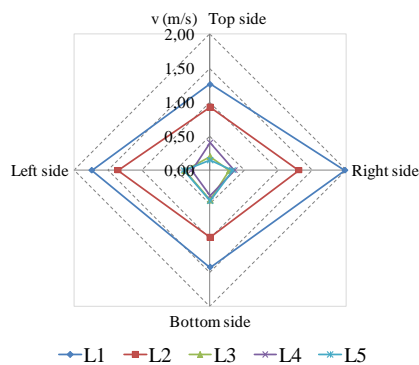
a)   b)

Figure 3.4 a) Velocity profile generated by the ceiling-mounted mixing diffuser, b) Airflow smoke visualization

The velocity profiles obtained shows practically a complete symmetry in the airflow generated by the diffuser at the five heights. However, the results show higher velocity values in the right and left sides of the diffuser, which corresponds to the sides with the largest separation distance from the walls. It may mean a significant influence on the room geometry in the velocity profile

The quasy-symmetry airflow pattern generated by the diffuser is also possible to see with smoke visualization, see figure 3.4(b).

In order to find the characteristic equation of the jet in one of the sides of the diffuser, the vertical line with the five anemometers is moved to 0.53 and 0.83 m from the diffuser on the left side of the diffuser. Figure 3.5 shows the anemometer positions and the velocity profiles obtained at each distance from the diffuser.
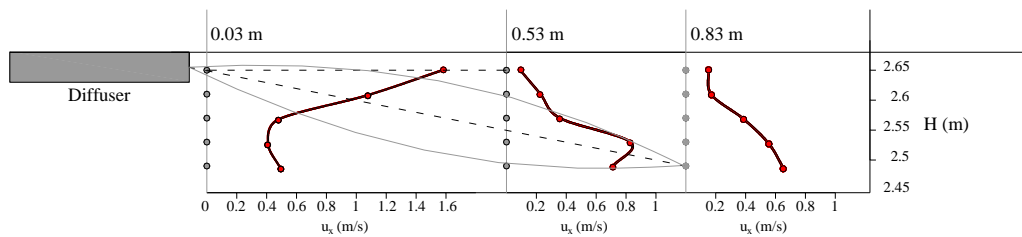
Figure 3.5 Placement of the anemometers respect to the diffuser (grey) and velocity results obtained for each anemometer (red)

For the closest distance, 0.03 m from the diffuser, the maximum velocities are obtained at the heights closest to the ceiling. However, at 0.53 m and 0.83 m from the diffuser the maximum velocities are obtained at the heights of 2.53 and 2.49 m respectively.

The results correspond to the typical developed region of a jet, which entrains the air in the room and disperse the air with a certain angle from the ceiling, which correspond to 15° for this case. The velocity decay of the jet is calculated using the maximum velocity values measured at the separation distances of 0.03 m, 0.53 m and 0.83 m from the diffuser, which corresponds with the anemometers placed at the height of 2.65 m, 2.53 m and 2.49 m respectively.
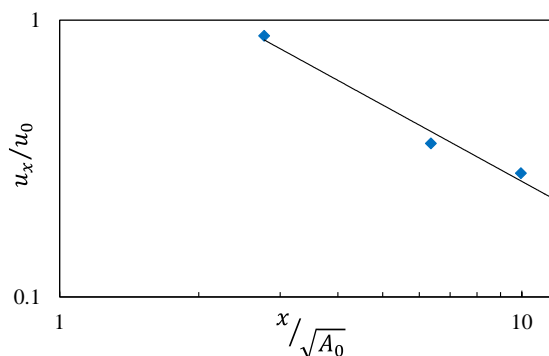
Figure 3.6 Log-log graph representing the velocity decay of the mixing diffuser

Figure 3.6 represents the dimensionless velocity u_x/u_0 as a function of the dimensionless

distance $x/\sqrt{A_0}$ in a log-log graph. The slope of the straight line in the graph represents the velocity decay of the jet, which is -0.92.

   The data of the free opening area of the diffuser is provided by the manufacturer, 0.0227 m^2, and the maximum velocity, u$_0$, is calculated as the division of the volume flow rate, 198 m^3/h and the diffuser free area. The value of the constant decay coefficient, K_v, obtained is 2.5, which is a typical value in this kind of diffusers.

3.4   Airflow pattern for the displacement diffuser

The cold air spread at a low velocity in the room by a displacement ventilation system "displaces" the previous air in a room, without producing mixing process. A semi-circular wall mounted displacement diffuser is used to condition the test room and its air flow pattern is measured and visualized with smoke.

   Seven anemometers are place along a horizontal line at 0.01 m height from the floor in order to measure the velocity profile. The horizontal line formed a 45º angle with the center line of the room along the x axis. The first anemometer is placed at 0.20 m from the diffuser and the rest are placed equidistance at 0.20 m from each other.
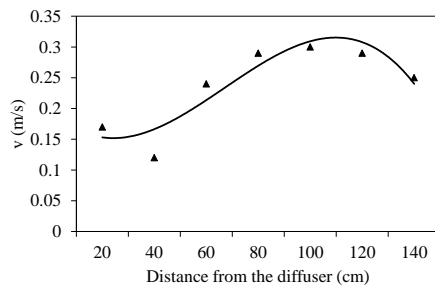
a)   b)

Figure 3.7 a) Velocity profile generated by the wall-mounted displacement diffuser along at horizontal line at 0.01 m from the floor, b) Airflow smoke visualization

The results show an acceleration of the flow at distances larger than 0.60 m from the diffuser due to the flow of the heavier cold air to the lower part of the room. This velocity is reduced to a value close to 0.20 m/s at 1.40 m from the diffuser, see figure 3.7(a). The stratified and radial flow generated by the cold supply air, which is common with a wall-mounted displacement diffuser (Nielsen 2000), is shown in figure 3.7(b).

3.5 Airflow pattern for the low-velocity vertical diffuser

In order to measure the velocity profile of a ceiling-mounted low velocity textile diffuser, twelve hot-sphere anemometers are placed along the horizontal line, T1, at 0.80 m from the ceiling, see figure 3.8(a).

The positions of the anemometers in relation to the front wall are shown in table 3.1.

Table 3.1 Position of the anemometers along the horizontal line, T1

Anemometer	y (m)	Anemometer	y (m)
1	0.04	7	0.31
2	0.09	8	0.38
3	0.12	9	0.48
4	0.18	10	0.58
5	0.22	11	0.78
6	0.27	12	0.98

The textile diffuser generates an expected downward flow that is not disturbed by any heat load in the room (the radiator is placed in the opposite side of the room).

The velocity profile measured shows high velocity values in the region close to the wall and lower values in the measurements below the diffuser, see figure 3.8(b).
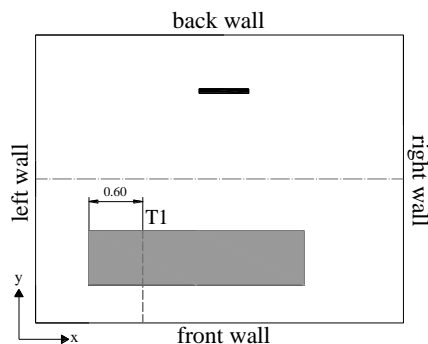
a)   b)
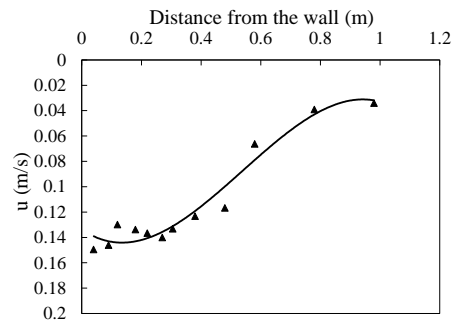
Figure 3.8 a) Placement of the measuring line T1 (diffusers in grey), b) Velocity profile measured at 0.8 m the diffuser along the line T1

This acceleration of the flow close to the wall is due to the Coanda effect generated by the wall, which is also visualized by smoke. Figure 3.9 shows the development of the flow at three different instants of time, where it is possible to notice the tendency of the air to flow to the wall side.

a)   b)   c)

Figure 3.9 Smoke visualization of the flow at three instants of time a) 1s, b) 2.5 s, c) 4.5 s

3.6   Discussion of the results

The results presented show the airflow pattern generated by the different ventilation strategies in the test room. They help us to gain knowledge about the different air characteristics that can be created in a room by the different ventilation systems. This data will be useful to understand the indoor environment conditions created in a room by the different ventilation systems when a person or several people are placed in the room. The following chapters will study the influence of these airflow patterns and other parameters on the dispersion of human exhaled contaminants in a room.

CHAPTER 4
Dispersion of human exhaled contaminants in a room

People that occupy a room are not only very significant heat loads but they can also be the most relevant source of biological contaminants, as the human exhaled air can contain different pathogens such as viruses or bacteria. Expiratory droplet nuclei generated by an infected person can spread in the air through the airflow pattern and may increase the pathogen concentration in different indoor environment areas. The purpose of this study is to investigate the influence of the indoor conditions generated by different air distribution strategies on the behaviour and trajectory of the human exhalation flow. It is also the objective to find a possible correlation between the velocity and contaminant concentration of the exhalation flow and its trajectory. This chapter will also analyse the influence of the thermal plume generated by a manikin, simulating a standing person, in the air quality that this manikin breathes. Papers I, IV and VI address the results of this chapter.

4.1 Experimental conditions in the room with one manikin

A breathing thermal manikin is used to simulate a standing person in a room, which is conditioned by different ventilation strategies: non-mechanical ventilation (NV), mixing ventilation (MV), displacement ventilation (DV), and low-velocity vertical ventilation, which generates downward flow (DWF) and upward flow (UWF) areas in the room.

The manikin inhales through the nose and exhales through the mouth. The temperature of the exhalation flow is set at 34°C for all the tests. A tracer gas, N_2O, is added to the exhalation flow in order to simulate small exhaled particles as its distribution in the air is identical to the distribution of droplet nuclei (Tang et al., 2011; Yin et al., 2011).

For the different ventilation systems used, the breathing function of the manikin changes as is shown in table 4.1. Figure 4.1 shows the velocity measurements of the exhalation at the mouth of the manikin for the two different breathing functions used. During the time that the exhalation has a velocity close to zero the manikin is inhaling through the nose. The resulting breathing function of the manikin is quite similar to the normal breathing of a person and is considered a sinusoidal function of time (Gupta et al., 2010).

Table 4.1 Breathing functions of the source manikin

		SOURCE MANIKIN		
		Volume rate (l/exhalation)	Breathing frequency (breaths /minute)	Maximum velocity (m/s)
Group A	NV MV DV	0.57	19.0	4.74
Group B	DWF UWF	0.75	14.6	5.76

a)   b)
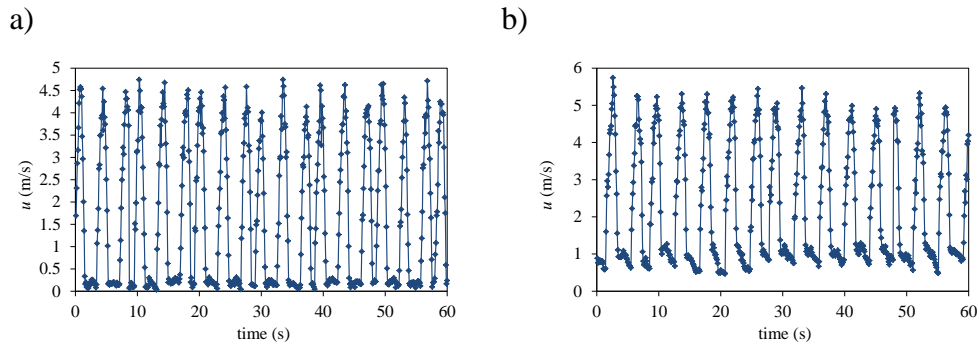
Figure 4.1 Exhalation velocity profiles for the two groups of cases. a) *Group A*, b) *Group B*

For the experiments, the source manikin is used to investigate the influence of different ventilation strategies on the behaviour of the exhalation flow. Different ventilation strategies produce different airflow patterns, temperature distribution and therefore different temperature differences between the exhalation flow and the surrounding air. These facts can directly affect the direction, trajectory and distance that the exhalation jet flows. The penetration distance of this contaminated flow is a crucial factor in order to study the risk of cross-infection in a room when it is occupied by several people.

The experimental work to study the exhalation flow under different ventilation strategies consists of five tests. Table 4.3 shows a sketch of each of the cases studied. For the tests, the standing thermal breathing manikin is placed in the room together with a radiator. The heat load released by the manikin is 94W while the radiator is responsible for 394 W. The position of the manikin and the radiator for each case, as well as the measuring lines used to place the sensors, are shown in figure 4.2.

Additionally, for the displacement ventilation case, the influence of the thermal plume on the air quality that the manikin breathes is also studied. In this case the source manikin is operated under three different heat fluxes; corresponding with different surface temperatures, in order to study the thermal plume generated by different metabolic rates, see table 4.2. The heat load of the radiator is maintained at 394 W.

Table 4.2 Heat load released by the manikin for the study of the thermal plume

SOURCE MANIKIN	
Heat load (W)	Surface temperature (°C)
0	-
94	29.9
120	31.0

a)

b)

c)

d)
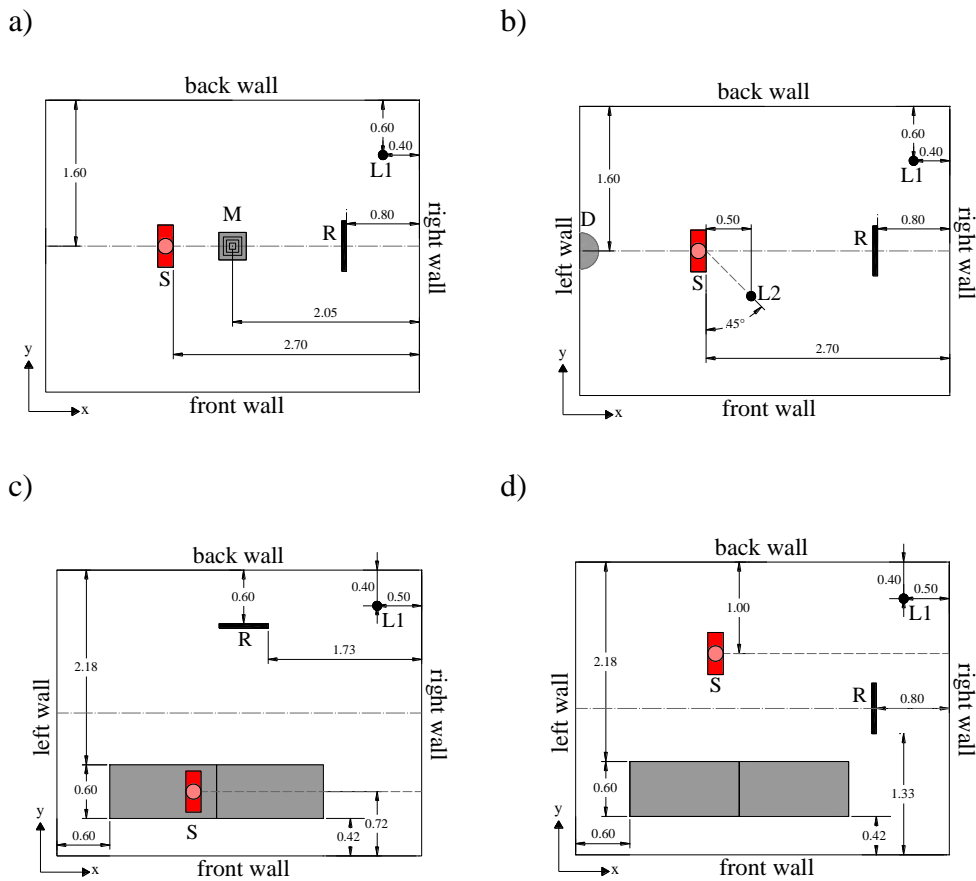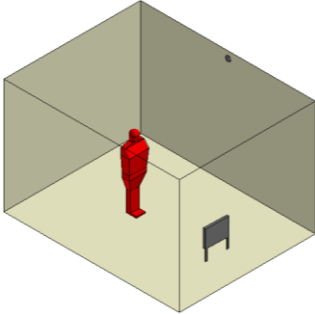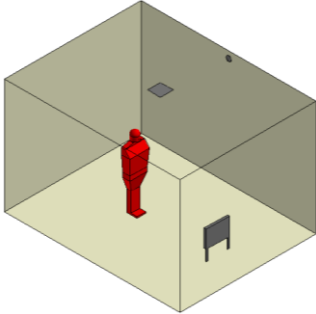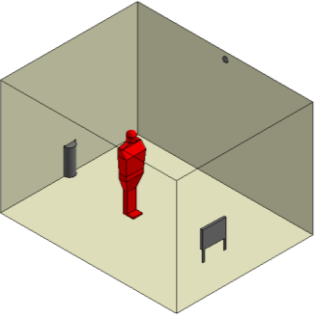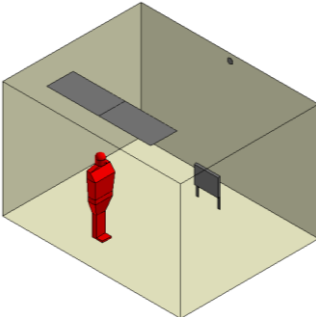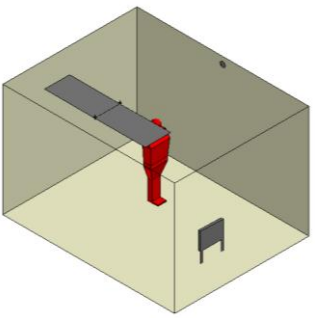
Figure 4.2 Placement of the source manikin (S), radiator (R), vertical lines, L1 and L2 and diffusers a) Mixing ventilation (M) and without mechanical ventilation, b) Displacement ventilation (D), c) Vertical ventilation with the textile diffuser (T) for the downward flow position, d) Vertical ventilation with the textile diffuser (T) for the upward flow position

Table 4.3 Position of the manikin with the different ventilation strategies

GROUP A		
Non-mechanical ventilation	Mixing ventilation	Displacement ventilation

GROUP B	
Low-velocity vertical ventilation	
Downward flow	Upward flow

4.2 Influence of the thermal plume on the air quality a person breathes

This part of the chapter will investigate the PME (*Personal Micro Environment*) of the manikin under displacement ventilation conditions. The aim is to increase the knowledge of how the thermal plume generated by a person affects the PME and therefore the concentration of contaminants in the inhalation area.

An experimental study in the room with the displacement ventilation system is carried out. The convective transport mechanism, which is found in the thermal plume around a person, influences the human exposure to pollutants in this environment (Murakami, 2004).

In this case the source manikin is operated in three different heat fluxes; see table 4.2, to simulate different metabolic rates.

During the experiments ten concentration probes were placed in the room. Three concentration tubes were fixed to the surface of the manikin at three different heights: hips (0.95 m), chest (1.25 m) and nose (1.53 m in the inhalation tube of the manikin). The other seven tubes were situated along the vertical lines L1 and L2, four along L1 at the heights of 0.05 m, 1.25 m, 1.80 m and 2.15 m and three in L2 at the heights of 0.95 m, 1.25 m and 1.53 m, see figure 2b.

Figure 4.3 shows the vertical contaminant distribution in the room along L1 and L2. The results show a strong vertical contaminant gradient typical of a displacement ventilation system along the two vertical lines. For L1, the contaminant distribution is almost the same for the three heat loads used. However, for L2 the contaminant concentration increases with the heat load released from the manikin.

a)

b)
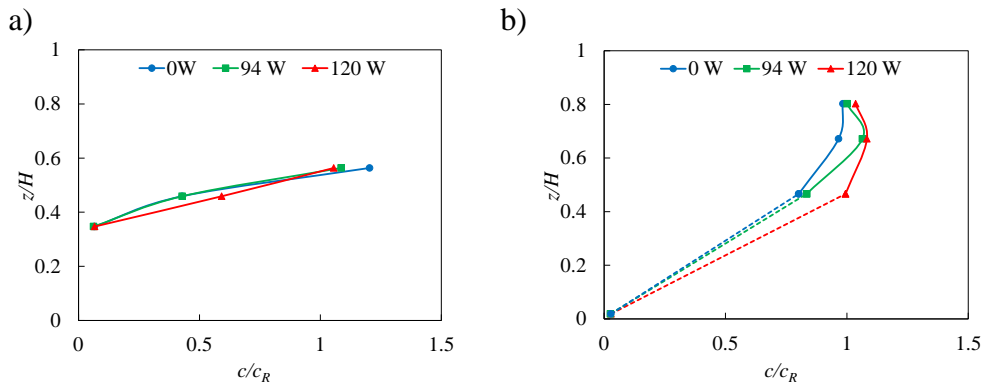
Figure 4.3 Concentration values along the vertical lines using the displacement ventilation strategy. a) L1 in the room, b) L2 at 0.50 m from the manikin

The contaminant concentration in the surface of the manikin at three different heights, the hips, the chest and the inhalation through the nose are show in figure 4.4.
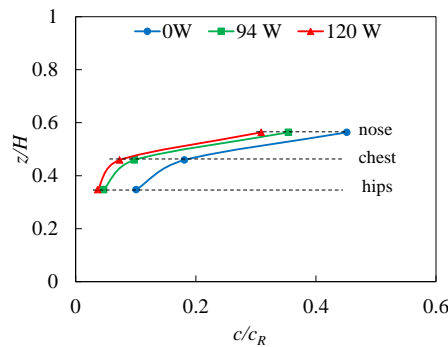
Figure 4.4 Concentration values in the thermal plume of the manikin at the height of the hips, chest and in the inhalation using the displacement ventilation strategy

The three cases considered 0 W, 94 W and 120 W, show a similar shape of the contaminant

concentration profile where the highest amount of contaminants is in the inhalation area. This is due to the typical distribution of contaminants in a displacement ventilated room where the lower area is maintained cleaner than the upper area of the room; see figure 4.3.

The air inhaled by a manikin comes from the lower part of the room, due to the convective flows, (Hayashi et al., 2002, Zhu et al., 2005, Murakami 2004). A strong thermal plume induces more clean air from the lower area of the room that flows upwards to the inhalation area. In consequence, the higher the heat flux is the lower the concentration of contaminants is in the inhalation area.

4.3 Study of the exhalation flow

In this section, the main objective of the experimental tests, *Groups A and B*, is to observe and determine the centreline of the exhalation flow under different ventilation strategies in the room, considering the exhalation as a non-isothermal jet. After this, it is possible to relate the trajectory of the exhalation jet with the maximum velocity and concentration values measured along the centreline.

4.3.1 Thermal conditions in the room

The environmental conditions created by the different ventilation systems in the room can directly affect the trajectory of the exhalation flow. In each of the cases studied one vertical line, L1, with five thermocouples placed at the heights of: 0.1 m, 0.6 m, 1.1 m, 1.8 m and 2.1 m, is located in the room, see figure 4.2. The vertical temperature distributions found for the displacement ventilation, mixing ventilation and vertical ventilation cases are shown in figure 4.5.
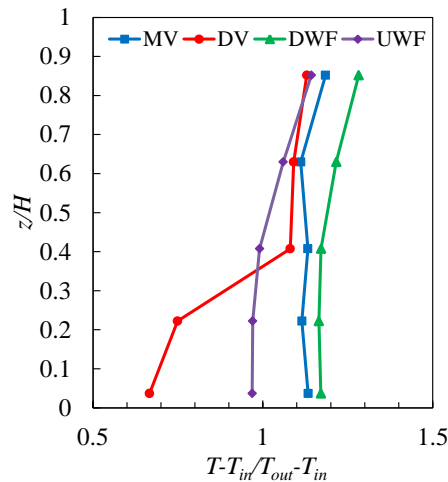
Figure 4.5 Vertical temperature distributions in the room along L1 for the four cases with mechanical ventilation

It is possible to see the typical vertical temperature stratification for the displacement ventilation case. For the mixing ventilation case the temperature values are very close to 1.0, which means that the air is fully mixed in the room. The temperature level for the cases of vertical ventilation, DWF and UWF, is slightly higher than in the other two cases and shows a constant temperature level close to 1.0 as was measured in the mixing ventilation case.

4.3.2   Centreline of the exhalation flow

The exhalation flow can be described as a non-isothermal jet. In this way, the exhalation jet will entrain the air in the room increasing the width of the jet as the distance from the mouth increases. However, the penetration length of the exhalation flow can vary with the different ambient conditions created in the room. During these tests, five gas samplers and five anemometers are used to measure the concentration and velocity in the exhalation flow of the breathing. The sensors are situated along the centreline of the exhalation flow in order to measure the peak centreline values. These five positions are found visualizing the exhalation flow with smoke, see figure 4.6. Five anemometers are placed along the visualized centreline to measure the instantaneous velocity. After placing the anemometers, smoke is used to confirm that their positions correspond to the centreline of the exhalation airflow previously visualized. This process is repeated until the five positions along the centreline are found.

a)   b)   c)
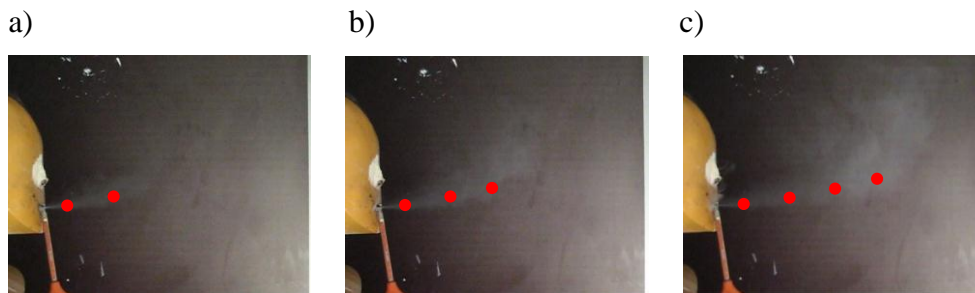
Figure 4.6 Smoke visualization of the exhalation jet in the displacement ventilation case and placement of the probes along the centreline at different time intervals a) 0.1 s, b) 0.3 s and c) 0.55 s

During the experiments special care was taken to find the best position of the manikin to generate a horizontal airflow exhalation. Figure 4.6 illustrates the visualization of the jet with smoke in order to find the centreline of the exhalation at different instants of time. It is important to notice that the further the probes are from the mouth the more the velocity of the exhalation jet is affected by the turbulence. This fact makes the process of finding the centreline of the jet more difficult at further distances from the mouth.

The positions of the anemometers and concentration tubes placed to take measurements along the centreline of the exhalation flow for each case: non-mechanical ventilation (NV), mixing ventilation (MV), displacement ventilation (DV) and vertical ventilation, downward (DWF) and upward (UWF) positions, are shown in figure 4.7. The position of each sensor in the room is given in table 4.4.

mechanical ventilation (NV)

ng ventilation (MV)

Figure 4.7 Placement of the anemometers and concentration tubes along the centreline of the exhalation flow respect to the manikin for each case studied

Table 4.4 Position of the anemometers and concentration tubes along the centreline of the exhalation flow

	Non-mechanical ventilation (NV)				
Horizontal distance (m)	0.04	0.08	0.15	0.25	0.45
Height (m)	1.52	1.525	1.535	1.575	1.615
	Mixing ventilation (MV)				
Horizontal distance (m)	0.04	0.085	0.145	0.23	0.315
Height (m)	1.52	1.528	1.55	1.57	1.61
	Displacement ventilation (DV)				
Horizontal distance (m)	0.04	0.14	0.34	0.54	0.74
Height (m)	1.52	1.525	1.535	1.545	1.575
	Vertical ventilation (DWF)				
Horizontal distance (m)	0.04	0.16	0.27	0.40	0.65
Height (m)	1.525	1.545	1.56	1.575	1.60
	Vertical ventilation (UWF)				
Horizontal distance (m)	0.01	0.095	0.23	0.44	0.65
Height (m)	1.52	1.53	1.537	1.565	1.585

4.3.3 Airflow model of exhalation flows

Considering the human exhalation flow as an instantaneous non-isothermal turbulent jet, it is possible to relate its trajectory with other characteristic parameters by an equation similar to the one proposed by Baturin (1972) for steady state flow. The theory of the non-isothermal jets describes their centreline as curved. Looking at the velocity and

concentration probes positions to find the centreline of the exhalation jet, figure 4.7, it is possible to observe the different curved trajectories obtained for the different ventilation strategies, see figure 4.8.
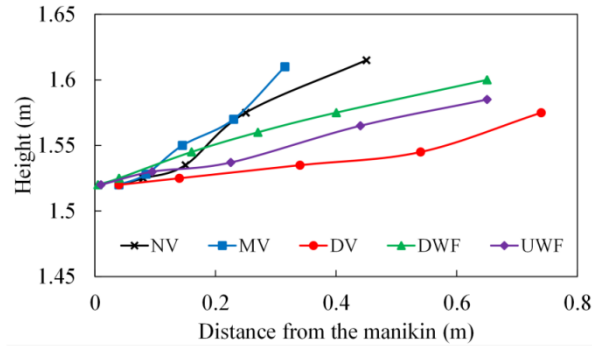
Figure 4.8 Centreline of the exhalation jets for the five ventilation principles

The Archimedes number is used to measure the motion due to density difference. Considering the exhalation flow as a non-isothermal jet with a temperature T_0 different from the temperature in the room, T_{amb}, the buoyancy can directly affect the exhalation flow. It is possible to characterize the exhalation flow by the following Archimedes number:

$$\text{Ar} = \frac{\beta \, \text{g} \, \Delta \text{T} \, \sqrt{a_0}}{\text{u}_0^2} \qquad (4.1)$$

where β, g, a_0, u_0 and ΔT are volume expansion coefficient, gravitational acceleration, mouth opening surface (123 mm^2), maximum velocity of the exhalation flow and temperature difference between the exhalation flow, T_0, and the ambience in the room, T_{amb}. T_{amb} is obtained as the average value of two temperature values given by two thermocouples placed 1.3 m and 1.7 m height at 0.40 m from the manikin.

Table 4.5 shows the temperature of the surroundings of the exhalation flow, T_{amb}, the temperature difference, ΔT, with the exhalation airflow temperature, T_0, and the corresponding Ar number obtained.

For the displacement ventilation case, the Ar number obtained is lower than for the other two cases with the same breathing function, mixing ventilation and the case without mechanical ventilation. It means that the strength of free convection is larger for the displacement ventilation case and therefore the exhalation jet projects less upward. This fact is directly related with the temperature difference, ΔT, which shows the lowest value for the displacement ventilation case. For this case, the vertical temperature stratification maintains the temperature at the height of the exhalation higher than in the rest of cases. This fact produces a lower temperature difference with the exhalation flow. The stable temperature layer generated by the displacement ventilation system at the height of the breathing maintains the exhalation flow more stable and reduces the mixing process of the exhalation flow with the surrounding air. It can make difficult for the exhalation flow to project to the upper part of the room and to entrain the surrounding air reducing the

contaminant concentration. This phenomenon will provoke a higher contaminant concentration around the height of the breathing (Bjørn and Nielsen, 2003; Li et al., 2011).

Table 4.5 Temperature data obtained for the five ventilation strategies, T_0=34 °C

Ventilation strategy	T_{amb} (°C)	ΔT (T_0-T_{amb})	Ar *10^7
Non-mechanical ventilation (NV)	22.8	11.2	9.6
Mixing ventilation (MV)	22.9	11.1	9.5
Displacement ventilation (DV)	23.6	10.4	8.9
Vertical ventilation (DWF)	22.3	11.1	6.8
Vertical ventilation (UWF)	22.9	10.7	6.5

For the mixing ventilation and without mechanical ventilation cases, the exhalation jets flow upper than in the displacement case and shows higher Ar numbers and temperature difference, ΔT. The exhalation jets are nearly the same for the two cases (with mixing and non-mechanical ventilation) which agrees with the results obtained by Liu et al., 2009.

For the vertical ventilation cases, the Ar number obtained are lower than in the displacement ventilation because of the larger value of the velocity inlet of the breathing. However, the trajectories of the exhalation jets flow slightly more upward than in the displacement ventilation case due to the higher temperature difference, ΔT.

Therefore, the penetration distance is directly affected by the temperature conditions in the surroundings of the manikin that are created by the different ventilation strategies. It is especially important the microenvironment generated around the thermal manikin since the surrounding air temperature influences the convective transport and can make the exhalation flow in different directions.

4.3.4   Velocity and concentration decay

The maximum velocity and concentration decays of the exhalation jet for each case are shown in figure 4.9. The maximum velocities at each point of the centreline are obtained as the average values of the maximum velocity values measured in the breathing during each experiment. For the concentration decay the maximum concentration value obtained during the measurements is used. The maximum velocity and concentration values along the centreline, u_x and c_x, are given as a function of the distance to the manikin´s mouth.

a)

b)

c)

d)

e)
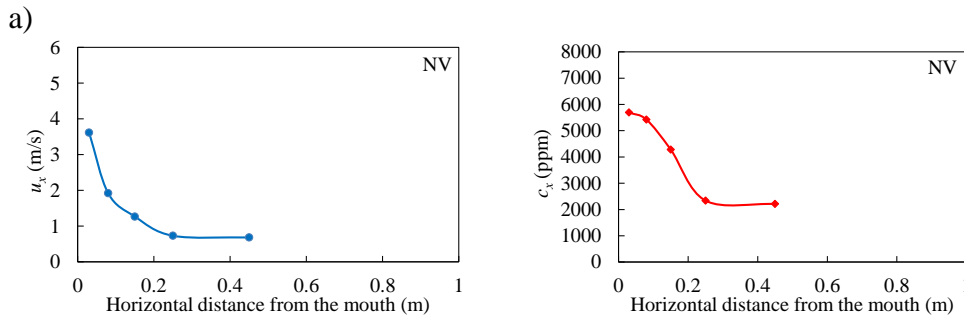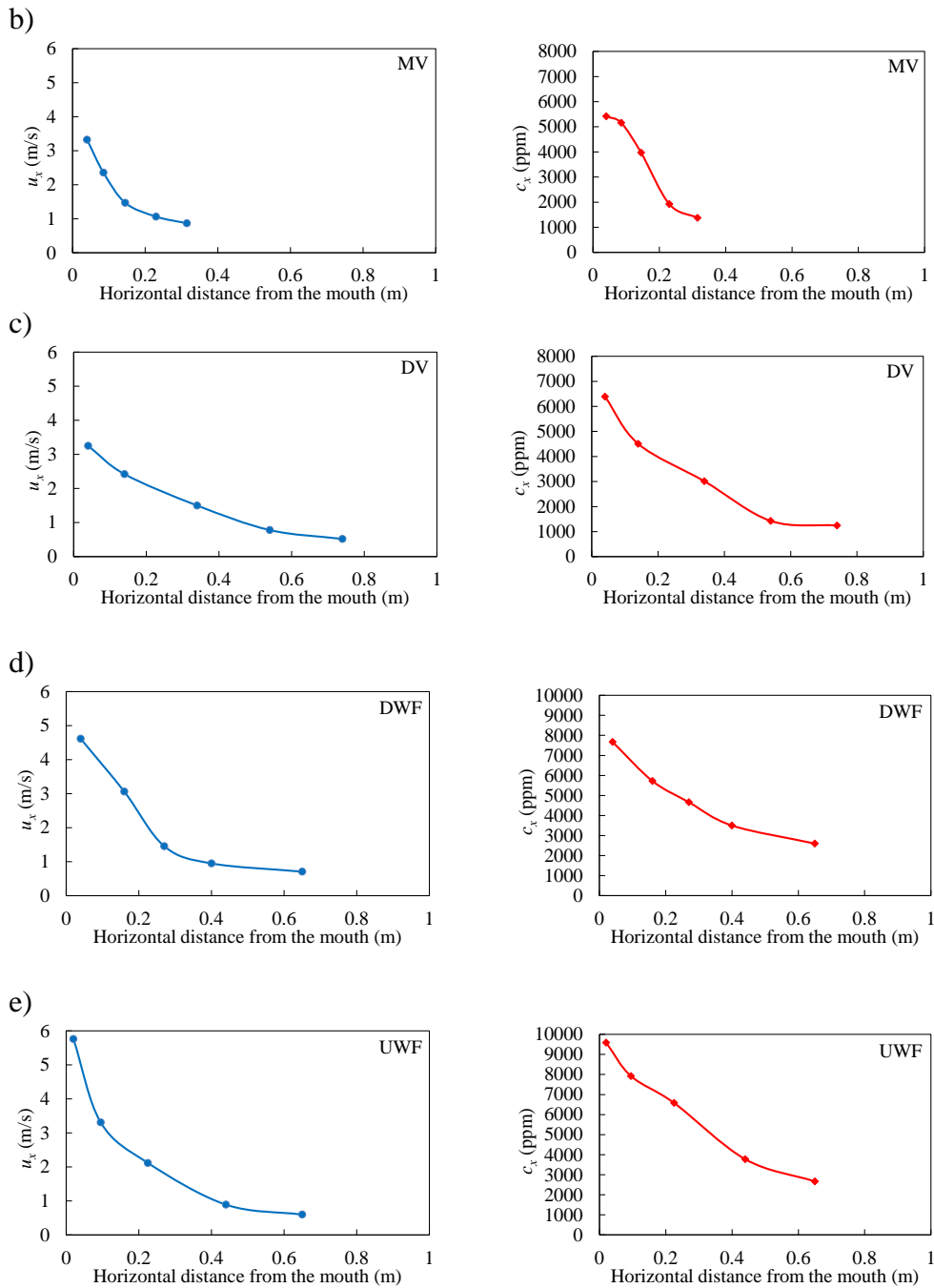
Figure 4.9 Velocity and concentration decay of the exhalation jet for the five cases studied. a) Non-mechanical ventilation, b) Mixing ventilation, c) Displacement ventilation, d) Vertical ventilation in the downward flow area, e) Vertical ventilation in the upward flow area

Nielsen et al. (2009) have shown that peak values for exhalation velocity of the instantaneous human exhalation flow can be described by an expression where the peak velocity is a linear function of the reciprocal horizontal distance from the mouth. This relation is expressed by the following equation, similar to the expression for the centreline velocity in a free jet:

$$\frac{u_x}{u_o} = K_{\exp} \cdot \left(\frac{x}{\sqrt{a_o}} \right)^{n_1} \qquad (4.2)$$

where K_{exp} is a characteristic constant, a_0 the area of the mouth, x the horizontal distance from the mouth where the measurements are taken, and u_x and u_o are the peak values of the velocity at distance x and in the mouth respectively. For the cases of Group A and B, the velocity values measured at the manikin´s mouth are 4.74 m/s and 5.76 m/s, respectively.

In the same way, peak concentration values of the samples measured during breathing are also related to positions, as shown in the following equation:

$$\frac{c_x - c_s}{c_o - c_s} = K_c \cdot \left(\frac{x}{\sqrt{a_o}} \right)^{n_2} \qquad (4.3)$$

where K_c is a characteristic constant and c_x, c_0 and c_S are peak concentration values measured at a horizontal distance x from the mouth, in the mouth and in the surroundings, respectively. The values of c_s are measured at the chest of the manikin. It is important to point out that the measured peak concentration is influenced by the measuring equipment where some averaging takes place. The concentration values at the mouth for the tests of Groups A and B are 6687 ppm and 9599 ppm, respectively.

The values of the characteristic constants and exponents, for the five cases studied, are shown in table 4.6.

Table 4.6 Characteristic velocity and concentration constants and exponents for the exhalation jets

Ventilation strategy	c_s (ppm)	K_{exp}	n_1	K_c	n_2
Non-mechanical ventilation (NV)	262	4.5	-0.66	8.5	-0.43
Mixing ventilation (MV)	47	4.5	-0.68	6.3	-0.69
Displacement ventilation (DV)	58	7.5	-0.64	10.8	-0.63
Vertical ventilation (DWF)	208	6.6	-0.70	11.6	-0.39
Vertical ventilation (UWF)	206	5.8	-0.64	12.1	-0.36

Figure 4.10 is the graphic representation of the equations (4.2) and (4.3) for the exhalation flow with the five air distribution principles. The dimensionless velocity u_x/u_0 and concentration cx-cs/c0-cs are shown as a function of the dimensionless distance x/a0 in a log-log   graph.

e)
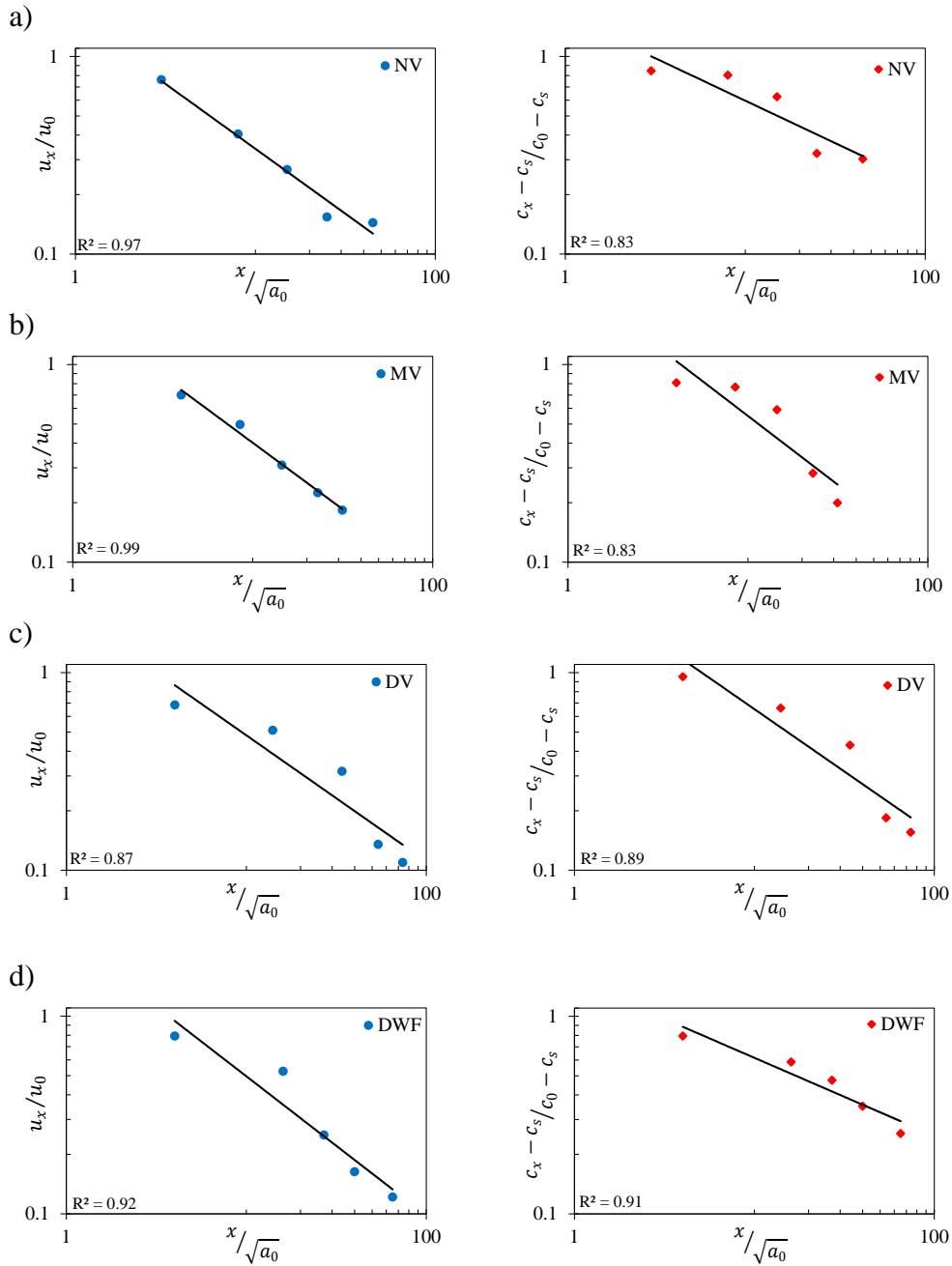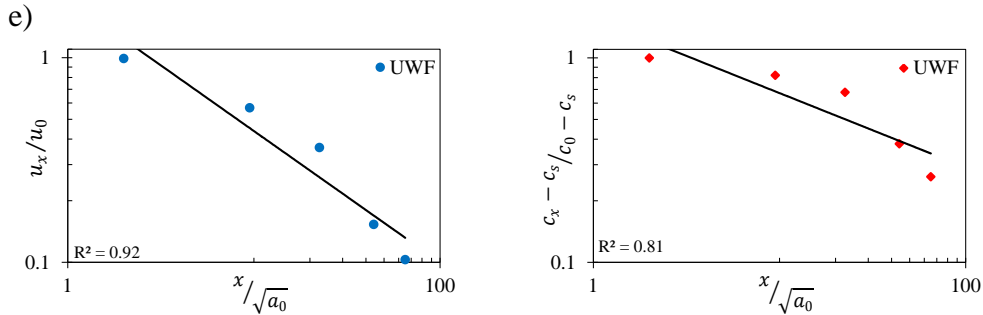
Figure 4.10 Velocity and concentration level along the centreline of the exhalation jet versus distance to the mouth in a log-log graph for the different ventilation strategies. a) non-mechanical ventilation, b) mixing ventilation, c) displacement ventilation, d) vertical ventilation with downward flow, e) vertical ventilation with upward flow

Finally, figure 4.11 compares the velocity and concentration decays obtained for the five cases studied in a log-log graph. For the velocity results, figure 4.11(a), it is possible to observe a very similar slope, in all the cases with a numeric value close to -0.65. This value is not very different from -0.5, the slope obtained for a plane free jet. However, the concentration results are less homogenous and the slope varies from case to case, see figure 4.11(b).

a)   b)
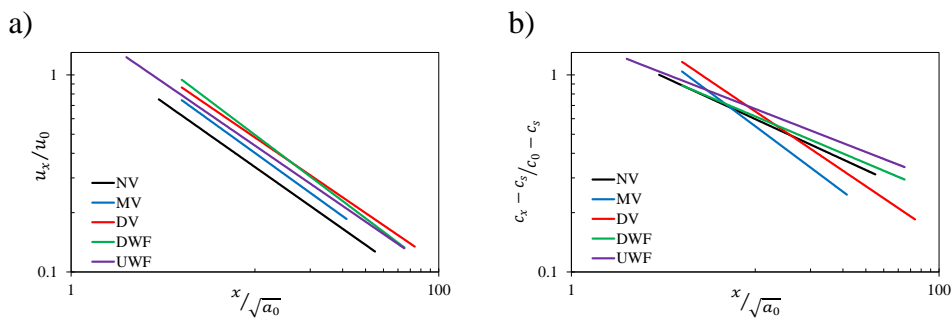
Figure 4.11 a) Comparison of the velocity decay in a log-log graph, b) Comparison of the concentration decay in a log-log graph

4.4 Conclusions

The results show that the thermal plume generated by a person influences the air quality in the breathing area. For the displacement ventilation case studied, the higher heat load released by the manikin, the higher amount of air is induced to the inhalation area by the thermal plume. Therefore the lower contaminant concentration is found in the breathing area because the displacement ventilation works with two zones in the room, a clean lower area and a contaminated upper area.

Different ventilation systems create different airflow patterns and different temperature distributions in a room. The temperature difference between the exhalation flow and the ambience directly affects the direction and penetration length of the exhalation flow. Using the same initial velocity of the breathing, the larger the temperature difference between the exhalation and the surrounding air is, the more upward the jet flows.

The maximum velocity decay and the maximum average concentration decay in the exhalation can be described by simple expressions that show the variables as proportional to the reciprocal horizontal distance from the mouth.

CHAPTER 5
Cross-infection between people in a room

When several people are placed in the same room the dispersion of exhaled contaminants can produce a risk of cross-infection between people. An infectious person can exhale airborne pollutants that are spread in the air. A susceptible healthy person placed in the same room may be exposed in a higher or lower level to the exhaled contaminants. This level of exposure depends not only on the air distribution system but also on people´s different positions, the distance between them, direction of exhalation and surrounding temperature and temperature gradient. In this chapter experimental measurements using two breathing thermal manikins and four different ventilation strategies are carried out. The main objective of this chapter is to study the key factors in indoor environments that may affect the exposure level to contaminants and therefore the risk of cross-infection. All the results are addressed in paper V and paper VI.

5.1 Evidences of cross-infection risk in indoor environments

In recent years, an interest in understanding the mechanism of airborne infection between people in the same room has increased significantly. Several studies have shown evidence that relate the ventilation systems with the distribution of contaminants and airborne transmission of diseases in rooms (Li et al., 2005; Li et al., 2007; He et al., 2005; Mui et al., 2009); Richmond-Bryant, 2009). Displacement ventilation system was supposed to be a very efficient system producing a clean area in the breathing zone of the room (He et al., 2005) and preventing the risk of cross-infection between people in a room (Gao and Niu, 2006). However, the temperature gradient may, on the other hand, result in high concentration at different heights, e.g. the breathing zone as shown by Bjørn and Nielsen (2002) and Qian et al. (2006), causing a reduced protection against the exposure to contaminants. On the other hand, Nielsen et al. (2008) showed that full mixing of the air can limit the concentration of the pollutants in the breathing zone of the exposed person. However, there are a lot of key factors that may influence the efficiency of the ventilation systems in removing contaminants in a room. Location of the exhaust and supply openings is one of the factors that directly affect the dispersion of contaminants in indoor environments. Some authors determined the influence of these factors in the spread of

contaminants in hospital wards (Nielsen, 2009; Chung and Hsu, 2001; Qian et al., 2008; Nielsen et al., 2010; Lim et al., 2010) and isolation rooms (Cheong and Phua, 2006). Woloszyn et al., 2004 also concluded that the presence of obstacles in a room will condition the airflow pattern and the contaminant distribution in a room. In the same way, the position of thermal loads and people in a room also influence the airflow patterns (Liu et al., 2009; Lee et al., 2005).

The results presented in this chapter show the results of the personal exposure between two manikins in a room with different ventilation strategies and different separation distances and relative positions between the manikins in the room. Paper V and VI address the result of the experiments.

5.2   Methods

For the experimental tests described in this chapter, two breathing thermal manikins are used. One of them is considered the infectious one, the source manikin, and the other is the one exposed to the exhaled contaminants, the target manikin. Both manikins inhale through the nose and exhale through the mouth. It is possible to find a complete description of the breathing cycles of each manikin in Chapter 2. The source manikin exhales the contaminants simulated by a tracer gas, N_2O. It has been proved by several studies (Gao and Niu, 2007; Yin et al., 2011) that the use of tracer gas is a valid way to simulate the small droplets generated by the human breathing.

The thermal conditions in the room are maintained at the same level for all the experimental tests. Each manikin is responsible of 94 W while the radiator placed in the room is responsible of 300 W. The air change rate is set at 5.6 h^{-1}.

The separation distance and relative position between the manikins and respect to the diffusers have been changed in order to gain knowledge about the influence of these key factors on the exposure level.
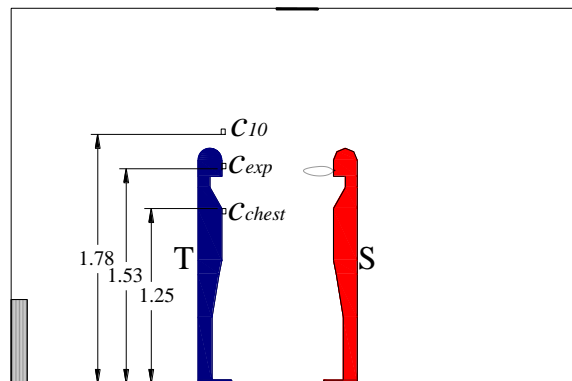
Figure 5.1 Sketch of the test room with the source (S) and the target (T) manikins and location of the concentration tubes at the chest (c_{chest}), the inhalation (c_{exp}) and above the manikin (c_{10}). The separation distance between the manikins in the pictures is 0.80 m. All measurements in meters

The results of the exposure level are shown as dimensionless values of the concentration at

different positions at the target manikin, see figure 5.1: the chest, c_{chest}, the inhalation through the nose, c_{exp}, and 0.1 m above the manikin, c_{10}. The exposure is calculated using the average concentration values in the inhalation of the target manikin divided by the exhaust concentration of the room. Using this expression a higher exposure is equivalent to a higher risk of airborne infection between the contaminated and the exposed person simulated by the source and the target manikins, respectively. This expression for the exposure is called "susceptible exposure index" by Qian and Li (2010).The exposure at the chest and above the head of the target manikin is also calculated using the average concentration at these positions divided by the exhaust concentration of the room, in order to analyze the contaminant exposure in the microenvironment around the manikin.

5.3 Two manikins within a room with displacement ventilation

5.3.1 Layout of the tests

For the tests carried out with the displacement ventilation system different relative positions of the manikins are studied. Four relative positions: face to face, face to back, face to side and with the source manikin seated are studied, see figure 5.2.

a)   b)   c)   d)
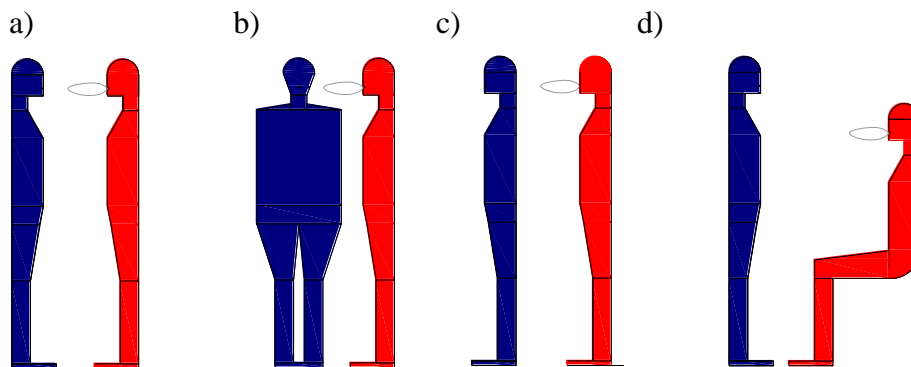
Figure 5.2 Relative positions of the manikins (source in red and target in blue) a) Manikins standing face to face, b) Manikins standing face to side, c) Manikins standing face to back, d) Source manikin seated and target manikin standing

During all the experiments, the manikins are placed along the centreline of the room in the direction of the *x* axis. The source manikin was always placed at 0.80 m from the radiator and the target manikin was moved to obtain the different separation distances: 0.35 m, 0.50 m, 0.80 m and 1.10 m, see figure 5.3. For the test with the source manikin seated, the position of the source manikin respect to the radiator was the same but the separation distances between the manikins were 0.70 and 1.10 m, owing to the geometry of the manikins. In the case with the target manikin turned 90°, face to side case, the target manikin is facing the back wall and its nose is placed at the same line of the *x* axis. The vertical temperature distribution in the room was measured with five thermocouples along

the vertical line L1 at the heights of 0.1 m, 0.6 m, 1.1 m, 1.7 m and 2.3 m, see figure 5.3. A summary of the tests carried out is shown in table 5.1.
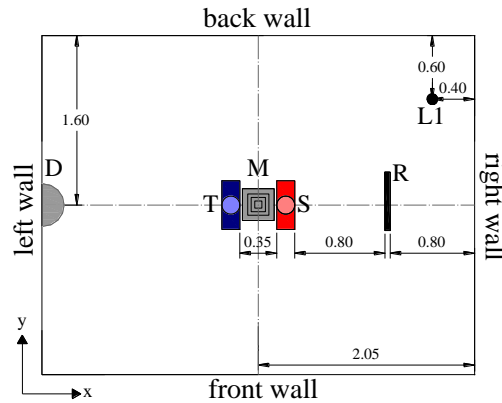
Figure 5.3 Experimental setup with the two manikins (T, target manikin; S, source manikin) for the tests with the displacement diffuser (D) and the mixing diffuser (M), vertical measuring line (L1) and radiator (R). The position of the target manikin was moved to obtain the different separation distances. All measurements in meters

Table 5.1 Experimental tests with two manikins and displacement ventilation

Test	Position of the manikins	Distance between the manikins
1	Two manikins standing face to face	a) 0.35 m
		b) 0.50 m
		c) 0.80 m
		d) 1.10 m
2	Two manikins standing face to side	a) 0.35 m
		b) 0.50 m
		c) 0.80 m
		d) 1.10 m
3	Two manikins standing back to face	a) 0.35 m
		b) 0.50 m
		c) 0.80 m
		d) 1.10 m
4	Source sitting and target standing	a) 0.70 m
		b) 1.10 m

5.3.2 Results

The vertical temperature distribution in the room along the line L1 was measured for the displacement and mixing ventilation tests. The temperature conditions maintained for each of the tests are presented in figure 5.4, where it is possible to see a typical vertical temperature gradient for the displacement ventilation case.
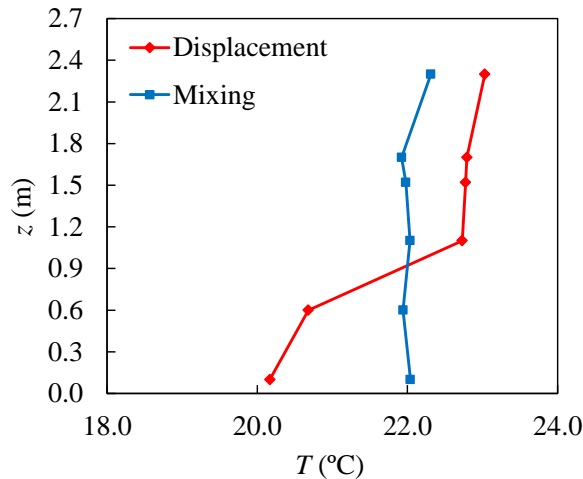
Figure 5.4 Vertical temperature distributions at L1 for the displacement and mixing ventilation tests

Figure 5.5 shows the concentration results for tests 1, 2, 3 and 4. For test 1, figure 5.5(a), which corresponds with the manikins facing each other, a clean area is maintained at the height of the chest in all the cases with an exposure level close to zero. This is typical of displacement ventilation, although the cleanest zone may be lower. Displacement ventilation can create a clean low zone, but it will also create a zone with higher concentration of exhaled contaminants because the exhalation is a weak heat source, see Li et al. (2011). This high level of concentration is shown in the exposure of the target manikin, reaching a maximum value of 12.0 at a separation distance of 0.35 m. However, this concentration exposure c_{exp}/c_R decreases as the separation distance increases.

This result is similar to the data obtained by Bjørn and Nielsen (2002) and Nielsen et al. (2008) for the face to face values, and it shows that the contaminated exhalation flow can penetrate the breathing zone of a standing person who faces the manikin, and produces an exposure level of several times the return concentration in the room. The concentration above the head of the target manikin is also high. This effect is provoked by the exhalation flow that rises due to the exhalation temperature and the temperature difference with the surrounding air.

Figure 5.5(b) shows the results for test 2, with the target manikin turned 90°. The exposure concentration c_{exp}/c_R is also high, with values very close to 7.0 and 6.0 for the separation distances of 0.35 m and 0.50 m respectively. However, the value is significantly reduced when the distance is more than 0.50 m. It is important to notice that the concentration values above the head of the target manikin are higher than the exposure values. The relative position of the target manikin may cause a different microenvironment and allow the contaminated exhalation flow to move upward above the head of the target manikin. The results close to zero at the chest height are due to the contaminant

stratification as discussed in test 1.

The target manikin has its back to the source in test 3. The results show that the exposure concentrations at all the separation distances are close to 1.0, which corresponds to a situation of fully mixed air, see figure 5.5(c). The exposure levels, and therefore the infection risk, are reduced significantly.

Personal exposure, c_{exp}/c_R, and concentration values above the target manikin, c_{10}/c_R, for test 4, which corresponds to the case with the source manikin seated, hardly vary with the distance, see figure 5.5(d) At the chest height the concentration value is directly influenced by the primary flow from the source manikin, which is exhaling the air at almost the same height as the chest, 1.23 m. When the source manikin is at 0.70 m from the target, the concentration of pollutants c_{chest}/c_R at the chest is almost 10. However, it is possible to see a significant decrease in the concentration value when the separation distance between the two manikins increases to 1.10 m. In this position, the exhaled air from the source manikin moves above chest height before reaching the chest of the target manikin.
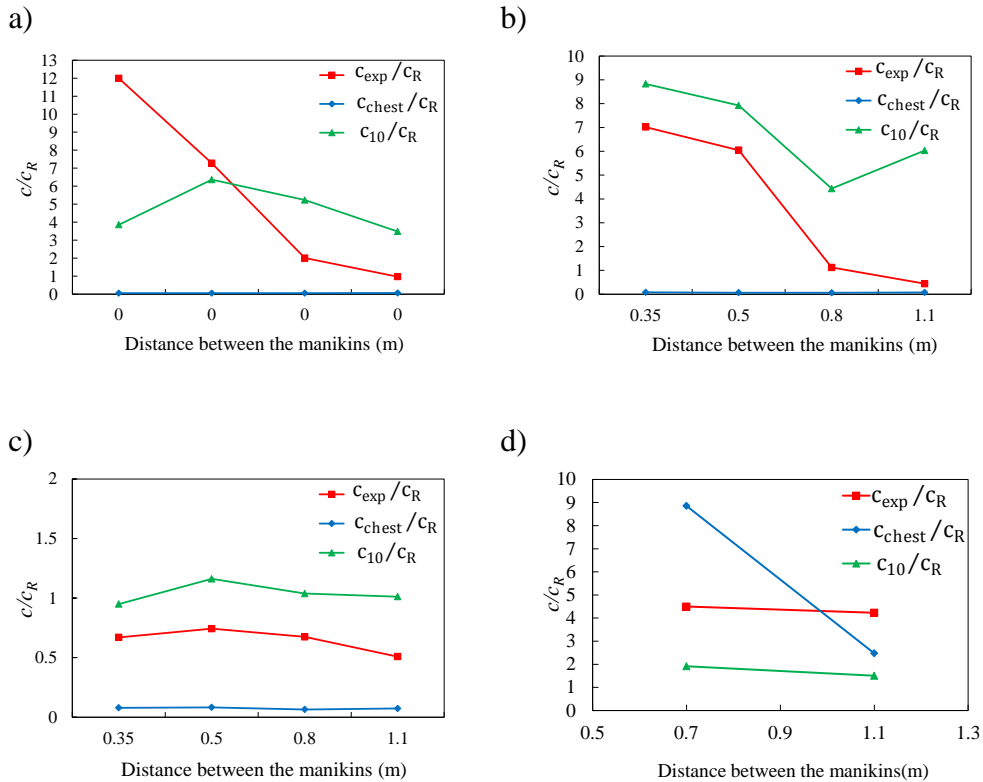
Figure 5.5 Comparison of the exposure concentration values in the inhalation (c_{exp}/c_R), the chest (c_{chest}/c_R), and above the target manikin (c_{10}/c_R) for the displacement ventilation tests a) test 1, b) test 2, c) test 3, d) test 4

5.3.3 Comparison of the personal exposure levels

Figure 5.6 shows the exposure of the target manikin, given as c_{exp}/c_R, where c_{exp} is the concentration in the target manikin´s inhalation, and c_R is the return concentration.

For the face to back situation the value of c_{exp}/c_R is ~0.5, which is due to the inhalation of the manikin from the low clean area of the room. The exposure is maintained at the same level for all the separation distances due to the lack of direct exposure from the source exhalation.

When the manikins are side to face and the separation distance is 1.10 m exposure value close to 0.5 is also obtained. However, when the distance decreases the concentration values increase significantly, reaching a maximum value close to 7.0 for the separation distance of 0.35 m.

The face to face test shows the largest exposure values. For distances lower than 0.80 m it is possible to see a remarkable increase in the direct exposure of the target manikin, due to the direct influence of the exhalation flow of the source manikin. This is a serious fact to take in consideration regarding the protection against cross-infection risk in rooms with this vertical temperature gradient.

Finally, when the source manikin is seated, the exposure value remains high, close to 5.0 for the two separation distances studied. This fact may be due to the low position of the source exhalation flow that rises to the upper part generating higher contaminant concentration level at the height of the target inhalation. A detailed description of the exhalation flow can be found in chapter 4.
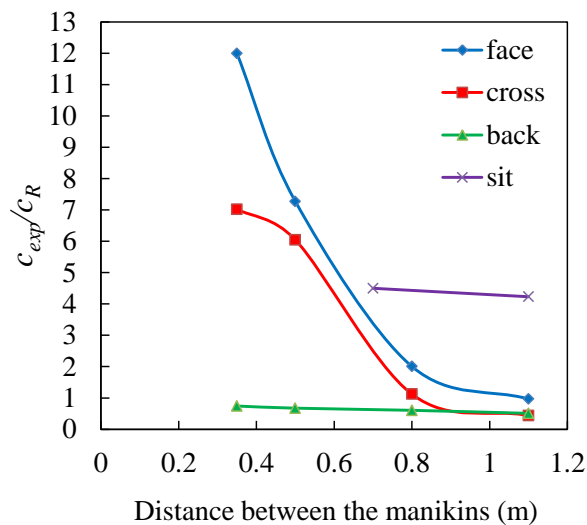
Figure 5.6 Comparison of the personal exposure obtained for the four displacement ventilation cases: face to face (face), face to side (cross), face to back (back) and with the source manikin seated (sit)

Figure 5.7 shows a comparison of the contaminant concentration data measured for the different relative positions over time and for the different separation distances.

It is possible to see that the peak values of concentration exposure are higher than the average values shown in the rest of figures. It means that the personal exposure at some

instants of time can be higher than the average values show in the rest of the graphs of this chapter.

a)

b)
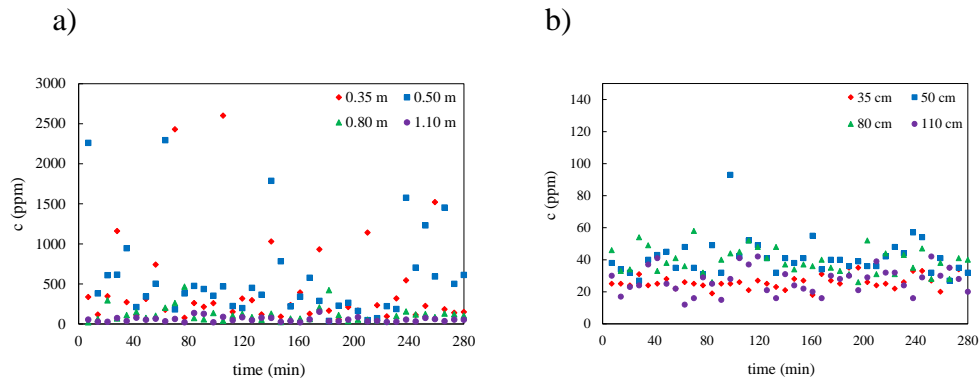
Figure 5.7 Concentration measurement over 280 minutes for two displacement ventilation tests a) test 1 (face to face), b) test 2 (face to back)

5.4 Two manikins within a room with mixing ventilation

5.4.1 Layout of the tests

For the study of the cross-infection risk between two people of the same height in a room with a mixing ventilation system, two relative positions between the manikins were studied: standing face to face and with the target manikin standing and the source manikin seated, see table 5.2. The placement of the manikins and the radiator was the same as for the displacement ventilation case see figure 5.3. The relative position of the source manikin respect to the radiator was maintained during the test while the target manikin was moved to obtain the four different separation distances: 0.35 m, 0.50 m, 0.80 m and 1.10 m.

Table 5.2 Experimental tests with two manikins and displacement ventilation

Test	Position of the manikins	Distance between the manikins
1	Two manikins standing face to face	a) 0.35 m
		b) 0.50 m
		c) 0.80 m
		d) 1.10 m
2	Source sitting and target standing	a) 0.70 m
		b) 1.10 m

The vertical temperature distribution measured in the room along the line L1 shows a typical temperature distribution of a mixing ventilation system, without any vertical gradient; see figure 5.4.

5.4.2 Results

The concentration results for tests 1 and 2 are shown in figure 5.8. For test 1, figure 5.8(a), the values of the exposure concentration, and the concentration at the chest of the target manikin, are observed to be around 1.0, which indicates a fully mixed value in the thermal plume around the target manikin and in the inhalation zone. However, although the concentration values above the head of the target manikin are around 1.0 for the largest distances, the pollution level increases when the separation distance is decreased to less than 0.80 m. This is due to a direct influence of the source manikin´s exhalation flow in this area, especially when the separation distance is 0.35 m, where it is possible to observe a maximum value close to 1.4. These results agree with the observed location of the breathing flow profile in the mixing ventilation case, see chapter 4.

For test 2, see figure 5.8(b), the concentration results show values very close to 1.0 for all the separation distances, typical of a fully mixing case. A separation distance of 0.70 m between the manikins is enough to dilute the contaminants of the exhalation flow generating concentration values close to 1.0 at all the positions around the target manikin, the chest (c_{chest}/c_R), the inhalation (c_{exp}/c_R) and above the head (c_{10}/c_R).

a)   b)
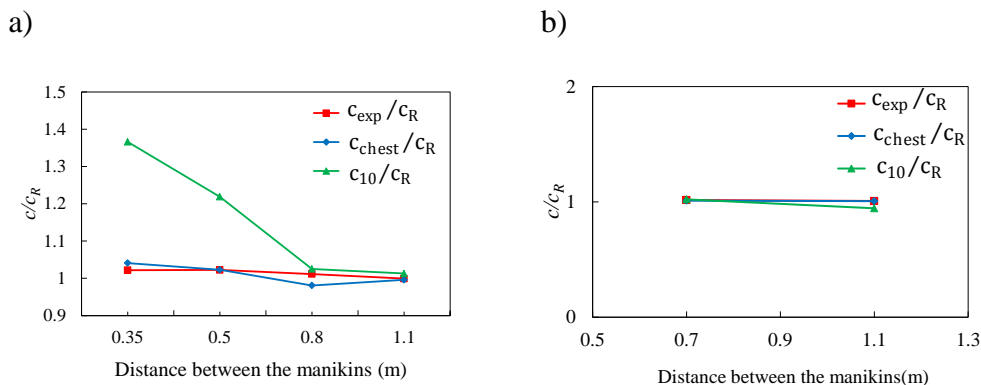
Figure 5.8 Comparison of the exposure concentration values in the inhalation (c_{exp}/c_R), the chest (c_{chest}/c_R), and above the target manikin (c_{10}/c_R) for the mixing ventilation tests a) test 1, b) test 2

5.5 Two manikins within a room without mechanical ventilation

Experimental tests with the manikins standing and facing each other in the room with no mechanical ventilation system were carried out. The placement of the manikins was the same than in the mixing and displacement ventilation cases, and the separation distances between them were: 0.35 m, 0.50 m, 0.80 m and 1.10 m.

The steady state conditions are, in this case, maintained by having an open door between

the laboratory and the test room. The temperature in the laboratory is maintained at 22±1°C by a radiator based heating system. The volume and size of the laboratory ensure the steady state conditions during the measuring period.
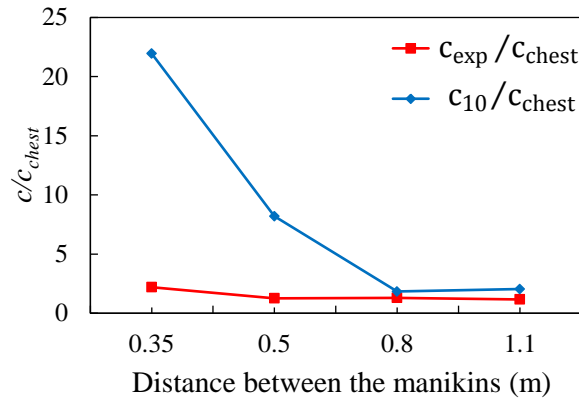
Figure 5.9 Comparison of the exposure concentration values in the inhalation (c_{exp}/c_{chest}) and above the target manikin (c_{10}/c_{chest})

As there is no ventilation with return flow, the concentrations in the inhalation area and above the head of the target manikin have been compared to the concentration of the air at the chest of the target manikin. The exposure concentration values c_{exp}/c_{chest} are kept around 1.0, except for the case with the smaller separation distance where the value obtained is 2.2, as is shown in figure 5.9. However, it is possible to see much higher values of gas concentration above the head of the manikin, especially at distances of 0.50 m and 0.35 m. The behaviour of the airflow in the room is controlled by convective flows and the boundary layers of the manikins. Because of that, a concentration of pollutants from the exhalation flow of the source manikin is built up above the head of the target manikin, and the exhalation flow will influence the measurements when the separation distance is reduced.

5.6 Two manikins within a room with low velocity vertical ventilation

5.6.1 Layout of the tests

This study consists of three experimental tests summarized in table 5.3, where different conditions in the room are changed. For tests 1 and 2, the manikins are placed in the downward flow area generated by the textile diffuser, while for the test 3 the manikins are placed in the upward flow area generated by the diffusers. The placement of the manikins for each test is shown in figure 5.10.

Table 5.3 Experimental tests with two manikins and low-impulse velocity ventilation

Test	Sketch of the manikins in the room	Distance between the manikins
1		a) 0.35 m b) 0.50 m c) 0.80 m d) 1.10 m
2		a) 0.35 m b) 0.50 m c) 1.10 m
3		a) 0.35 m b) 0.50 m c) 0.80 m d) 1.10 m

Figures in table 5.3 show the textile diffusers, the circular exhaust opening, the radiator, the source manikin (in red) and the target manikin exposed to the contaminants (in blue).

Four additional cases were carried out in the room and the results are addressed in paper VI. This section only describes the three more significant ones.
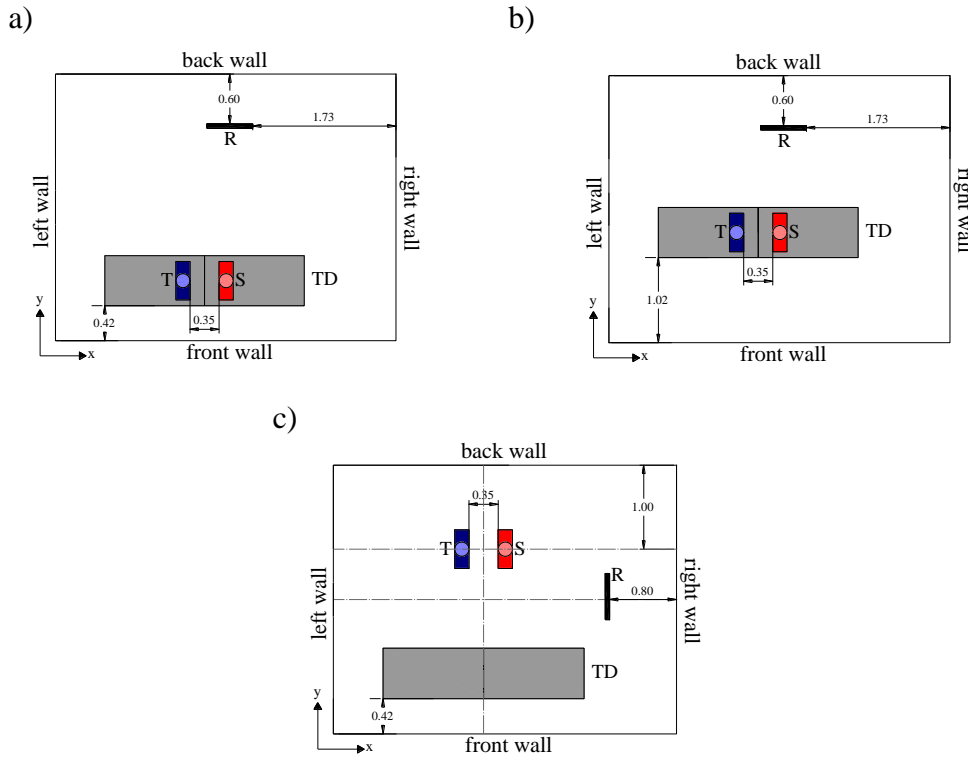
Figure 5.10 Layout of the room with the radiator (R), target manikin (T), source manikin (S) and textile diffuser (TD), a) test 1, b) test 2, c) test 3 (The distance between the manikins changed for the different tests)

5.6.2 Results

The results of the personal exposure, c_{exp}/c_R, and contaminant concentration at the chest, c_{chest}/c_R, and above the target manikin, c_{10}/c_R, for the different tests are shown in figure 5.11. Figure 5.11(a) shows a high exposure value, close to 6.0, for a distance of 0.35 m between the manikins. This may be due to the micro-environment generated by the manikins and observed with smoke visualization. More details about the micro-environment can be found in paper VI. The thermal plume of the two manikin at this short distance generate a significant upward flow that makes it difficult for the clean, supplied air to entrain the air between the manikins, reducing the mixing process. This phenomenon allows the contaminated exhalation flow from the source to penetrate the breathing area of the target manikin. The exposure decreases when the separation distance increases, as was found in the displacement ventilation tests. The concentration above the target manikin is maintained very low at all the distances due to the direct influence of the clean air from the diffuser. At the chest, the contaminant concentration is low and close to 1.0. For the separation distances of 0.35 m and 0.50 m the increase of the concentration values may be due to the

lack of influence of the air from the diffuser that also produces a high exposure.

a)

b)

c)
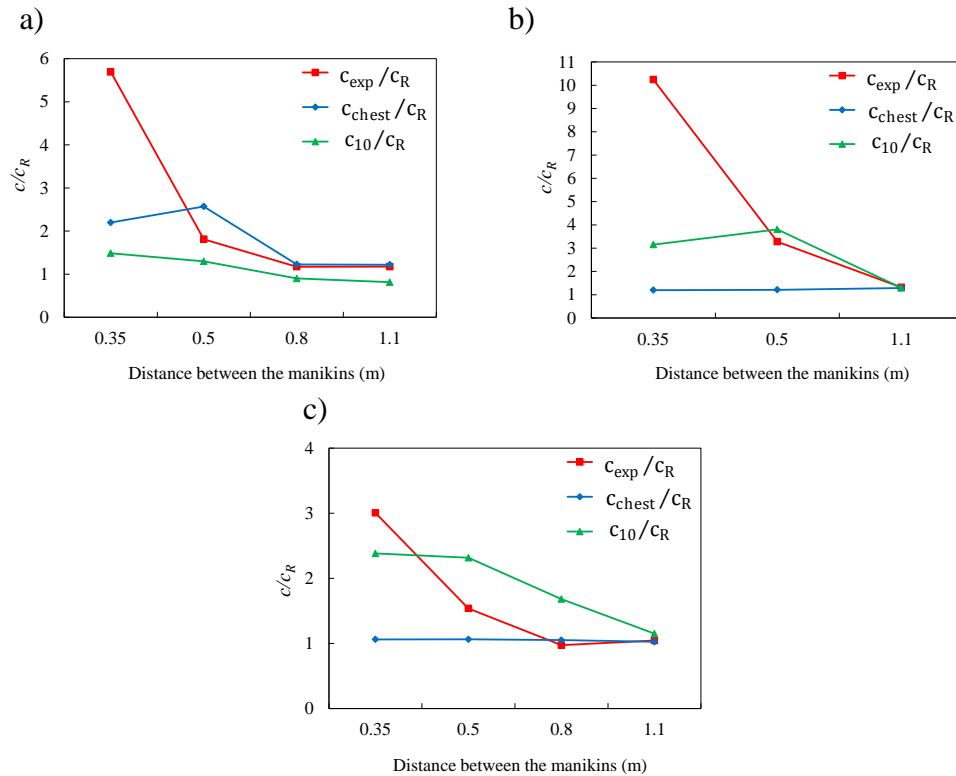
Figure 5.11 Comparison of the exposure concentration values in the inhalation (c_{exp}/c_R), the chest (c_{chest}/c_R), and above the target manikin (c_{10}/c_R) for the low-velocity vertical ventilation tests a) test 1, b) test 2, c) test 3

For test 2, the personal exposure values are significantly high, while the contaminant concentration at the height of the chest shows a value close to 1.0 for all the separation distances, see figure 5.11(b) This phenomenon may be due to the upward flow generated by the thermal plumes of the manikins, which deflect the clean, supplied air around the manikins and induce it to the upper part. In this way, the height of the chest is maintained clean and higher concentration values are found at the inhalation and above the manikin. The contaminant concentration in the inhalation of the target manikin is also directly influenced by the exhalation flow of the source manikin for a distance of 0.35 m.

It is important to notice the influence that the parallel wall close to the diffusers may have on the personal exposure. For test 1, the personal exposure values are lower than for test 2. This may be due to the influence of the wall that drives the downward flow generated by the diffuser close to the manikins and help to create a mixing process in the breathing area. A Coanda effect generated by this wall has been visualized with smoke and can be found in chapter 3.

Test 3 shows the results for the test where the two manikins are placed in the upward flow area of the room, see figure 5.11(c). The results show that c_{chest}/c_R is kept close to 1.0 at all the separation distances. The personal exposure, c_{exp}/c_R, is also kept close to 1.0 when the manikins are separated 0.80 m and 1.10 m. However, this value increases significantly

for 0.50 m and reaches a maximum value of 3.0 for 0.35 m. This maximum value is due, like in the rest of the cases, to the direct influence of the source exhalation flow that penetrates into in the breathing area of the target manikin at this short distance, increasing the level of contaminants, even when the dominating airflow is upward. However, the personal exposure is lower than for the two downward cases studied, test 1 and 2. It is especially surprising that the protection from cross infection is larger in this area outside the vertical downward flow below the ceiling mounted diffuser. The measurements support the theory that upward or downward flow around the manikins has a strong influence on the exposure of the target manikin and it is a question on the deflection of the exhalation and an influence of the temperature difference. Experiments with manikins of different heights show a similar problem, namely the importance of the target manikin´s location in the exhalation flow of the source manikin, Liu et al. (2010).

The contaminant concentration above the target manikin, c_{10}/c_R, are the maximum value obtained in tests with a separation distance of 0.50 m, 0.80 m and 1.10 m. For a distance of 0.35 m reaches a maximum value, close to 2.5. The high values produced at this location are due to the upward flow generated by the room air flow and the exhalation flow. Contaminants rise to the upper part of the room, keeping the chest and breathing area free of contaminants.

5.7 Comparison of the results for the different ventilation strategies

The relation between the personal exposure to exhaled contaminants and different ventilation strategies (local temperature distributions) in a room has been analyzed. Figure 5.12 compares the exposure of the target manikin with the different ventilation systems.
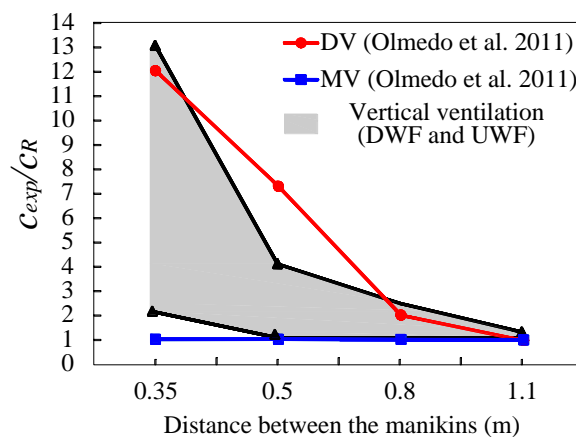
Figure 5.12 Comparison of the personal exposure concentration values for the different ventilation systems studied: displacement ventilation (DV), mixing ventilation (MV) and low-velocity vertical ventilation (grey area)

The distance between the two thermal manikins used to simulate two standing people in a room has been varied. The separation distance has been found to be a key factor in the risk of cross-infection between two people (both exhaling through the mouth). For all the

ventilation strategies used, a separation distance higher than 0.8 m decreases significantly the personal exposure of the target manikin.

The displacement ventilation system produces a large contaminant concentration at the height of the breathing provoked by the "lock-up phenomenon". The vertical thermal stratification generated by this kind of systems maintains the exhaled contaminants trapped at the height of the breathing zone. This fact produces a high risk of airborne cross-infection to the target manikin, which is significantly high at distances lower than 0.8 m.

However the mixing ventilation maintains a more stable contaminant concentration in the breathing area of the target manikin for all the separation distances. The mixing process and the temperature difference produce a dilution and a direction of the exhaled contaminants in the air that maintains the personal exposure at lower levels irrespective of the distance between the manikins.

Finally, the downward flow ventilation is supposed to create a protection against the airborne cross-infection to the target manikin. However, the results show that the thermal plumes created by the thermal manikins disturb the downward flow and can induce a mixing process in the room. The personal exposure varies in a wide range for the different cases studied, which show that the layout of the room and the relative position of people is a factor to take into account if the risk of airborne cross-infection wants to be reduced.

CHAPTER 6
Conclusions and future work

Following are the conclusions and proposals for future work that are deduced from the research made within this thesis.

The human exhalation flow and the dispersion of exhaled contaminants in a room have been analyzed using different ventilation strategies: displacement ventilation, mixing ventilation, non-mechanical ventilation and low-velocity vertical ventilation.

The different air distribution systems create a different micro-environment around the thermal manikin and especially around its breathing area. This fact makes the exhalation flows with different trajectories for the different ventilation systems. The vertical temperature gradient connected to a displacement ventilation system retains the exhalation at head height of surrounding persons, while mixing ventilation allows the exhalation to rise above head height due to temperature difference between exhalation and the surrounding air. This temperature difference is directly connected to the direction of the exhalation flow.

The exhalation flow can be described by simple expressions, using the peak velocity and peak mean concentration values, which show these variables as proportional to the reciprocal horizontal distance from the mouth.

Experiments with cross infection risk between two persons (source manikin and target manikin) show that the air distribution systems and especially the microenvironment they create are of importance to the exhalation flow between the manikins.

The relative positions as well as the separation distance between the manikins have been found to be key factors in order to reduce the risk of airborne cross-infection between people in a room. For a downward ventilation system it is also important the relative position of the people respect to the diffuser as well as the layout of the room.

Neither the displacement ventilation nor the downward ventilation systems produce any special protection to cross-infection when the separation distance between people (manikins) is lower than 0.80 m.

The possibility of realizing numerical simulations to study the airborne route of cross-infection between people in a room would be a very powerful tool. This offers many possibilities for the study of airflow patterns and dispersion of exhaled contaminants. Many parameters that may influence the risk of airborne cross-infection in a room should be taken into account in future works with numerical or experimental results, such as: breathing functions, difference in heights of people, number of people in a room, activity level of persons or air velocity and turbulence level in the micro-environment around the persons.

Bibliography

Badeau, A., Afshari, A., Goldsmith, T. and Frazer, D. (2002) Preliminary prediction of flow and particle concentration produced from natural human cough dispersion, *Proceedings of the Second Joint EMBS/BMES Conference*, Houston, USA , 23-26.

Baturin, V.V. (1972) *Fundamentals of Industrial Ventilation*, Oxford, New York, Pergamon Press.

Bjørn, E. (1999) Simulation of human respiration with breathing thermal manikin, *Proceedings of Third International Meeting on Thermal Manikin Testing*, Stockholm, Sweden, National Institute for Working Life, 78-81.

Bjørn, E. and Nielsen, P.V. (2002) Dispersal of exhaled air and personal exposure in displacement ventilated room, *Indoor Air*, **12**, 147-164.

Brohus, H. and Nielsen, P.V. (1996) Personal exposure in displacement ventilated rooms, *Indoor Air*, **6**, 157-167.

CDC (2003) *Guidelines for Environmental Infection Control in Health-Care facilities*, USA, U.S. Department of health and human services centers for disease control and prevention (CDC).

CDC (2005) *Guidelines for preventing the transmission of Mycobacterium tuberculosis in Health-Care Settings*, USA, U.S. Department of health and human services centers for disease control and prevention (CDC).

Chao, C. Y. H., Wan, M. P. and Sze To, G. N. (2008) Transport and removal of expiratory droplets in hospital ward environment, *Aerosol. Sci. Technol.*, **42**(5), 377-394.

Chao, C. Y. H., Wan, M. P., Morawska, L., Johnson, G. R., Ristovski, Z. D., Hargreaves, M., Mengersen, K., Corbett, S., Li, Y., Xie, X. and Katoshevski, D. (2009) Characterization of expiration air jets and droplet size distributions immediately at the mouth opening, *J. Aerosol Sci.*, **40**, 122-133.

Chen, Q., and Moser, A. (1991) Simulation of a multiple-nozzle diffuser, *Proc. of 12th AIVC Conference*, **2**, 1-14.

Chen, C., Zhao, B., Cui, W., Dong, L., An, N. and Ouyang, X. (2010) The effectiveness of an air cleaner in controlling droplet/aerosol particle dispersion emitted from a patient´s mouth in the indoor environment of dental clinics, *J.R. Soc. Interface,* **7**, 1105-1118.

Chen, C. and Zhao, B. (2010) Some questions on dispersion of human exhaled droplets in ventilation room: answers from numerical investigation, *Indoor Air,* **20**, 95-111.

Cheong, K.W.D. and Phua, S.Y. (2006) Development of ventilation design strategy for effective removal of pollutant in the isolation room of a hospital, *Build. Environ.*, **41**, 1161–1170.

Chow, T.T. and Yang, X.Y. (2004) Ventilation performance in operating theatres against airborne infection: review of research activities and practical guidance, *J. Hosp. Infect.*, **56**, 85–92.

Chung, K.C. and Hsu, S.P. (2001) Effect of ventilation pattern on room air and contaminant distribution, *Build. Environ*., **36**(9), 989-998.

Clark, R.P. and Edholm, O.G. (1985) Man and his thermal environment, London, E. Arnold Publishing Co.

Craven, B.A. and Settles, G.S. (2006) A computational and experimental iinvestigation of the human thermal plume, J. Fluids Eng., 128(6), 1251-1259.

Effros, R. M., Wahlen, K. and Bosbous, M. (2002) Dilution of respiratory solutes on exhaled condensates, *Am. J. Resp. Crit. Care,* **165**, 663-669.

Einberg, G. and Hagstrom, K. (2005) CFD modelling of an industrial air diffuser - predicting velocity and temperature in the near zone. *Build. Environ*., **40**(5), 601-615.

Gao, N. and Niu, J. (2006) Transient CFD simulation of the respiration process and inter-person exposure assessment, *Build. Environ.*, **41**, 1214-1222.

Gao, N. and Niu, J. (2007) Modeling particle dispersion and deposition in indoor environments, *Build. Environ.*, **41**, 3862–3876.

Gupta, J.K., Lin, C. and Chen, Q. (2009) Flow dynamics and characterization of a cough, *Indoor Air,* **19**, 517-525.

Gupta, J.K., Lin, C. and Chen, Q. (2010) Characterizing exhaled airflow from breathing and talking, *Indoor Air,* **20**, 31-39.

Hayashi, T., Ishizu, Y., Kato, S. and Murakami, S. (2002) CFD analysis on characteristics of contaminated indoor air ventilation and its application in the evaluation of the effects of contaminant inhalation by a human occupant, *Build. Environ.*, **37**, 219-230.

He, G., Yang, X. and Srebric, J. (2005) Removal of contaminants released from room surfaces by displacement and mixing ventilation: modeling and validation, *Indoor Air*, **15**, 367-380.

Huo, Y. and Haghighat, F. (2000) A systematic approach to describe the air terminal device CFD simulation for room air distribution analysis, *Build. Environ.*, **35**(6), 563-576.

Jensen, R.L., Pedersen, D.N., Nielsen, P.V. and Topp. C. (2001) Personal exposure between people in a mixing ventilated room, *Proceedings of the 4th International Conference on Indoor Air Quality, Ventilation & Energy Conservation* I: 33–40. Hunan University.

Jiang, Z., Chen, Q. and Moser, A. (1992) Comparison of Displacement and Mixing Diffusers, *Indoor Air,* **2**, 168–179.

Koskela, H. (2004) Momentum source model for CFD - simulation of nozzle duct air diffuser, *Energ. Buildings*, **36,** 1011-1020.

Lee, E., Khan, J.A., Feigley, C.E., Ahmed, M.R. and Hussey, J.R. (2007) An investigation of air inlet types in mixing ventilation, *Build. Environ.*, **42**, 1089-1098.

Li, Y., Yu, I.T.S., Xu, P., Lee, J.H.W., Wong, T.W., Ooi P.L. and Sleigh A.C. (2004) Predicting super spreading events during the 2003 Sever Acute Respiratory Syndrome epidemics in Hong Kong and Singapore, *Am. J. Epidemiol.*, **160**(8), 719-728.

Li, Y., Huang, X., Yu, I.T.S., Wong, T.W. and Qian, H. (2004) Role of air distribution in SARS transmission during largest nosocomial outbreak in Hong Kong, *Indoor Air,* **15**, 83-95.

Li, Y., Leung, G.M., Tang, J.W., Yang, X., Chao, C.Y.H., Lin, J.Z., Lu, J.W., Nielsen, P.V., Niu, J., Qian, H., Sleigh, A.C., Su, H.-J.J., Sundell, J., Wong, T.W. and Yuen, P.L. (2007) Role of ventilation in airborne transmission of infectious agents in the built environment - a multidisciplinary systematic review, *Indoor Air*, **17**, 2-18.

Li, Y., Nielsen, P.V. and Sandberg, M. (2011) Displacement ventilation in hospital environments, *Ashrae J.,* **53**(6), 86-88.

Lim, T., Cho, J. and Kim, B.S. (2010) The predictions of infection risk of indoor airborne transmission of diseases in high-rise hospitals: tracer gas simulation, *Energ. Buildings,* **42**, 1172–1181.

Liu, L., Li, Y., Nielsen, P.V., Jensen, R.L., Litewnicki and M. and Zajas, J. (2009) An experimental study of human exhalation during breathing and coughing in a mixing ventilated room, *Proc. 9th Int. Conf. Healthy Buildings*, Syracuse, NY, USA.

Liu, J., Wang, H. and Wen, W. (2009) Numerical simulation on a horizontal airflow for airborne particles control in hospital operating room, *Build. Environ.*, **44**, 2284-2289.

Liu, L., Li, Y., Nielsen, P.V. and Jensen, R.L. (2010) An experimental study of exhaled substance exposure between two standing manikins, *Proceedings of 16th ASHRAE IAQ Conference,* Kuala Lumpur, Malaysia.

Morawska, L. (2006) Droplet fate in indoor environments, or can we prevent the spread of infection?, *Indoor Air*, **16**, 335-347.

Morawska, L., Johnson, G.R., Ristovski, Z.D., Hargreaves, M., Mengersen, K., Corbett, S., Chao, C.Y.H., Li ,Y. and Katoshevski, D. (2009) Size distribution and sites of origin of droplets expelled from the human respiratory tract during expiratory activities, *J. Aerosol Sci.*, **40**, 256-269.

Mui, K.W., Wonga, L.T., Wu, C.L. and Lai, A.C.K. (2009) Numerical modeling of exhaled droplet nuclei dispersion and mixing in indoor environments, *J. Hazardous Materials*, **167**, 736-744.

Murakami, S. (2004) Analysis and design of micro-climate around the human body with respiration by CFD, *Indoor Air*, **14**(7), 144–156.

Nicas, M., Nazaroff, W.W. and Hubbard, A. (2005) Toward understanding the risk of secondary airborne infection: Emission of respirable pathogens, *J. Occup. Environ. Hyg.,* **2**, 143-154.

Nielsen, P.V. (1995) Lecture notes on mixing ventilation, Department of Building Technology and Structural Engineering, Aalborg University, Aalborg, Denmark.

Nielsen P.V. (1997a) The box method – a practical procedure for introduction of an air terminal device in CFD calculation. Department of Building Technology and Structural Engineering, Aalborg University, Aalborg, Denmark.

Nielsen, P.V. (1997b) The prescribed velocity method - A practical procedure for introduction of an air terminal device in CFD calculation. Department of Building Technology and Structural Engineering, Aalborg University, Aalborg, Denmark.

Nielsen, P.V. (2000) Velocity distribution in a room ventilated by displacement ventilation and wall-mounted air terminal devices, *Energ. Buildings*, **31**, 179–187.

Nielsen, P.V. (2007) Analysis and design of room air distribution systems. *HVAC&R. Res.*, **13**(6), 987-997.

Nielsen, P.V., Bartholomaeussen, N.M., Jakubowska, E., Jiang, H., Jonsson, O.T., Krawiecka, K., Mierzejewski, A., Thomas, S.J., Trampczynska, K., Polak, M. and Soennichsen, M. (2007) Chair with integrated personalized ventilation for minimizing cross infection, *Proceedings of 10th International Conference on Air Distribution in Rooms*, Helsinki, Finland.

Nielsen, P.V., Buus, M., Winther, F.V. and Thilageswaran, M. (2008) Contaminant flow in the microenvironment between people under different ventilation conditions, *ASHRAE Trans.*, **114**, part 2.

Nielsen, P.V. (2009) Control of airborne infectious diseases in ventilated spaces, *J.R. Soc. Interface*, **6**, 747-755.

Nielsen, P.V., Jensen, R.L., Litewnicki and M. and Zajas, J. (2009) Experiments on the microenvironment and breathing of a person in isothermal and stratified surroundings, *Proc. 9th Int. Conf. Healthy Buildings*, Syracuse, NY, USA.

Nielsen, P.V., Li, Y., Buus, M. and Winther, F.V. (2010) Risk of cross-infection in a hospital ward with downward ventilation, *Build. Environ.*, **45**, 2008–2014.

Nielsen, P.V., Olmedo, I., Ruiz de Adana, M., Grzelecki, P. and Jensen R.L. (2011) Airborne cross infection between two people in a displacement ventilated room, *Int. J. HVAC & R Res.* (in press).

Olmedo, I., Nielsen, P.V., Ruiz de Adana, M., Jensen, R.L. and Grzelecki, P. (2011) Distribution of exhaled contaminants and personal exposure in a room using three different air distribution strategies, *Indoor Air*, doi: 10.1111/j.1600-0668.2011.00736.x.

Qian, H., Li, Y., Nielsen, P.V., Hyldgaard, C.E., Wong, T.W. and Chwang, A.T.Y. (2006) Dispersion of exhaled droplet nuclei in a two-bed hospital ward with three different ventilation systems, *Indoor Air*, **16**, 111-128.

Qian, H., Li, Y., Nielsen, P.V. and Hyldgaard, C.E. (2008) Dispersion of exhalation pollutants in a two-bed hospital ward with a downward ventilation system. *Build. Environ.*, **43**, 344–354.

Qian, H. and Li, Y. (2010) Removal of exhaled particles by ventilation and deposition in a multibed airborne infection isolation room. *Indoor Air*, **20**, 284-297.

Richmond-Bryant, J. (2009) Transport of exhaled particulate matter in airborne infection isolation rooms, *Build. Environ.,* **44**, 44–55.

Roy, C.J and Milton, D.K. (2004) Airborne Transmission of communicable infection — The elusive pathway, *New Engl. J. Med.,* **350**(17), 1710-1712.

Schwarz, K., Biller, H., Windt, H., Koch, W. and Hohlfeld J.M. (2010) Characterization of exhaled particles from the healthy human lung — A systematic analysis in relation to pulmonary function variables, *J. Aerosol Med.*, **23**(6), 371-379.

Srebric, J. and Chen, Q. (2002) Simplified numerical models for complex air supply diffusers, *HVAC&R. Res.*, **8**(3), 277-294.

Srebric, J., Vukovica, V., He, G. and Yang, X. (2008) CFD boundary conditions for contaminant dispersion, heat transfer and airflow simulations around human occupants in indoor environments, *Build. Environ.*, **43**, 294-303.

Tang, J., Liebner, T., Brent, C. and Gary, S. (2009) A schlieren optical study of the human cough with and without wearing a mask for aerosol infection control, *J.R. Soc. Interface,* **6**, 727-736.

Tang, J.W., Noakes, C.J., Nielsen, P.V., Eames, I., Nicolle, A., Li, Y. and Settles, G.S. (2011) Observing and quantifying airflows in the infection control of aerosol - and airborne-transmitted diseases: an overview of approaches, *J. Hosp. Infect.,* **77**, 213-222.

Wan, M. P. and Chao, C. Y. H. (2007) Transport characteristics of expiratory droplet nuclei in indoor environments with different ventilation airflow patterns, *J. Biomech. Eng.*, **129**, 341-353.

Wan, M.P., Sze To, G. N., Chao, C. Y. H., Fang, L., and Melikov, A. (2009) Modeling the fate of expiratory aerosols and the associated infection risk in an aircraft cabin environment. *Aerosol Sci. Tech*., **43**, 322-343.

Wells, W.F. (1934) On air-borne infection. Study II. Droplets and droplet nuclei, *Am. J. Hyg.*, **20**, 611–618.

Woloszyn, M, Virgone, J. and Mélen, S. (2004) Diagonal air-distribution system for operating rooms: experiment and modeling, *Build. Environ.*, **39**, 1171-1178.

Xie, X., Li, Y., Chwang, A.T.Y., Ho, P.L. and Seto, W.H. (2007) How far droplets can move in indoor environments – revisiting the Wells evaporation-falling curve, *Indoor Air*, **17**, 221–225.

Yang, Y., Sze-To, G.N. and Chao, C.Y.H. (2011) Estimation of the aerodynamic sizes of single bacterium-laden expiratory aerosols using stochastic modeling with experimental validation*, Aerosol. Sci. Technol*., **46**(1), 1-12.

Yin, Y., Gupta, J.K., Zhang, X., Liu, J. and Chen Q. (2011) Distributions of respiratory contaminants from a patient with different postures and exhaling modes in a single - bed inpatient room, *Build. Environ.*, **46**(1), 75-81.

Yu, I.T.S., Li, Y., Wong, T.W., Tam, W., Phil., M., Chan, A.T., Lee, J.H.W., Leung D.Y.C. and Ho, T. (2004) Evidence of airborne transmission of the Severe Acute Respiratory Syndrome virus, *New Engl. J. Med.*, **350**(17), 1731-1739.

Zhao, B., Zhang, Z. and Li, X (2005) Numerical study of the transport of droplets or particles generated by respiratory system indoors, *Build. Environ.*, **40**, 1032-1039

Zhu, S., Kato, S., Murakami, S. and Hayashi, T. (2005) Study on inhalation region by means of CFD analysis and experiment, *Build. Environ.*, **40**, 1329–1336.

Zhu, K., Kato, S. and Yang, J. (2006a) Investigation into airborne transport characteristics of airflow due to coughing in a stagnant indoor environment, *ASHRAE Trans*., **112**(2), 123-133.

Zhu, K., Kato, S. and Yang, J. (2006b) Study on transport characteristics of saliva droplets produced by coughing in a calm indoor environment, *Build. Environ.,* **41**, 1691–1702.

Zhu, K. and Kato, S. (2006) Investigating how viruses are transmitted by coughing, *ASHRAE IAQ Applications*, **7**, 3-6.

Zukowska, D., Melikov, A. and Popiolek, Z. (2008) Impact of thermal plumes generated by occupant simulators with different complexity of body geometry on airflow pattern in rooms, *Proc. 7th Int. Thermal Manikin and Modeling Meeting*, Coimbra, Portugal.

Appendix A
Calibration of the equipment

A. 1 Calibration of the thermocouples

During the experiments several thermocouples were used to measure the temperature at different positions in the room. Before that, the thermocouples were calibrated in order to obtain an accurate value of temperature.

Two calibrate the thermocouples two devices were used:

- ✓ Precision thermometer used to measure the temperature of reference for the thermocouples, see figure A.1 (a).
- ✓ Thermal calibration bath, ISOCAL 6, manufactured by Isotech. This device allowed the calibration of three thermocouples at the same time, see figure A.1 (b).

Figure A.1 a) Precision thermometer used for the calibration of the thermocouples, b) Thermal calibration bath, ISOCAL 6

After a stabilization time of about 15 minutes, the temperature calibration device maintained the bath temperature stable in order to compare the measurements of three thermocouples with the measurement of the precision thermometer. This process was carried out at three different temperatures: 15°C, 30°C and 45°C to obtain the calibration curve and the corresponding calibration equation for each thermocouple. The calibration curve/equation compares the measurements values of the precision thermometers with each thermocouple. The measurements of the thermocouples are adjusted to a linear equation of the following type:

$$T_r = a + bT_m \quad (A.1)$$

where T_r is the temperature measured by the precision thermometer and T_m is the temperature measured by the thermocouples.

Figure B.2 shows one of the calibration curve and equation obtained for one of the thermocouple type K.
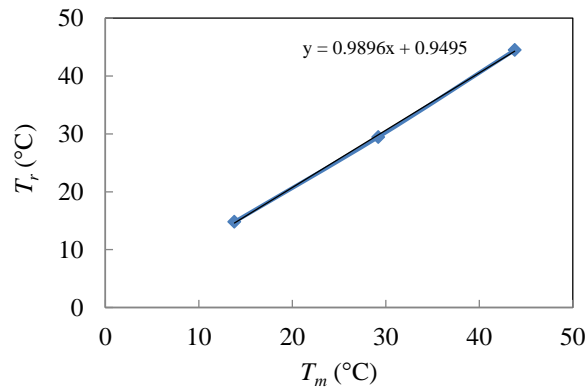
Figure A.2 Calibration curve and equation obtained for one of the thermocouples

The calibration curve of each thermocouple was used in the post-process of the temperature data of all the experiments.

A.2   Calibration of the anemometers

Hot sphere anemometers, DANTEC 54R50 were used to measure the velocity of the air at different positions in the room during the experiments. Results of measurements were logged in a computer with the corresponding DANTEC software, see figure A.3.

Additionally, for the calibration process of the anemometers a wind tunnel was used to expose the anemometers to a fixed velocity using different orifice plates, see figure A.4.

During this process the computer software measured the voltage difference generated by the anemometers while a manometer connected to the wind tunnel measured the pressure difference (true velocity).

The measured pressure difference was related by a linear equation with the velocity of the air (true velocity).

Inés Olmedo
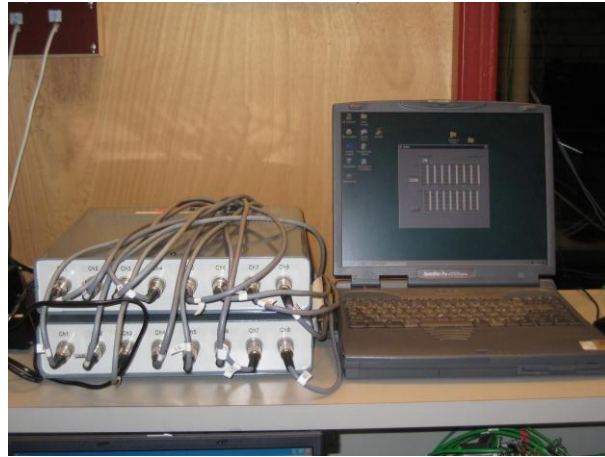
Figure A.3 Anemometers connected to the computer

A calibration curve established a relation between the voltage and the true velocity measured by the thermocouples and the manometer, respectively, that is added in the computer software to take the velocity measurements.

Figure A.4 Wind tunnel where the anemometers were placed to be calibrated

Appendix B
Study of the human breathing flow profile in a room with three different ventilation strategies

ASHRAE
IAQ Conference
Malaysia 2010

Study of the Human Breathing Flow Profile in a Room with Three Different Ventilation Strategies

Inés Olmedo

Peter V. Nielsen, PhD
Fellow ASHRAE

Manuel Ruiz de Adana, PhD

Piotr Grzelecki

Rasmus L. Jensen, PhD

ABSTRACT

This study investigates the characteristics of human exhalation through the mouth with three different ventilation strategies: displacement ventilation, mixing ventilation and without ventilation.

Experiments were conducted with one breathing thermal manikin in a full scale test room where the exhalation airflow was analyzed. In order to simulate the gaseous exhaled substances in human breathing, N_2O was used as a tracer gas. The concentration of N_2O and the velocity of the exhaled flow were measured in the center line of the exhalation flow.

The velocity decay of the exhalation flow versus distance was analyzed for the three ventilation strategies. The relationship between gas concentration values and distance from the manikin was also examined.

The measurements showed that the exhalation flow of breathing depends to some extent on the air distribution system. Two equations could be applied to describe the relationship between distance from the manikin and, respectively, peak velocity values and maximum mean gas-concentration values.

INTRODUCTION

When studying the risk of cross infection between people in a room, the human breathing cycle, pulmonary ventilation rate and characteristics of the exhaled air, such as temperature or humidity, are relevant factors. The exhalation from a source manikin will not only influence the macroenvironment of the room but also follow a horizontal direction and penetrate the breathing zone of another person, see Nielsen et al. (2008). The exhaled flow can also behave differently depending on the air distribution system installed in the room, giving rise to a higher or lower risk of infection to the target manikin.

It is thus important to establish which system best protects people from possible cross infection. While a displacement ventilation system generates a vertical temperature gradient in the room, prompting a vertical concentration gradient and therefore varying levels of concentration, a mixing ventilation system will generate a fully-mixed air distribution, and both temperature and concentration values will tend to be approx-imately the same at any height in the room, see Nielsen et al. (2008) and Bjørn and Nielsen (2002).

Human exhalation flow and thermal manikins

The breathing cycle is known to approximate a sinusoidal function, due to alternating inhalation and exhalation periods, as reported by Gupta et al. (2010).

The exhalation flow can be seen as something between a vortex ring and partly an instantaneous turbulent jet. However, Nielsen et al. (2009) have shown that, if peak values for exhalation velocity are used, human exhalation flow behaves in a similar manner to a free jet; consequently, the same equations can be applied to obtain velocities at different distances from the mouth.

The center line velocities of a flow, based on Abramovich (1984), can be expressed by the following equation:

$$\frac{u_x}{u_o} = K_{exp} \cdot \left(\frac{x}{\sqrt{a_o}} \right)^{n1} \tag{1}$$

Inés Olmedo is a PhD student and *Manuel Ruiz de Adana* is an associate professor in the Department of Chemical Physics and Applied Thermodynamics, University of Cordoba, Spain. *Peter V. Nielsen* is a professor, *Piotr Grzelecki* is a student, and *Rasmus L. Jensen* is a lecturer in the Department of Civil Engineering, Aalborg University, Sohngaardsholmsvej, Aalborg, Denmark.

where K_{exp} is the proportionality constant, x the distance from the mouth at which the measurements are made, u_x and u_o are peak values of the velocity at distance x and in the mouth, respectively and a_0 the area of the manikin's mouth. When studying a free jet, n_1 has a value of -1, which means that in a log-log graph representation of the equation, the slope of the line obtained is -1. Any other value of the constant n_1 could, of course, be expected to describe the relationship between the velocity of the exhalation flow and the distance from the manikin.

In the same way, peak mean concentration values measured during breathing are also related to positions, as shown in the following equation:

$$\frac{c_x - c_R}{c_o - c_R} = K_c \cdot \left(\frac{x}{\sqrt{a_o}} \right)^{n2} \tag{2}$$

where K_c is the proportionality constant and c_x, c_o and c_R are concentration values at a distance x from the mouth, in the mouth and in the surroundings.

In order to obtain reliable measurements of concentrations at different points in a room, careful consideration must be given to the characteristics of the thermal manikins used. The plume generated by a manikin, as well as the breathing cycle, influences the airflow pattern in the room, as reported by Melikov and Kaczmarczyk (2006) and by Liu et al. (2009 A).

METHODS

Test room

Experiments to ascertain the behavior of human breathing under different air distribution systems were conducted in a full-scale test chamber 4.10 m (13.45 ft) (L), 3.2 m (10.49 ft) (W) and 2.7 m (8.85 ft) (H), under steady-state conditions. Two different air-distribution systems were tested: displacement ventilation and mixing ventilation. The positions of the two air diffusers and exhaust openings are shown in Figure 1(A). Each of the experiments was carried out with only one

diffuser but with both exhausts. A third experiment was performed with no ventilation.

Manikin and thermal loads

A breathing thermal manikin without clothes, with an artificial lung, exhaling through the mouth and inhaling through the nose, was used to simulate human breathing in each case. The exhalation rate was 11 l/min, the volume of exhaled air was set to 0.75 l per exhalation and the temperature at 34ºC (93.2F). The heat power of the manikin was set to 94 W (320.74 Btu/h). The manikin was 1.68 m high and the total unclothed surface area was about 1.4 m^2. The details of shape and size of the manikin can be found in Bjørn (1999).

A T-connection in the tube which connects the artificial lungs and the mouth of the manikin is used to dose the tracer gas, N_2O, in order to simulate the human exhalation flow and to be able to measure concentration values of the breathing flow at different distances from the manikin. The connection is made close to the artificial lungs in order to assure a complete mixing of the gas with the air. The amount of tracer gas exhaled through the source manikin's mouth was 0.005 l/s (0.1765 ft^3/s).The area of the manikin's mouth, a_0, was 123 mm^2.(0.19 in^2)

In addition, a radiator was situated in the room, with a thermal load of 394 W (1344 Btu/h).

Both the manikin and the radiator were situated in the centre line of the room, along the x axis, see figure 1. The distance between the radiator and the right wall was 0.8 m and the separation distance between the radiator and the nose of the manikin was 2.05 m (6.72 ft). A sketch of the position of the manikin and radiator is shown in figure 1 (B).

During the tests with displacement and mixing ventilation, the air change rate used was 5.6 h^{-1} and the temperature of the air supply to the room was set to 16 ºC (60.8F) in order to obtain a temperature of 20ºC (68F) in the occupied area. A third test with non-ventilation was performed, keeping the temperature at 21ºC (69.8F). During this experiment the conditions were also kept steady, maintaining the same
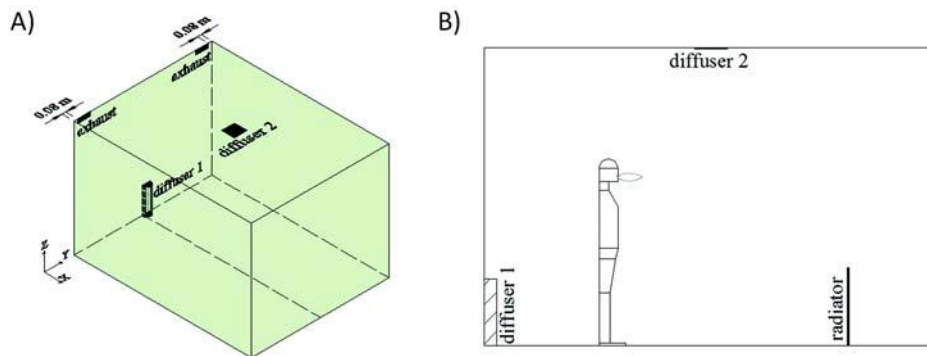
Figure 1 *A) Sketch of the test room showing the position of the two mounted diffusers (diffuser 1, wall mounted displacement diffuser; diffuser 2, square ceiling diffuser) and the exhausts. B) Placement of the radiator and manikin in the center plane of room.*
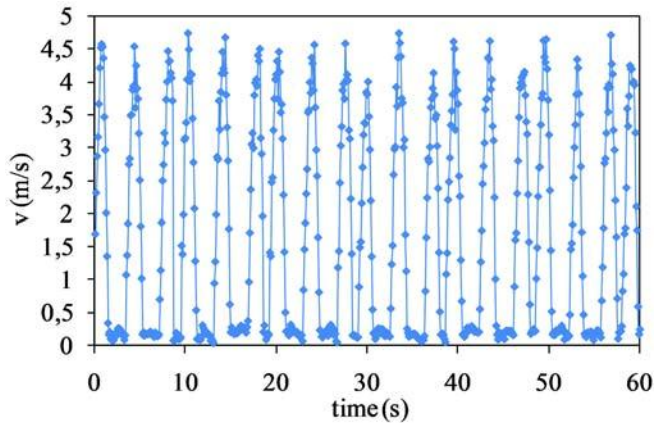
Figure 2 *Velocity values at the mouth outlet. Data were recorded every 100 ms.*

Figure 3 *Center line of the exhalation flow from the manikin with the three air distribution strategies. The height of the manikin's mouth is 1.52 m (4.98 ft).*

temperature within the test chamber and in the laboratory inside which it is placed.

Air velocity was measured at five points along the center line of the exhalation flow, using Dantec 54R10 hot sphere anemometers. NO_2 concentrations were measured with a Multigas Monitor type 1412 and two Multipoint Sampler and Dosers type 1303, both manufactured by Brüel & Kjaer.

MEASUREMENTS AND DISCUSSION

The first measurements were taken in order to obtain valuable information on breathing flow. The velocity and concentration of the exhalation flow were measured at the mouth outlet to determine the initial values, u_0 and c_0. At this point, the horizontal distance from the mouth to the measurement point was 0 m. Measurements were taken over four hours to chart time-dependent changes in exhalation. Results are provided in Figure 2, which shows the frequency and breathing mode of the manikin. The breathing pattern approximated to a half sinusoidal function and frequency did not change over time. The time for exhalation from the mouth and for inhalation from the nose are 1.75 s each one.

The peak velocity value obtained with the measurements was 4.74 m/s (15.55 ft/s) (u_0). For the N_2O gas concentration the maximum mean value obtained during the test was 6687 ppm (c_0).

In order to analyze exhalation flow under the three air-distribution systems, five anemometers and five concentration tubes were placed in the center line of the jet at different distances from the manikin. The correct positions were established using smoke visualization and prior instantaneous recording of peak velocity values. Moreover, the velocity of the air was measured in the same five positions without the breathing of the manikin, in order to compare these values with the velocities of the exhalation flow in the different ventilation strategies. The values of the average of the five points
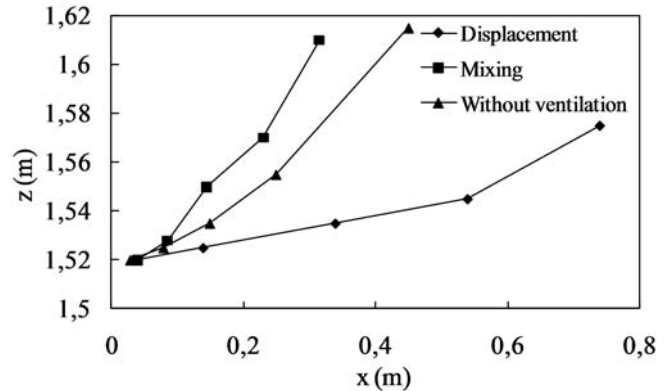
are 0.04 m/s (0.13ft/s), 0.08 m/s (0.26 ft/s) and 0.06 m/s (0.19 ft/s) for displacement and mixing ventilation and non-ventilation cases respectively. Figure 3 shows the center line of the exhalation flow where measurements were taken under the three air-distribution systems. There was a considerable resemblance between the stream lines obtained with mixing ventilation and with non-ventilation; similar findings have been reported by Liu et al. (2009 B).

Two samplings points, at 1.25m (4.1 ft) and 1.80 m (5.9 ft) height, for the C_R, concentration from the surroundings of the manikin, were situated at a distance of 0.50 m (1.64 ft) from the manikin and forming an angle of 45º with the center line of the room along the x axis. The value given for C_R is the average of both measurements.

Under displacement ventilation, the horizontal distance was greater than in the other tests. This could cause a higher risk of cross-infection to a person situated in the same room, as indicated by Nielsen et al. (2010).

Table 1 shows the position of the five measurement points, together with peak velocities and maximum mean concentration values obtained after four hours under the displacement ventilation system. The corresponding proportionality constants K_{exp} and K_c and exponents n_1 and n_2 obtained using equations (1) and (2) are also shown.

The mean value of factor K_{exp} for a standing person exhaling through the mouth under displacement ventilation was 7.52, a value very similar to that obtained by Nielsen et al. (2009 C).

The surrounding concentration c_R was 58 ppm and the corresponding mean K_c factor was 10.76.

Peak velocity values at the first and last measurement points for the displacement ventilation test are provided in Figure 4, which shows breathing frequency over time and charts the decline in velocity values with distance from the mouth. The influence of turbulence is also seen to be greatest at the point furthest from the mouth.

Velocity and concentration distributions of the exhalation flow at different distances are shown in Figure 5, using log-log axis. Values obtained for absolute constants n_1 and n_2 were -0.64 and -0.63, respectively.

The parameters measured under mixing ventilation were also measured in the center line of the jet under mixing ventilation. The position of measuring points and the results obtained are shown in Table 2.

The value of the proportionality constant for velocity was 4.48, lower than under displacement ventilation. Measured c_R surrounding the manikin was 47 ppm, giving a K_c value of 6.30.

Equations 1 and 2, with n_1 and n_2 values of -0.68 and -0.69 respectively, are also represented for mixing ventilation, in order to validate them as accurate expressions of the breathing profile, see figure 6.

Finally, velocity and concentration of the exhalation flow jet were also measured under non-ventilation but with steady-state conditions inside the room. Peak values were also found in the center line of the jet; measuring points and results are shown in Table 3.

Plots of equations (1) and (2) under non-ventilation are shown in Figure 7.

The K_{exp} value was 4.5, i.e. very similar to that recorded under mixing ventilation. This may be due to a similar temperature distribution in the area surrounding the manikin, prompted by the absence of vertical stratified temperature distribution; under displacement ventilation, this value differed considerably. The K_c value was 8.45, i.e. lower than that found under displacement ventilation; the concentration in the surroundings was 262 ppm. The calculated n_1 value was -0.66, while the n_2 value was -0.43. Of the three ventilation systems studied, this latter value differed most from the free-jet value of -1.

Graphical representations (log-log) of equation (1) with the three air-distribution systems studied are shown in Figure 8. The slope is similar in all three cases, with a value approaching -1, which corresponds to the n_1 value in equation (1). This suggests that the human exhalation flow can almost be

Table 1. Location of measuring points under displacement ventilation, peak values for velocity and concentration, and proportionality constants.

Horizontal distance, x (m)	0.04	0.14	0.34	0.54	0.74
Height (m)	1.520	1.525	1.535	1.545	1.575
$u_{x,max}$ (m/s)	3.24	2.42	1.5	0.78	0.52
$c_{x,max}$ (ppm)	6388	4504	3008	1426	1243
K_{exp}			7.52		
K_c			10.76		
n_1			-0.64		
n_2			-0.63		
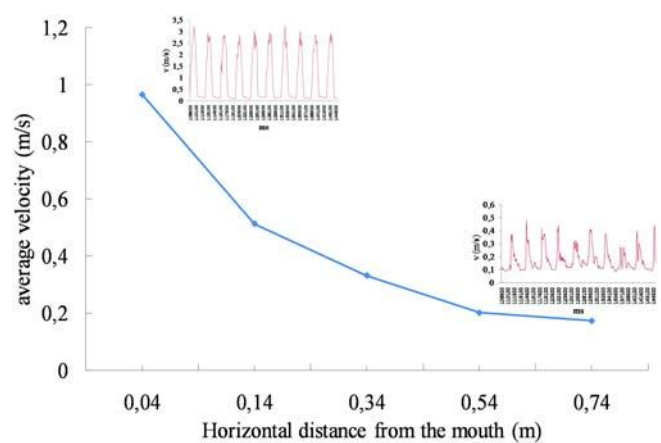
Figure 4 *Average exhalation flow velocity profile under displacement ventilation, and breathing frequency at the nearest and furthest measuring points.*
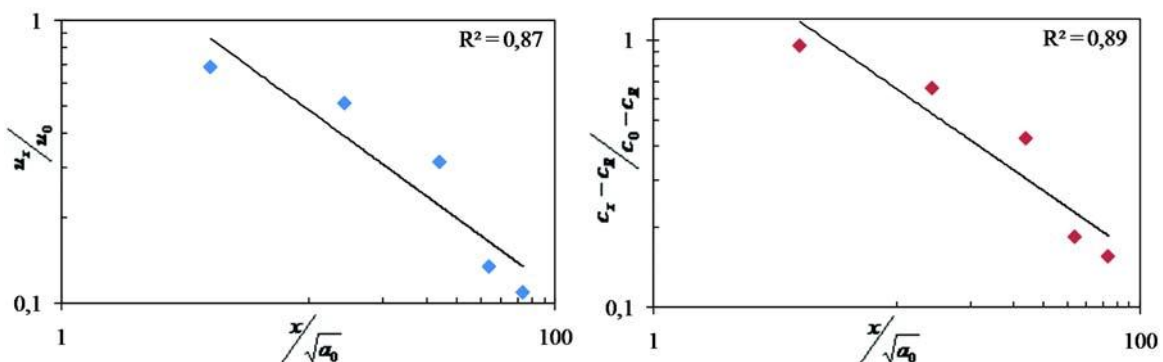
Figure 5 *Plot of equations 1 and 2 under displacement ventilation.*

described with a similar equation as a free jet, if peak velocity values in the center line of the exhalation flow are used.

Concentration values for the exhalation flow jets obtained under displacement ventilation, mixing ventilation and non-ventilation are shown in Figure 9, which plots in the form of a log-log graph the maximum mean concentrations measured over a four-hour period in each test. Under non-ventilation, however, the slope differed considerably from -1.

CONCLUSIONS

Human exhalation flow behavior depends on breathing flow and frequency, and on the heat released from the person; however, it is also influenced by the air-distribution system in the room. The penetration of the flow differed under the three ventilation system studied: displacement ventilation, mixing ventilation and non-ventilation.

Under displacement ventilation, the exhalation flow generated by the source manikin traveled a greater distance in the direction of flow than under the other two ventilation systems, indicating a higher risk of cross infection for one person placed in front of another. The shortest horizontal flow was obtained with the mixing ventilation system. Differences in exhalation flow behavior as a function of the type of air

distribution around the manikin are due to differences in temperature distribution inside the room, which are in turn dependent on the macroenvironment. The vertical temperature gradient produced under displacement ventilation maintained the horizontal flow of exhalation over a longer distance. Under mixing ventilation and non-ventilation, however, the absence of this gradient prompted an upward exhalation flow due to temperature differences and large mixing. This means an increased risk of cross infection for someone taller than the source person and standing closer to that person.

Human exhalation flow velocity can be represented by equation (1), using peak velocity values. In all three tested conditions, the slope describing exhaled flow behavior approached that of a free jet, with calculated values close to -1.

A correlation was also found between concentration values in the center line of the exhalation flow and the measuring position, expressed by equation 2. The concentration values used were maximum average measurements obtained over a four-hour period in each test. Under displacement and mixing ventilation, this equation yielded an expression similar to that of a free jet. However, under non-ventilation, the n_2 value for equation (2) differed from the free-jet value of -1. This could partly be due to a time-dependent increase in

Table 2. Location of the measuring points under mixing ventilation, peak values for velocity and concentration, and proportionality constants

Horizontal distance x (m)	0.040	0.085	0.145	0.230	0.315
Height (m)	1.520	1.528	1.550	1.570	1.610
$u_{x,max}$ (m/s)	3.32	2.36	1.47	1.06	0.86
$c_{x,max}$ (ppm)	5156	4013	3966	1921	1376
K_{exp}			4.48		
K_c			6.30		
n_1			-0.68		
n_2			-0.69		

Table 3. Location of the measuring under non-ventilation, peak values for velocity and concentration and proportionality constants

Horizontal distance, x (m)	0.03	0.08	0.15	0.25	0.45
Height (m)	1.520	1.525	1.535	1.575	1.615
$u_{x,max}$ (m/s)	3.62	1.92	1.27	0.73	0.68
$c_{x,max}$ (ppm)	5693	5423	4280	2338	2209
K_{exp}			4.50		
K_c			8.45		
n_1			-0.66		
n_2			-0.43		
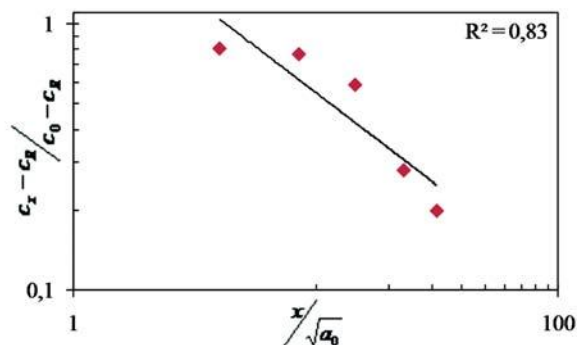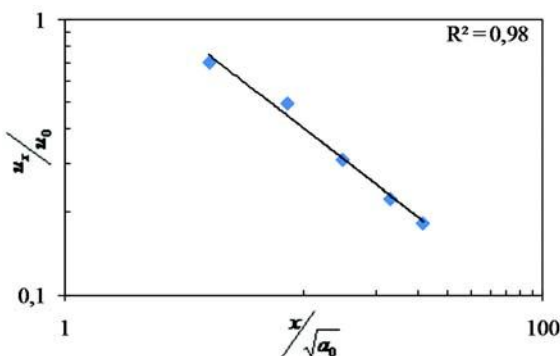
Figure 6 *Plot of equations 1 and 2 under mixing ventilation.*
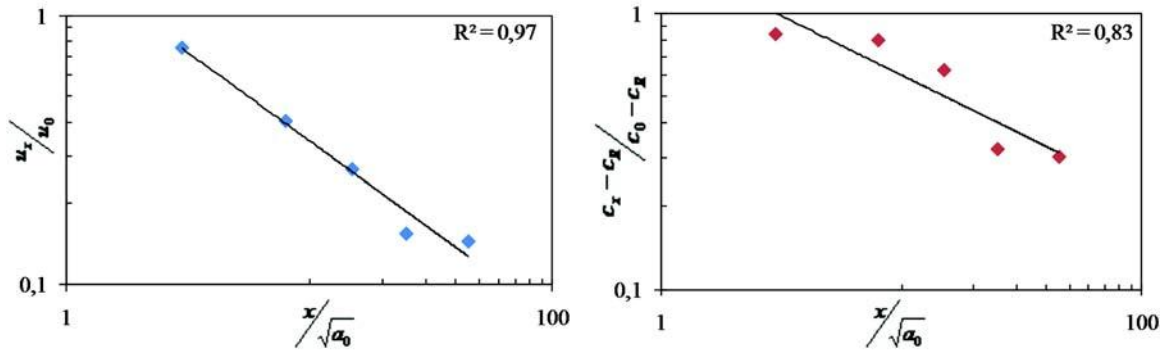
Figure 7 *Plot of equations 1 and 2 under non-ventilation.*
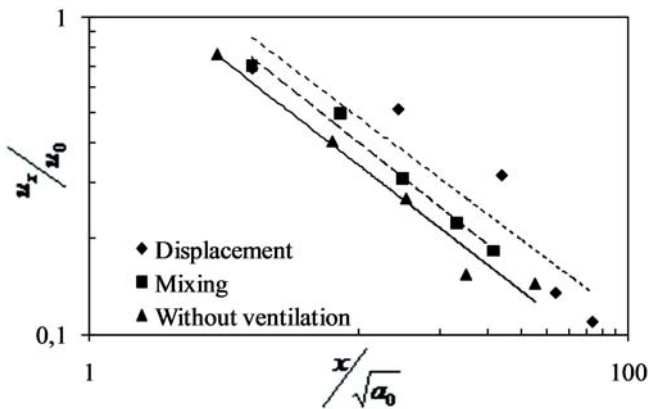
Figure 8 *Graphical representation of equation (1) in three non-isothermal situations: displacement ventilation, mixing ventilation and non-ventilation.*
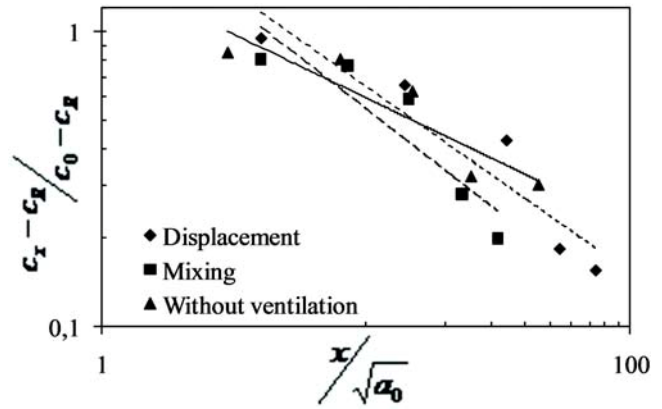
Figure 9 *Graphical representation of equation (2) in three non isothermal situations: displacement ventilation, mixing ventilation and without ventilation.*

concentration values around the manikin, due to the lack of ventilation.

REFERENCES

Abramovich, G. N. 1984. Theory of Turbulent Jets. Fastigiate, Moscow.

Bjørn, E. 1999. Simulation of Human Respiration with Breathing Thermal Manikin, Proceedings of Third International Meeting on Thermal Manikin Testing, National Institute for Working Life, Stockholm, SWEDEN, October 12-13, 1999.

Bjørn, E. and Nielsen, P.V. 2002. Dispersal of exhaled air and personal exposure in displacement ventilated room, Indoor Air, volume 12, no. 3, pp. 147-164.

Gupta, J.K., In, C., and Chen, Q. 2010. Characterizing exhaled airflow from breathing and talking, Indoor Air, volume 20, pp. 31-39.

Melikov, A. and Kaczmarczyk, J. 2006. Measurement and prediction of indoor air quality using a breathing thermal manikin, Indoor Air, volume 17, pp. 50-59.

Liu, L., I Y., Nielsen P.V., Jensen R.L., Littleneck M., and Sages J. 2009 B. An experimental study of human exhalation during breathing and coughing in a mixing ventilated room. Healthy Buildings 2009, Syracuse.

Liu, L., Nielsen P.V., I Y., Jensen R.L., Littleneck M., and Sages J. 2009 A. The thermal plume above a human body exposed to different air distribution strategies. Healthy Buildings 2009, Syracuse.

Nielsen, P.V., Buus, M., Wi nth er, F.V. and Theologizers, M. 2008. Contaminant flow in the microenvironment between people under different ventilation conditions, ASHRAE Transactions, 114, part 2.

Nielsen P.V., Jensen R.L., Littleneck M., and Sages J. 2009 C. Experiments on the microenvironment and breathing of a person in isothermal and stratified surroundings.

Healthy and Buildings 2009, Syracuse, NY, USA, 9th International Conference & Exhibition, September 13-17, 2009.

Nielsen P.V., Olmedo I., Ruiz de Adana M., Grasslike P., and Jensen R.L. 2010. Airborne Cross Infection between two people in a displacement ventilated room. Indoor Air Quality 2010, Malaysia.

Appendix C
Airborne cross-infection risk between two people standing in surroundings with a vertical temperature gradient

Airborne Cross-Infection Risk between Two People Standing in Surroundings with a Vertical Temperature Gradient

Peter V. Nielsen PhD ASHRAE Fellow[a]*, Inés Olmedo[b], Manuel Ruiz de Adana PhD[b], Piotr Grzelecki[a], Rasmus L. Jensen PhD[a]

[a]*Department of Civil Engineering, Aalborg University, Sohngaardsholmsvej 57, 9000, Aalborg, Denmark*
[b]*Department of Chemical Physics and Applied Thermodynamics, University of Cordoba, Spain*
**Corresponding email: pvn@civil.aau.dk*

ABSTRACT

Transmission of exhaled small particles from one person to another in an indoor environment can take place, both directly (in the microenvironment around the persons) and via the room air distribution. The impact of these transmission routes for two persons is investigated in details by evaluating the exposure to gaseous substances (simulating particles < 5 μm) in a room with a vertical temperature gradient obtained by displacement ventilation. Experiments are conducted with two breathing thermal manikins. One manikin is the source, and the other manikin is the target. In the experiments the distance between the two manikins varies from 1.1 m (43 in) to 0.35 m (14 in).

A tracer gas N_2O is used to represent the gaseous substances exhaled by the source manikin. The concentration of N_2O is measured to study the impact of the following parameters on the exposure: distance between manikins, positions as face to face, face to the side of the target manikin, face to the back of the target manikin, and a seated source manikin. The exposure increases with decreasing distance between the manikins, and the highest values are obtained in the face to face position. Face to the side is also creating some exposure of the target manikin, while face towards the target manikin's back does not give any direct exposure through the microenvironment. The thermal stratification in the room supports a significant exposure of the target manikin when the source manikin is seated and breathing towards the chest of a standing manikin.

KEYWORDS: *Exposure, Tracer gas, Displacement ventilation, Vertical temperature gradient, Breathing thermal manikin, Microenvironment, Cross-Infection risk.*

INTRODUCTION

More and more people are spending a considerable amount of time in the indoor environment, and it is therefore important to provide a good air quality and to minimise the danger of e.g. cross-infection risk and passive smoking.

Different air distribution systems offer different possibilities of protecting people against pollutants as bacteria and viruses. The pollutants are mixed with the room air and removed by a diluting process. If the pollutant source is also a heat source, a displacement system offers possibilities to work with two zones, a low zone with clean air and an upper zone with polluted air. It is possible to design a system with a low exposure of people under certain conditions, however, high exposure can also exist in certain situations in rooms with displacement flow, see Bjørn and Nielsen (2002), and Qian et al. (2006).

The measurements show that apart from the type of air distribution system, it is also important to work with the transport processes in people's microenvironment if they are standing close to each other.

THE MICROENVIRONMENT AROUND PEOPLE

Figure 1 indicates the problems to be considered. The room can be ventilated by an air distribution system which generates a fully mixed flow in the occupied zone, or as in this case, a displacement ventilation system which generates different zones and a vertical temperature gradient. If one of the persons in the occupied zone is a source of an airborne contaminant (as in cross-infection problems or in case of passive smoking), a concentration level around the other persons close to the source can rise to a high level independent of the general concentration level of the occupied zone. In other words, if the air distribution system is designed for an efficient ventilation of the room, there will still be a microenvironment around people close to each other which can not be influenced by this system.
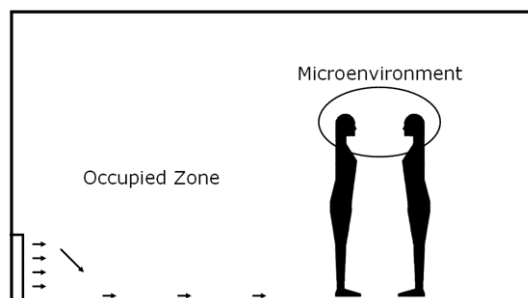
Figure 1. The measurements show that independent of the type of air distribution system it is important to work with the transport processes in people's microenvironment if they are standing close to each other.

The microenvironment around two persons is addressed in Figure 2. The two persons are considered to be source and target. The exhalation from the source person can be divided into two parts. One part of the exhalation flows into the macroenvironment (the occupied zone), and the general air distribution system in the room dilutes and transports this part out in the room and creates a concentration distribution around the target person, c_{oc}. The other part of the exhalation from the source person flows direct to the target person's breathing zone, or to this person's thermal boundary layer. The target person is exposed to the level c_{exp}, and this exposure therefore consists of an indirect exposure from the macroenvironment, c_{oc}, and a direct exposure from the source person's exhalation, see Figure 2. The concentration, c_{oc}, is measured in the experiments at the standing target person's chest. This concentration is also the the target person's inhalation concentration if this person is not influenced by a direct exposure, because the inhalation normally originates from the thermal boundary layer, Brohus and Nielsen (1996), and Bjørn and Nielsen (2002).
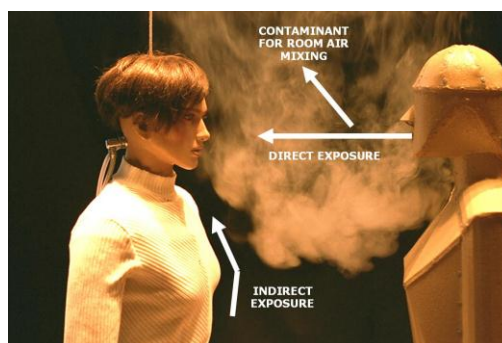
Figure 2. A source manikin and a target manikin. The contaminant flow between the two manikins is indicated by smoke.

The concentrations c_{exp} and c_{oc} are in the following text given in a dimensionless form where the concentrations are divided by the return flow concentration c_R. $c_{oc}/c_R = 1.0$ corresponds to a fully mixed exposure level. It is always desirable to have an exposure level smaller than 1.0.

Parameters that influence the cross-infection risk between people situated close to each other in a ventilated room can be summarised as:

- Distances between the persons
- Positions and orientations of the persons
- Breathing process (breathing through the mouth or through the nose, opening of mouth, coughing, speaking)
- Difference in the height of the persons
- Activity levels of the persons
- Number of persons
- Temperature and vertical temperature gradient in the microenvironment around the persons
- Air velocity (speed and direction) in the microenvironment around the persons
- Turbulence level of the air flow in the microenvironment around the persons

The last three points are the result of room load and type of air distribution system in the room.

This article shows the effect of distance between two persons in a microenvironment with a vertical temperature gradient as well as the effect of the orientations of the persons in this environment. Some effects of the activity level are also mentioned.

Work on cross-infection risk between people of different height is shown by Liu et al. (2010), and work with different air distribution systems is shown by Nielsen et al. (2008).

MANIKINS AND CONCENTRATION DISTRIBUTION

The source and the target manikins are simulated by life-sized breathing thermal manikins. Both manikins use exhalation through the mouth, because this is considered to be the worst-case scenario, see Nielsen et al. (2008). The direction of the exhalation is horizontal. The source manikin's mouth is an opening of 123 mm^2 and has a semi-ellipsoid form. The target manikin's mouth is a circle with a diameter of 12 mm (0.47 in). The exhalation frequency is 19 exh/min for the source manikin and 15.5 for the target manikin. The flow (minute volume MV) is 11 l/m (0.39 cfm) for the source manikin and 10 l/m (0.35 cfm) for the target manikin. The source manikin has a total heat release of 94 W (321 Btu/h) and the target manikin a release of 102 W (348 Btu/h). Both manikins have an exhalation temperature of 34 ^{o}C (93 ^{o}F). N$_2$O is used as tracer gas in the experiments and is supplied to the exhalation of the source manikin at a rate of 0.3 l/min (0.01 cfm). The exposure to the tracer gas is measured in the nose of the target manikin.

Tracer gas is not influenced by buoyancy, and the results are therefore only valid for the situation where bacteria and viruses are transported by droplets (droplet nuclei) smaller than 5 - 10 μm. Droplet nuclei smaller than 5 μm exhibit a settling velocity below 1 m/h in still air, and can therefore follow the persons' exhalation flows and the ambient air flows in for example a hospital ward. Large droplets are also part of the cross-infection process, but they settle either on surfaces close to the source of the infection, or they evaporate, decrease in size and follow the air flow as droplet nuclei. The transport of fine particles is important because they are easier to inhaile than the coarser particles as shown by Wells (1955).

Tracer gas concentration can not be directly used as a measure of the health risk, but it can give an indication of this risk. The health risk can be estimated from the Wells-Riley model which, among other things, gives a link between the concentration in a person's inhalation and the connected risk of infection (Riley et al. 1978). All the measurements and discussions in this article are based on steady state conditions, however, the

Wells-Riley model introduces the time as a parameter, as e.g. the number of infected sources over a period of time.

The concentration distribution is measured by an INNOVA Multi Gas Monitor, Sampler and Doser. Velocities are measured by Dantec 54R10 hot sphere anemometers, and temperatures by thermocouples type K and grant Squirrel SQ1600 meter and logger.

TEST ROOM

The geometry of the test room is 4.1 m (length) × 3.2 m (width) × 2.7 m (height) (13.5 ft × 10.5 ft × 8.9 ft). Figure 3 shows the locations of diffuser and the two manikins and a single radiator used to supply an extra heat load. They are all located along the symmetry line of the room. The radiator supplies a heat load to ensure a typical vertical temperature gradient for displacement ventilation. The load is 300 W (1024 Btu/h) in cases with two manikins, and 400 W (1365 Btu/h) in cases with one manikin. The total heat load to the room is thus ~500 W (~1700 Btu/h). The air change rate for all the experiments is 5.6 h^{-1}, and the room temperature is close to 23 °C (73 °F).
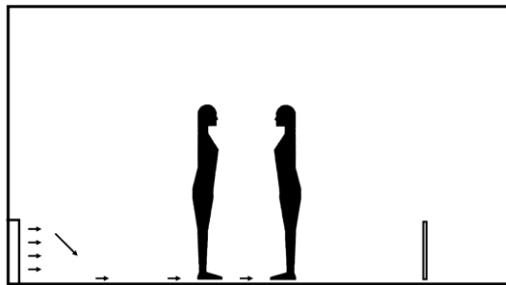
Figure 3. Location of diffuser, thermal manikins and radiator in the room.

MEASUREMENTS AND DISCUSSION

The microenvironment is examined for the following four positions of the manikins (persons): face to face, face to the side of the target manikin, face to the back of the target manikin, and a seated source manikin, see Figure 4, where the source manikin is white and the target manikin is black.
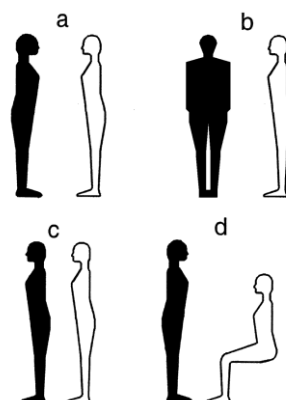
Figure 4. Positions of manikins. a) face to face, b) face to side of target manikin, c) face to back of target manikin, d) seated source manikin. Source manikin is white, and target manikin is black.

Measurements are made at the following four distances between the manikins in standing position: 110 cm (43 in), 80 cm (31.5 in), 50 cm (20 in), 35 cm (14 in), and at the two distances 70 cm (27.6 in) and 100 cm (39.4 in) in the case with the seated manikin. The distance is measured from tip of the nose to tip of the nose in the face to face position, and from tip of the nose to the back of the head in the face to back position. The distance is measured from tip of the nose to tip of the nose when the position is face to the side of the target manikin.

The vertical temperature distribution in the room is typical of displacement ventilation. Figure 5 shows how the flow in the room is stratified with the warm air in a layer below the ceiling. T, T_o, T_R are local temperature, supply temperature and return temperature, respectively. It is typical that the upper layer of warm air reaches down into the occupied zone for a standing person at the given flow rate. Although the manikins inhale through their mouths in the upper zone, they inhale a large amount of air from the lower (cleaner) zone because this air is transported up to the breathing zone by the thermal boundary layer around the manikins, (Brohus and Nielsen 1996). The temperature is uninfluenced by the changes in the positions of the manikins, which should also be expected. The vertical temperature distribution influences the measurements in the microenvironment around the manikins and it also influences the cross-infection risk.
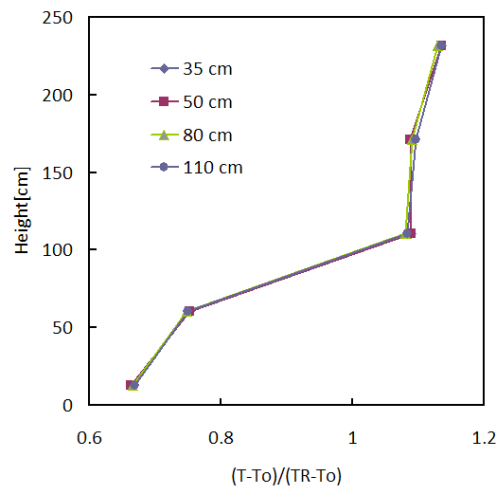
Figure 5. Vertical temperature distribution in the room. The temperature distribution is measured for different distances between the manikins.
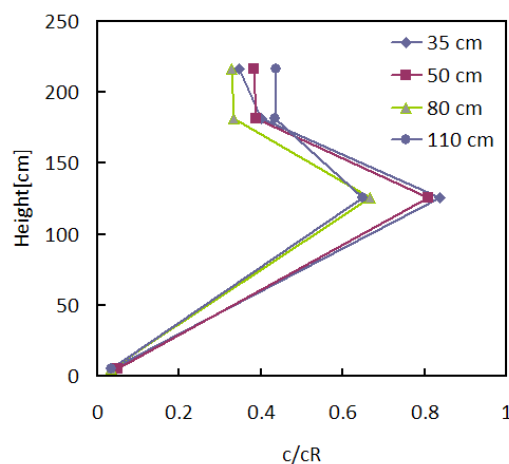
Figure 6. Vertical concentration distribution of tracer gas in the room. The concentration distribution is measured for different distances between the manikins.

The vertical concentration distribution of tracer gas also shows stratification in the room. The measurements in Figure 6 indicate that the exhaled tracer gas from the source manikin stratifies in a layer at the height of ~1.5 m (~60 in), which is also proved by smoke experiments. This effect is obtained in the process where the hot air from the radiator rises in a plume to the ceiling regions, like the plumes from the manikins. The exhalation from the manikin is slightly colder, 34 $^{\circ}$C (93 $^{\circ}$F), and it only reaches a restricted level in the vertical temperature distribution in the room. The concentration in Figure 6 is given in a dimensionless form, where the local concentration is divided by the return concentration, c_R. The values in the figure are dependent on the horizontal location of the measuring line which is unusual in a displacement ventilation case. The measurements are made at a position behind the source manikin's direction of exhalation, but it is shown that much higher values are found in the upper part of the room if the exhalation has the opposite direction. This explains the fact that the concentration is smaller than 1.0 in the ceiling regions opposite to the return openings.

A detailed study of the exhalation flow from a single manikin, Olmedo et al. (2010), shows how the exhalation vortex moves slightly upwards, Figure 7. The entrainment from the surroundings decreases the temperature in the flow, and the exhalation stratifies at a thermally neutral height as indicated in Figure 6, see also Nielsen et al. (2009).
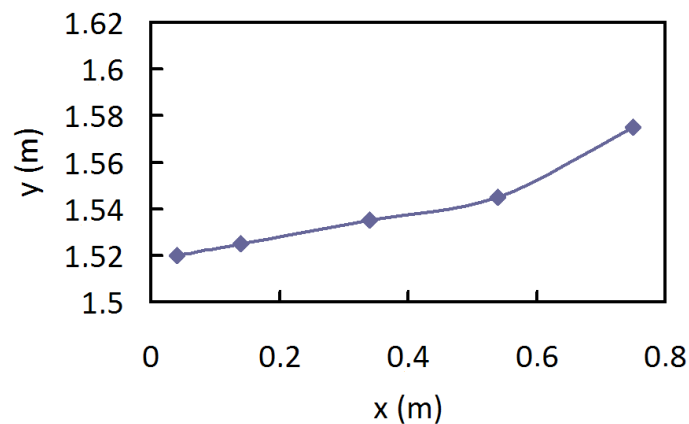
Figure 7. Centre line of the instantaneous exhalation flow from a manikin standing in a room with displacement flow. Olmedo et al. (2010).

The temperature, contaminants, and stream line distribution in Figures 5, 6 and 7 are dependent on the load of the room (air change rate and temperature difference), but they can be considered as typical values for a standard room and for a hospital patient ward.
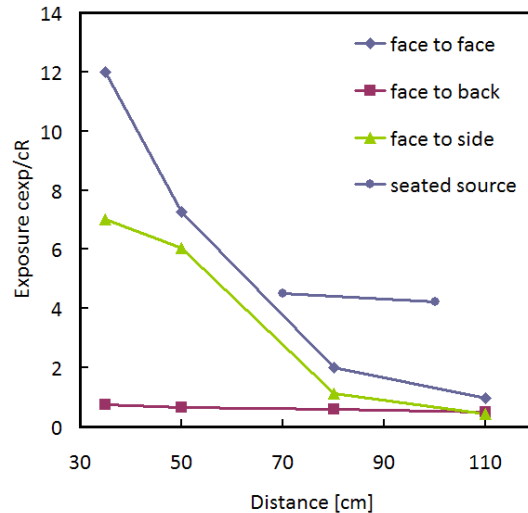
Figure 8. Exposure of the target manikin versus distance between the two manikins. Measurements for the four positions, face to face, face to side of target manikin, face to back of target manikin and seated source manikin. Exposure is given as c_{exp}/c_R.

The exposure shown in Figure 8 is given as c_{exp}/c_R, where c_{exp} is the concentration in the target manikin's inhalation, and c_R is the return concentration. When the distance between the manikins is 110 cm (43 in), the target manikin inhales a concentration which is equal to the background concentration in the room (indirect exposure, see Figure 2). The two manikins do not have a common microenvironment with respect to cross-infection considerations. The concentration c_{exp}/c_R is ~0.5 for face to the side and face to the back, which is typical of displacement ventilation where the inhalation contains air from the lower zone in the room, Brohus and Nielsen (1996). c_{exp}/c_R is ~1.0 for the face to face situation, and the higher value indicates that a small fraction of direct exposure takes place at a distance of 110 cm.

There is a remarkable increase in the direct exposure when the distance between the manikins is smaller than 80 cm for the cases face to face and face to side of the target manikin. The exposure increases up to 12 times the concentration in a fully mixed situation, in the face to face situation, and up to 7.0 times in the face to the side of the target manikin situation, when the distance is 35 cm (14 in). With respect to the protection against cross-infection this is a serious setback for systems generating a vertical temperature gradient.

Protection from cross-infection seems to be high in the face to back situation. The exposure c_{exp}/c_R does only reach 0.75 at a distance of 35 cm (14 in), which is below a fully mixed case.

The two manikins are of the same height. Figure 7 indicates that people of different heights could be more exposed, or less, than found in our measurements. The centre line of the exhalation, and the target manikins boundary layer can, in certain positions, lead to a higher direct exposure than found in Figure 8.

Figure 8 shows that there is a high and rather constant level of cross-infection risk in the case with a seated source manikin and a standing target manikin, where c_{exp}/c_R is equal to 4.5. The main reason for that level may be the low position of the source manikin's exhalation zone and the rising exhalation flow (Figure 7). Therefore, this is a situation where different heights are an important parameter. A similar situation with a high exposure from a seated manikin is shown by Bjørn and Nielsen (2002), see Figure 9.

Figure 9. Smoke experiment with two manikins in a room with a vertical temperature gradient. The smoke indecates a layer of high concentration exhaled from the seated source manikin.

The measurements in Figure 8 are averaged values, all measured over a period of four hours. The air distribution system and the heat loads are in steady state conditions, but the breathing frequencies of the two manikins are slightly different, which cause a large variation in the instantaneous exposure. Figure 10 shows the variation in exposures. It is seen that the exposure is low even at a short distance of 35 cm (14 in), in some periods. The peaks of the exposure may even be higher than shown in the figure, because the measuring equipment averages the value in every single measuring frequency.
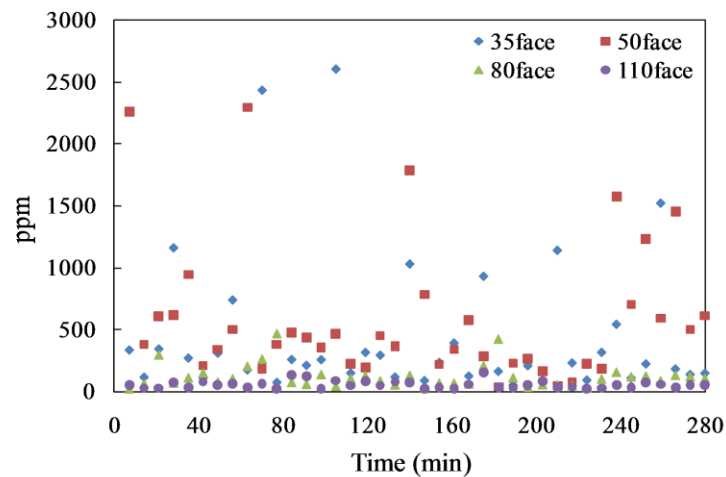
Figure 10. Instantaneous measurements of exposure during 280 min. for the face to face case. The vertical axis show the direct measured concentration of tracer gas in ppm.The values can not be compared to values in other graphs. 35 face, 50 face, 80 face and 110 face indicates the four different distances between the manikins, all in the case face to face.

A given measurement in a dimensionless form, as c_{exp}/c_R, is valid for all situations, which have the same geometry and the same Archimedes number according to the similarity principles (Nielsen 2001). The Archimedes number is expressed by the heat load (temperature difference, $T_R - T_o$) and the velocity (flow rate to the room, q_o) as well as the velocity (flow rate) generated by the breathing thermal manikins.

The concentration in the return flow is given by

$$c_R = \frac{S}{q_o} \qquad\qquad (1)$$

where S is the source. The flow rate q_o is equal to 0.055 m^3/s (117 cfm) in all the experiments. It is assumed that the source S is about 20 pathogen carrying droplet nuclei per seconds. It is seen in Equation (1) that c_R is

equal to 363 droplet nuclei per m^3 in this case. If the exposure, c_{exp}/c_R, for the target person is 10 (Figure 8) it then corresponds to an exposure of 3630 droplet nuclei per m^3 (103 droplet nuclei per cubic feet).

The importance of the flow rate to the room can be seen from Equation (1). An increase in the air change rate from 5.6 h^{-1} to 11.2 h^{-1} decreases c_R from 363 to 182 droplet nuclei pr. m^3. The exposure in Figure 8 is dependent on the corresponding change in the Archimedes number, but if it is assumed that the level of 10 will be maintained, then the exposure of the target person decreases from 3630 to 1820 droplet nuclei pr. m^3.

The activity level and the corresponding breathing frequency of the manikins (persons) are also important. Figure 11 shows the total amount of air, MV, inhaled and exhaled by a woman per minute at different activity levels. In the experiments the target manikin has a flow rate, MV, of 10 l/m (0.35 cfm), and the source manikin a flow rate, MV, of 11 l/m (0.39 cfm). This level of flow rate corresponds to a metabolic rate of 1.3 to 1.4 met, which is a typical activity level of a standing person, Figure 11.
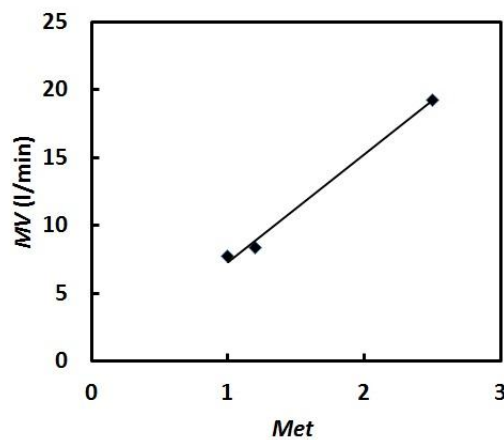
Figure 11. Minute volume (MV) versus metabolic rate for a woman, Adams (1993).

The importance of the activity level can be seen from the following example where it is assumed that the exposure of the target person c_{exp}/c_R is 10, and c_R has a level of 363 droplet nuclei pr. m^3 as in the first example. If the target person has a minute flow, MV, of 10 l/m (0.35 cfm), the target receives 36.3 droplet nuclei per minute. If the target person has a very high activity level, ~2.6 met, see Adams (1993), the minute flow is 20 l/m (0.7 cfm) and a total of 72.6 droplet nuclei are inhaled per minute by the target person, which is two times as much as in the first case.

The results of the experiments in Figure 8 are based on the given the flow rates to the two manikins. However, to some extent it is possible to make calculations as the ones mentioned above where the target manikins minute flow is changed. It will not be possible to make such a calculation for the source manikin. An increase in the activity level of the source manikin will change the dimensionless concentration distribution in the microenvironment around the two manikins, and it will give new results compared to the ones shown in figure 8.

The results in this article are based on measurements which all show that the exhalation flow from the breathing process is able to escape the thermal plume from the manikin (person). Qian et al. (2004) address this problem in connection with the definition of boundary conditions for CFD. Situations where the exhalation was weak, without possibility to escape from the body plume, were observed in connection with the measurements in this research work. New experiments with standing manikins and low activity level (1.2 met) as well as experiments with high activity level (2 met) all show situations where the exhalation flow did escape the thermal plume of the source manikin and reach the opposite manikin's inhalation. The heat load and the breathing flow

and frequency were adjusted according to figure 11. Nielsen at al. (2009) also shows that some exhalation is always trapped in the thermal plume in the beginning and in the end of a breathing cycle because the exhalation momentum flow is low in those situations. An important parameter is the area of the mouth, which is 123 mm2 in all the experiments. This is in good agreement with the results shown by Gupta et al. (2010). A larger area of the mouth, which could be the case in some situations, may decrease the momentum flow of the exhalation with the consequence that it will be entrained into the plume.

It should be noticed that the meaurements generally show that the cross-infection risk by airborne droplet nuclei may increase to a high level when people are standing close to each other (< 1m, see Figure 8). This has also been shown in rooms with other types of air distribution systems, Nielsen et al. (2008). This is a similar characteristics as the one connected to droplet infection, where there is a risk of infection when the distance between people is less than 1m, while the probability of infection is smaller at larger distances. Those similarities in the characteristics could make it difficult to distinguish between the two different principles of cross infection risk (airborne transmission and droplet spread transmission) as also pointed out by Li (2009).

CONCLUSIONS

Transmission of exhaled gaseous substances from one person to another in an indoor environment takes place, both in a direct way and via the room air distribution. In a room with displacement ventilation and a vertical temperature gradient, a direct exposure can take place when the distance between two persons is less than 80 cm (31.5 in).

The distance between people, positions of people as face to face, face to the side of the target person, face to the back of the target person, and a seated source person, have been studied. It is shown that the exposure increases with decreasing distance between people, and the highest values are obtained in the face to face position. Face to the side is also giving some exposure of a person, while face towards a person's back does not give any direct exposure via the microenvironment. The thermal stratification and the rising flow of the exhalation in the room support a significant exposure of a standing person when the source person is seated breathing towards the chest of a standing target person.

The exposure increases up to 12 times the level of a fully mixed situation in the face to face case, and up to 7 times in the face to the side of a person case, when the distance is 35 cm (14 in). This is a serious setback for the displacement ventilation system with respect to the protection against cross-infection.

It is indicated that people of different heights could be more exposed, or less, than found in the measurements. The centre line of the exhalation and people's boundary layer flow may, in certain positions, lead to even higher direct exposure than found in this paper.

The activity level of a person has a large influence on the cross-infection risk.

There is a similarity between the characteristics of infection risk by airborne transmission and by droplet-spread transmission, which could make it difficult to distinguish the two different principles of cross infection risk.

REFERENCES

Adams, W.C. 1993. Measurement of breathing rate and volume in routinely performed daily activities. *California Environmental Protection Agency*, Air Research Board, June 1993.

Bjørn, E., and P.V. Nielsen. 2002. Dispersal of exhaled air and personal exposure in displacement ventilated rooms. *Indoor Air* 12 (3): 147-164.

Brohus, H., and P.V. Nielsen. 1996. Personal exposure in displacement ventilated rooms. In: Indoor Air: *International Journal of Indoor Air Quality and Climate* 6 (3): 157-167.

Gupta, J.K., C.-H. Lin, and Q. Chen. 2010. Characterizing exhaled airflow from breathing and talking, Indoor Air: *International Journal of Indoor Air Quality and Climate* 20, 31-39.

Li, Y. 2009. Ventilation and airborne infection. *Proceedings of Healthy Buildings 2009*, Syracuse, NY, USA, 9th International Conference & Exhibition, September 13-17.

Liu, L., Y. Li, P.V. Nielsen, and R.J. Jensen. 2010. An experimental study of exhaled substance exposure between two standing manikins. *ASHRAE's IAQ 2010 Conference*. Kuala Lumpur.

Nielsen, P.V. Scale-model experiments, In: E. Tähti and H. Goodfellow. 2001. Handbook of Industrial Ventilation, *Academic Press*, San Diego.

Nielsen, P.V., F.V. Winther, M. Buus, M. Thilageswaran. 2008. Contaminant flow in the microenvironment between people under different ventilation conditions. The ASHRAE Annual Meeting, Salt Lake City, Utah, USA, 21st – 25th June, 2008. *ASHRAE Transactions* 114 (2): 632-640.

Nielsen, P.V., R.L. Jensen, M. Litewnicki, and J. Zajas. 2009. Experiments on the microenvironment and breathing of a person in isothermal and stratified surroundings. *Healthy Buildings 2009*. Syracuse, NY, USA, 9th International Conference & Exhibition, September 13-17.

Olmedo, I., P.V. Nielsen, M. Ruiz de Adana, R.L. Jensen, and P. Grzelecki. 2010. Study of the human breathing flow profile in a room with three different air distribution systems. *ASHRAE's IAQ 2010 Conference*. Kuala Lumpur.

Qian, H., P.V. Nielsen, Y. Li, and C.E. Hyldgaard. 2004. Airflow and contaminant distribution in hospital wards with a displacement ventilation system. In Guoqiang Zhang, Xuesong Hou, Jilin Yand, Liwei Tian, Cong Zheng (eds.), Built Environment and Public Health - *Proceedings of BEPH 2004*, Tsinghua University, pp. 355-364.

Qian, H., Y. Li, P.V. Nielsen, C.E. Hyldgaard, T. Wai Wong, and A.T.Y. Chwang. 2006. Dispersion of exhaled droplet nuclei in a two-bed hospital ward with three different ventilation systems. *Indoor Air* 16 (2): 111 – 128.

Riley, E.C., G. Murphy, and R.L. Riley. 1978. Airborne spread of measles in a suburban elementary-school. *American Journal of Epidemiology* 107: 421-432.

Wells, W.F. 1955. Airborne contagion and air hygiene: an ecological study of droplet infection. Cambridge, MA, *Harvard University Press*.

Appendix D
Airflow pattern generated by three air diffusers: Experimental and visual analysis

The paper presented in this Appendix is published in the *6 th Mediterranean Congress of Climatization*, Madrid/Spain 2-3 June 2011.

Airflow pattern generated by three air diffusers: Experimental and visual analysis

Inés Olmedo   **Peter V. Nielsen**   **Manuel Ruiz de Adana**

Rasmus L. Jensen

ABSTRACT

The correct description of air diffusers plays a crucial role in the CFD predictions of the airflow pattern into a room. The numerical simulation of air distribution in an indoor space is challenging because of the complicated airflow pattern generated.

Many authors have developed simplified geometry methods that approximate the diffusers to simplified openings where the discharge velocities and directions should be determined.

An experimental study has been carried out in order to take velocity measurements of the airflow pattern generated by three different air diffusers: displacement, mixing and a low impulse diffuser. Smoke visualization has been developed to determine the direction of the flow and observe the developed region of the jets.

Many conclusions can be drawn regarding the symmetry or unexpected asymmetry of the different airflow patterns, the impact of room conditions or developed regions of the jets. The experimental data obtained are crucial to validate CFD simulations with these diffusers in indoor spaces.

INTRODUCTION

The application of numerical methods for the analysis of the behaviour of airflow is being used increasingly. These techniques allow the possibility of having information about the airflow without the need to take measurements, in most of the cases.

However, it is important to determine the reliability of the simulations in question, so validation with experimental data is needed.

In the prediction of the airflow within a room one of the most influential parts is the terminal units, which will determine the behaviour of the air flowing into the room. Obviously, the terminal units provide a momentum flow to the air depending on the kind used.

Different studies (Lee, 2007; Srebric, 2006) have demonstrated the importance of the diffuser characteristics and the CFD boundary conditions in the distribution of airborne contaminant concentration, depending on the airflow generated, as well as furnishings and occupants, see also Nielsen (2004).

In the last years several authors have developed studies regarding different methods of simulation, analyzing the results that have been obtained. Some of the models which have been used for simulations in CFD up to now are the prescribed velocity method (Nielsen, 1997A), the box method (Nielsen, 1997B) and the momentum method (Chen and Moser, 1991). All of them requiere some previous experimental measurements, they have been validated and are recommended for the simulation of several diffusers (Kotani et al. 2002; Koskela, 2004; Huo et al 2000; Einberg et al. 2005; Srebric and Chen 2002). However, a comprehensive view of the airflow generated by the diffuser is a significant and necessary tool in order to prescribe the CFD boundary conditions in the most accurate way.

The purpose of this paper is to provide some useful data about the airflow generated by different air supply terminals. Smoke visualization has been used in order to obtain relevant information about the behaviour of the air close to the diffuser, as well as experimental velocity measurements that may define the velocity profile of the airflow generated by the diffusers.

METHODS

Test room

Figure 1 shows a sketch of the full-scale test room with the internal dimensions of 4.10 m (length), 3.20 m (width), and 2.70 m (height), used to carry out the experiments. The cold air is supplied at a temperature of 16ºC by three different diffusers: a wall-mounted semicircular diffuser, a four ways mixing diffuser and a ceiling-mounted textile diffuser, see figure 1. Only one diffuser was used in each test.

The textile diffuser consists of two terminal devices placed next to each other in the ceiling of the room. The position of the diffusers relative to the wall measured from the bottom left corner of the first diffuser is x: 0.60 m and y: 0.42 m. The centre of the displacement diffuser is placed in the middle of the left wall while the mixing diffuser is centred in the ceiling.

The air exchange rate was set to 5.6 h-1.
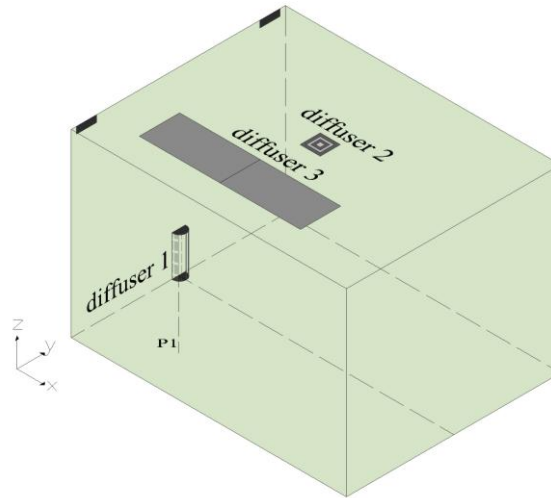
Figure 1 Sketch of the test room. Diffuser 1: Displacement diffuser placed in the middle of the wall; Diffuser 2: Mixing diffuser placed in the middle of the ceiling; Diffuser 3: Low-velocity textile diffuser.

The test chamber is provided with hot sphere anemometers, which were used to measure air velocity. The measurements were taken with a frequency of 10 ms for a period of 5 minutes in order to obtain stable values of the velocity.

RESULTS

Mixing diffuser

Figure 2(A) shows the velocity profile generated by the mixing diffuser. The measurements were taken at five different heights 2.65 m, 2.61 m, 2.57 m, 2.53 m and 2.49 m, which corresponds to L1, L2, L3, L4 and L5 respectively. Four anemometers were placed at 0.03 m from each side of the diffuser. The profile shows a symmetry in the airflow generated by the diffuser that is also possible to see with smoke visualization, see figure 2(B). The maximum velocities are obtained to the right and left sides of the

diffuser, which correspond to the sides with the largest separation distance from the walls, which means that the geometry of the room may influence the velocity profile.

A)
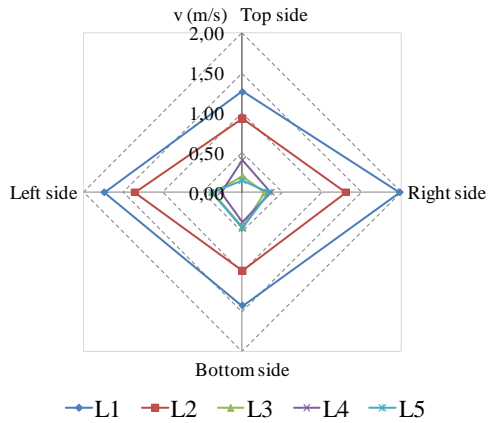
B)

Figure 2 (A) Velocity profile generated by the ceiling-mounted mixing diffuser (B) Airflow smoke visualization.

Displacement diffuser

Some measurements were also taken in order to define the velocity profile generated by the displacement diffuser at 0.01 m from the floor. Seven anemometers were placed along the line P1 separated by 0.20 m, see figure 1.

The results show an acceleration of the flow at 0.40 m from the diffuser. This velocity is reduced to a value close to 0.20 m/s at 1.40 m from the diffuser. Looking at figure 3(B) is possible to see the stratified flow generated by the cold supply air, which is common with a wall-mounted displacement diffuser.

A)

B)
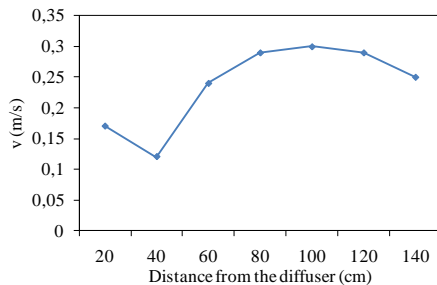
Low velocity diffuser

Finally a low impulse textile diffuser was also analyzed. The velocity was measured at twelve points along three horizontal lines placed 0.50 m below the diffuser, see figure 4.
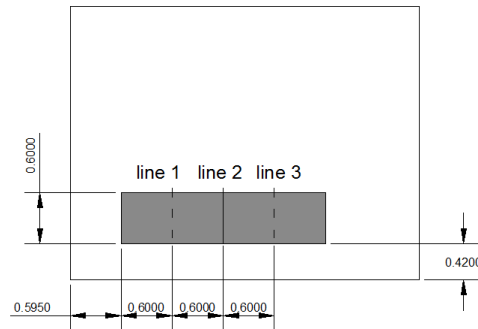
Figure 4 Top view of the test room with the horizontal lines along which the anemometers were placed.

Figure 5(A) shows the velocity profiles obtained along each of the lines. The maximum velocities are obtained close to the wall. The tendency of the air is to flow to the left part of the room which may be caused by the Coanda effect. This phenomenon has been visualized with smoke, see figure 5(B).
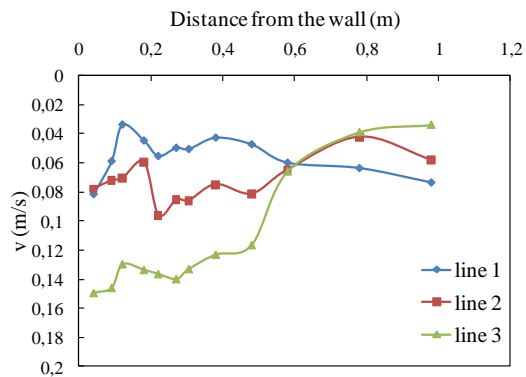
Figure 5 (A) Velocity profile of the textile diffuser at three different lines, (B) Smoke visualization of the airflow pattern.

CONCLUSIONS

Looking at the results, the following conclusions can be drawn:

- The position of the diffuser in the room has a significant influence on the airflow pattern generated. This influence is very large for the low-velocity textile diffuser where the effect of a very close wall to the diffuser has been observed, provoking a Coanda effect.

- Smoke visualization is a very useful tool in order to study the airflow pattern generated by different air terminal units. It can determine the most appropriate position of the anemometers in order to measure the velocity profile.

- The hypothesis of quasi-symmetry can be acceptable for the mixing ventilation case which has been validated by experimental measurements and smoke visualization.

REFERENCES

Chen, Q. and Moser, A. (1991) Simplification of a Multiple Nozzle Diffuser, Proc. Twelfth AIVC Conf., Vol. 2. Ottawa, Canada, 1-14.

Einberg, G., Hagström, K., Mustakallio, P., Koskela, H. and Holmberg, S. (2005) CFD modelling of an industrial air diffuser – predicting velocity and temperature in the near zone, *Building and Environment*, 40, 601-615.

Huo, Y., Haghighat, F., Zhang, J. and Shaw, C. (2000) A systematic approach to describe the air terminal device CFD simulation for room air distribution analysis, *Building and Environment*, 35, 563-576.

Koskela, H. (2004) Momentum source model for CFD-simulation of nozzle duct air diffuser, *Energy and Buildings*, 36, 1011-1020.

Kotani, H., Yamanaka, T. and Momoi, Y. (2002) CFD simulation of airflow in room with multi-cone ceiling diffuser using measured velocity and turbulent parameters in large space. *Proc. 8th Int. Conf. Air Distributions in Rooms (RoomVent 2002)*, Copenhagen, Denmark, 117-120.

Lee E. (2007) An investigation of air inlet types in mixing ventilation, *Building and Environment*, 42: 1089-1098.

Nielsen, P.V. (1997 A) The prescribed velocity method- A practical procedure for introduction of an air terminal device in CFD calculation. Department of Building Technology and Structural Engineering, Aalborg University 1997, Aalborg, Denmark.

Nielsen P.V. (1997 B) The box method – a practical procedure for introduction of an air terminal device in CFD calculation. Department of Building Technology and Structural Engineering, Aalborg University 1997, Aalborg, Denmark.

Nielsen, P.V. (2004) Computational fluid dynamics and room air movement, Indoor Air, 14(7): 134-143.

Srebric, J. and Chen, Q. (2002) Simplified numerical models for complex air supply diffusers, HVAC&Research, 8, 589-600.

Srebric J. (2006) CFD boundary conditions for contaminant dispersion, heat transfer and airflow simulations around human occupants in indoor environments, Building and Environment, 43: 294-303.

Appendix E
Experimental study about how the thermal plume affects the air quality a person breathes

EXPERIMENTAL STUDY ABOUT HOW THE THERMAL PLUME AFFECTS THE AIR QUALITY A PERSON BREATHES

Inés Olmedo[1], Peter V. Nielsen[2],Manuel Ruiz de Adana[1], Piotr Grzelecki[2], Rasmus L. Jensen[2]

[1]Department of Chemical Physics and Applied Thermodynamics, Córdoba University, Córdoba, Spain.
[2]Department of Civil Engineering, Aalborg University, Aalborg, Denmark.

Abstract

The Personal Micro Environment (PME) depends directly on the heat transfer in the surrounding environment. For the displacement ventilation systems the convective transport mechanism, which is found in the thermal plume around a person, influences the human exposure to pollutants.

The aim of this research is to increase the knowledge of how the thermal plume generated by a person affects the PME and therefore the concentration of contaminants in the inhalation area.

An experimental study in a displacement ventilation room was carried out. Experiments were developed in a full scale test chamber 4.10 m (length), 3.2 m (width), 2.7 m (height). The incoming air is distributed through a wall-mounted displacement diffuser. A breathing thermal manikin exhaling through the mouth and inhaling through the nose was used. A tracer gas, N_2O, was used to simulate the gaseous substances, which might be considered as biological contaminants, exhaled by the manikin.

The manikin was operated in three different heat fluxes with a value of: 0W, 94 W and 120 W.

During the experiments six concentration probes were situated in the room. Three concentration tubes were fixed on the surface of the manikin at three different heights: hips, chest and nose (inhalation). The three other tubes were situated in a vertical line at 0.50 m from the manikin and at the same three heights.

The results show the highest concentration of contaminants around the manikin when the manikin heat load is fixed to 0W. However, the concentration is significantly reduced in the case with 120 W, especially in the breathing area.

Keywords: thermal plumes, manikin, displacement ventilation, tracer gas

1   Introduction

Human exhalation flow is considered to be one of the most important biological contaminant sources in indoor environments. When a person is breathing, small droplets, that may contain pathogens, are generated and spread in the airflow. The contaminanted air can reach the breathing zone of other persons in the same room causing a risk of airborne cross-infection between people in the same room. This risk of cross-infection has been related to different parameters inside a room such as, the temperature gradient, the thermal loads or the airflow pattern generated by different ventilation systems (Nielsen et al. 2008; Nielsen et al.2010; Gao and Niu 2002).

The human body is not only a source of contaminants but also a heat source. The thermal plumes generated by the difference of temperature between the skin and the air generates an upward flow around the human body that makes the air from below the head go up and reach the inhalation area. This phenomenon has been studied by means of CFD (Hayashi et al. 2002) and experimental measurements (Zhu et al. 2005). Liu et al. (2009) studied the impact of different ventilation systems on the strenght of the thermal plumes generated by human bodies. Another recent study by Murakami (2004) concluded that the microenvironment around a human body directly affects the quality of air exhaled and inhaled by a person.

Therefore the heat flux emitted by a person is crucial to determine what is the quality of the inhaled air and from which parts around the human body it is coming.

When studying displacement ventilation the vertical temperature stratification provokes a clean area in the lower part of the room and a more polluted area close to the ceiling (Bjørn and Nielsen 2002). This kind of ventilation has also an effect on the thermal plume generated by a person making it weaker when large vertical temperature gradients take place (Kofoed and Nielsen 1990).

The aim of this study is to investigate the influence of the heat flux generated by a person in the origin and the quality of the air that a person is inhaling.

2   Methods

2.1   Test room and thermal manikin

Figure 1 shows a sketch of the full-scale test room used to carry out the experiment. The cold air was supplied by a wall-mounted semicircular diffuser, while two exhaust openings, same size, in the high part of the wall extract the air from the room, see figure 1.
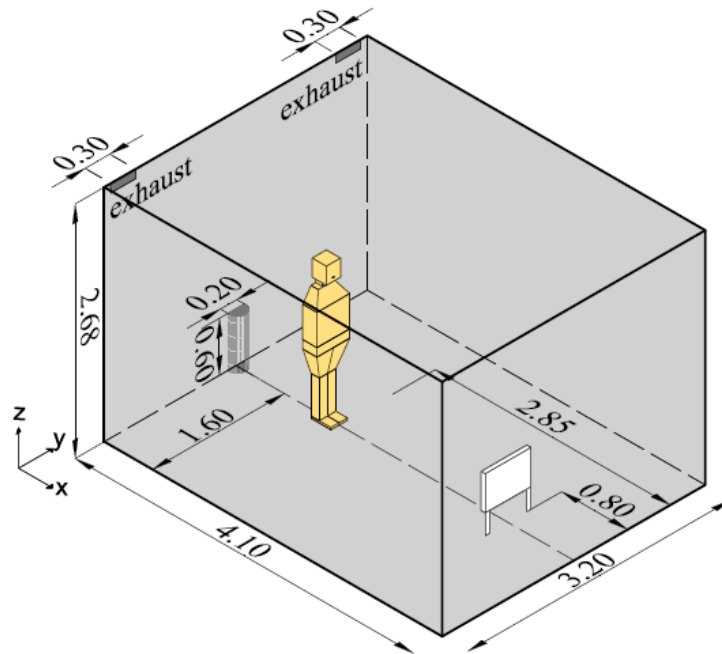
Figure 1. A) Sketch of the test room showing the position of the displacement diffuser, exhausts, radiator and thermal manikin.

A breathing thermal manikin without clothes, with an artificial lung, exhaling through the mouth and inhaling through the nose, was used to simulate human breathing. The exhalation rate was 11 l/min, the volume of exhaled air was set to 0.75 l per exhalation and the temperature at 34ºC. The heat power of the manikin was set to three different values: 0 W, 94 W corresponding to a superficial temperature of 29.9ºC and 120 W, superficial temperature of 31ºC. The manikin was 1.68 m high and the total unclothed surface area was about 1.4 m^2. The area of the manikin´s mouth, a_0, was 123 mm^2. The details of shape and size of the manikin can be found in Bjørn (1999). The same manikin is used as the contaminant source in the room by dosing the tracer gas, N_2O, in the exhalation flow thought the mouth of the manikin. This tracer gas is used to simulate the biological contaminants that can be contained in the exhaled air.

The velocity of the exhalation of the manikin was measured and it is possible to see the exhalation flow as a function of time in figure 2.
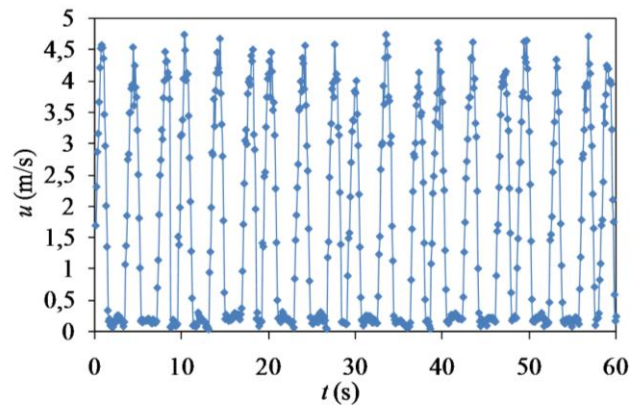
Figure 2. Velocity values at the mouth outlet. Data were recordered every 100 ms.

2.2   Measurements

N_2O concentrations were measured with a Multigas Monitor type 1412 and two Multipoint Sampler and Dosers type 1303, both manufactured by Brüel & Kjaer.

In addition, a radiator was situated in the room, with a thermal load of 394 W.

Both the manikin and the radiator were situated in the centre line of the room, along the x axis, see figure 1.

During the experiments the air change rate used was 5.6 h^{-1} and the temperature of the air supply to the room was set to 16 ºC in order to obtain a temperature of 20ºC in the occupied area.

The concentration measurements are taken in three vertical lines in the room, see figure 3.
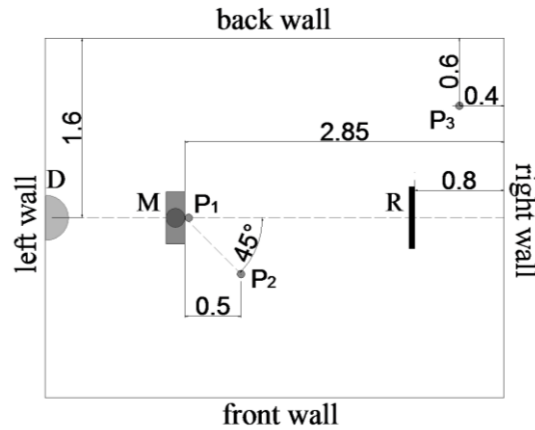
Figure 3. Placement of the vertical lines, P1, P2 and P3 in the room. All measurements in m.

3   Results

Figure 4 shows the contaminant concentration close to the manikin at threee different heights, the hips, the chest and the inhalation throught the nose. When increasing the heat flux of the manikin the concentration of contaminants was decreased at all heights. The three cases considered, 0 W, 94 W and 120 W, show a similar shape of the contaminants concentration profile where the highest amount of contaminants is in the inhalation area.
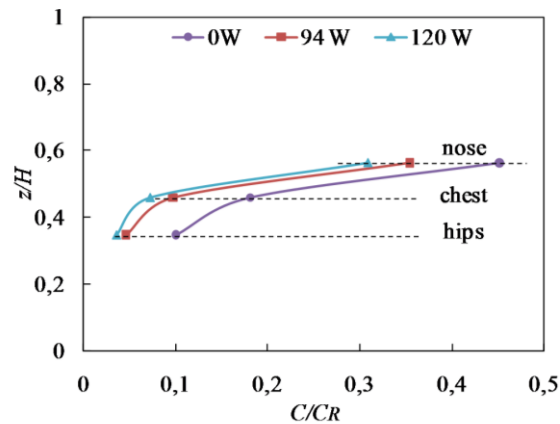
Figure 4. Concentration values in pole 1. The broken lines mark the heights of the nose, chest and hips of the manikin.

The same measurements were taken in pole 2, at 50 cm distance from the manikin. The results show a strong vertical contaminant gradient. The contaminant distribution is almost the same with the three heat loads used, see figure 5.
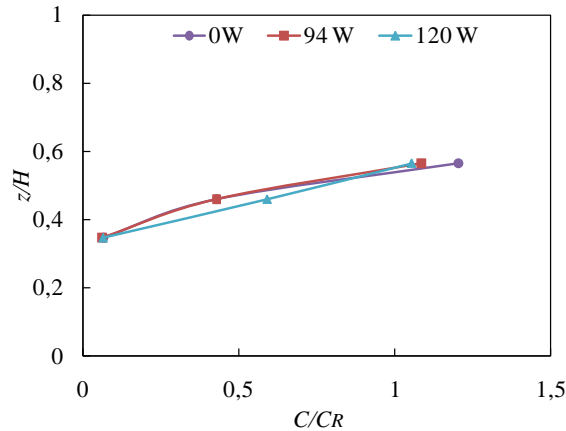
Figure 5. Concentration values in pole 2, at 50 cm from the manikin.

The vertical concentration gradient in the room for the three cases was measured in the vertical line, P3, showing a strong vertical gradient typical of a displacement ventilation system, see figure 6.
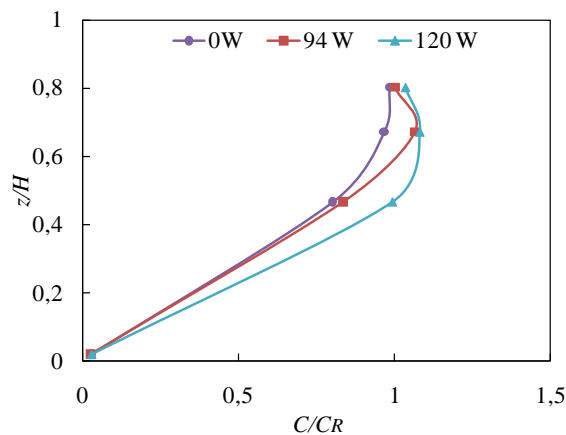
Figure 6. Concentration values in pole 3, in the room.

4   Conclusions

The concentration measurements taken in the boundary layer of the manikin show a high dependence on the heat flux emitted by the manikin. When increasing the thermal load of the manikin the contaminants concentration around the manikin decreases significantly. However, in the case without any heat load in the manikin the concentration around it is much higher than in the other two cases.

It means that the manikin´s heat load induces clean air from the bottom part of the room that goes up and reaches the chest and inhalation area (nose). The strength of the body plume influences the micro environment around a person and therefore affects the quality of the air a person inhales. In fact, the lower concentration of contaminants in the inhalation area is found in the case where the power was set to 120 W.

All in all, the results show an influence of the manikin´s boundary layer on the contaminant distribution around it which directly affects the air quality that a person is

breathing and can be determinant, e.g., in the risk of cross infection between people in a room.

Further studies are recommended in order to gain knowledge of the key parameters that directly can affect the air quality and contaminant distribution in indoor environments.

5   References

Bjørn, E. (1999) *Simulation of Human Respiration with Breathing Thermal Manikin*, Aalborg, Denmark, Department of Building and Structural Engineering, Aalborg University

Bjørn, E. and Nielsen, P.V. (2002) *Dispersal of exhaled air and personal exposure in displacement ventilated room*, Indoor Air, 12, 147-164

Gao, N., Niu, J. (2006) *Transient CFD simulation of the respiration process and inter-person exposure* assessment, Building and Environment, 41, 1214-1222

Hayashi, T., Ishizu, Y., Kato, S., and Murakami, S. (2002) *CFD analysis on the characteristics of contaminated indoor air ventilation and its application in the evaluation of the effects of contaminant inhalation by a human occupant*, Building and Environment, 37, pp. 219-230

Kofoed, P. and Nielsen, P.V. (1990) *Thermal plumes in ventilated rooms*. Room Vent 1990, Oslo

Liu, L., Nielsen P.V., Li Y., Jensen R.L., Litewnicki M., and Zajas J. (2009) A. *The thermal plume above a human body exposed to different air distribution strategies.* Healthy Buildings 2009, Syracuse

Murakami, S. (2004) *Analysis and design of micro-environment around the human body with respiration by CFD*, Indoor Air, 14, pp. 144-156

Nielsen, P.V., Buus, M., Winther, F.V. and Thilageswaran, M. (2008) *Contaminant flow in the microenvironment between people under different ventilation conditions,* ASHRAE Transactions, 114, part 2

Nielsen P.V., Olmedo I., Ruiz de Adana M., Grzelecki P., and Jensen R.L. (2010) *Airborne Cross Infection between two people in a displacement ventilated room*. Indoor Air Quality 2010, Malaysia

Zhu, S., Kato, S., Murakami, S., and Hayashi, T. (2005) *Study on inhalation region by means of CFD analysis and experiment*, Building and Environment, 40, pp. 1329-1336

Appendix F
Distribution of exhaled contaminants and personal exposure in a room using three different air distribution strategies

Distribution of exhaled contaminants and personal exposure in a room using three different air distribution strategies

Abstract The level of exposure to human exhaled contaminants in a room depends not only on the air distribution system but also on people's different positions, the distance between them, people's activity level and height, direction of exhalation, and the surrounding temperature and temperature gradient. Human exhalation is studied in detail for different distribution systems: displacement and mixing ventilation as well as a system without mechanical ventilation. Two thermal manikins breathing through the mouth are used to simulate the exposure to human exhaled contaminants. The position and distance between the manikins are changed to study the influence on the level of exposure. The results show that the air exhaled by a manikin flows a longer distance with a higher concentration in case of displacement ventilation than in the other two cases, indicating a significant exposure to the contaminants for one person positioned in front of another. However, in all three cases, the exhalation flow of the source penetrates the thermal plume, causing an increase in the concentration of contaminants in front of the target person. The results are significantly dependent on the distance and position between the two manikins in all three cases.

I. Olmedo[1], P. V. Nielsen[2], M. Ruiz de Adana[1], R. L. Jensen[2], P. Grzelecki[2]

[1]Department of Chemical Physics and Applied Thermodynamics, Córdoba University, Córdoba, Spain, [2]Department of Civil Engineering, Aalborg, Aalborg University, Denmark

Key words: Personal exposure; Human breathing; Thermal manikins; Displacement ventilation.

I. Olmedo
Department of Chemical Physics and Applied Thermodynamics
Leonardo Da Vinci Building-Campus of Rabanales km 396a, Madrid-Cadiz Road
14071 Córdoba, Córdoba University
Spain
Tel.: +34 957 212203
Fax: +34 957 218417
e-mail: ines.olmedo@uco.es

Practical Implications

Indoor environments are susceptible to contaminant exposure, as contaminants can easily spread in the air. Human breathing is one of the most important biological contaminant sources, as the exhaled air can contain different pathogens such as viruses and bacteria. This paper addresses the human exhalation flow and its behavior in connection with different ventilation strategies, as well as the interaction between two people in a room. This is a key factor for studying the airborne infection risk when the room is occupied by several persons. The paper only takes into account the airborne part of the infection risk.

Nomenclature

a_0	area of the manikin's mouth (m²)
c	tracer gas concentration (ppm)
c_0	peak concentration at the manikin's mouth (ppm)
c_{10}	tracer gas concentration 0.10 m above the head (ppm)
c_{chest}	tracer gas concentration at the chest (ppm)
c_{exp}	tracer gas concentration in the inhalation (ppm)
c_R	tracer gas concentration in the return (ppm)
c_s	tracer gas concentration surrounding the manikin (ppm)
c_x	tracer gas concentration at a horizontal distance from the mouth (ppm)
H	height of the test room (m)
K_c	characteristic concentration constant
K_{exp}	characteristic velocity constant
n_1	characteristic velocity exponent
n_2	characteristic concentration exponent
T	absolute air temperature (K)
T_0	exhaled air temperature (K)
T_{amb}	air temperature at the height of the manikin's mouth (K)
T_{in}	supply air temperature (K)
T_{out}	return air temperature (K)
u_0	peak velocity in the manikin's mouth (m/s)
u_x	peak velocity at a horizontal distance from the manikin's mouth (m/s)
x	horizontal distance (m)
z	vertical distance (m)

Introduction

There are different pathways of pathogen transport such as direct or indirect contact with an infected person, see Morawska et al. (2009). However, the transmission via inhalation of airborne particles is a very significant form of pathogen transport. Expiratory droplet nuclei generated by an infected person can spread in the air through the airflow pattern and may increase the pathogen concentration in different indoor environment areas, see Chao et al. (2009).

In recent years, an interest in understanding the mechanism of airborne infection between people in the same room has increased significantly. It is realized that an infectious person can spread airborne pollutants and provoke a possible cross-infection to other persons in the room (Richmond-Bryant et al., 2006). It can be illustrated by tracer gas experiments, see Bjørn and Nielsen, 2002 and Nielsen, 2009.

As the exposure to infectious airborne pathogens is higher in hospitals, some studies have focused the investigation on hospital rooms (Cheong and Phua, 2006; Nielsen et al., 2010; Qian et al., 2006, 2008). Some of these results show that the ventilation systems, the air exchange rate, the breathing functions, the thermal loads, and the position, orientation, and separation distance between people are crucial factors for understanding, controlling, and predicting the mechanisms of infectious disease transmission. Other recent studies by Li et al. (2005, 2007) reveal the importance of the ventilation systems in a possible cross-infection between people, concluding that there is a close connection between the ventilation systems and the infectious transmission in the air.

The personal exposure to pollutants in ventilated rooms has been studied involving full-scale experiments, (Bjørn and Nielsen, 2002; Brohus and Nielsen, 1996), and the results for an exposure of the target person show the influence of the separation distance between the source and the target person. The displacement ventilation system supplies cool air at floor level. The air is heated by the heat sources, such as the occupants, and creates a vertical temperature gradient, as well as two zones. The lower zone consists of clean supply air, and the upper zone of air is contaminated by the heat sources. This system was originally believed to be an efficient system producing a clean area in the breathing zone of the room (He et al., 2005). However, the temperature gradient may, on the other hand, result in high concentration at different heights, e.g., the breathing zone as shown by Bjørn and Nielsen (2002) and Qian et al. (2006), causing a reduced protection against the exposure to contaminants. Another recent study by Lee et al. (2005) concluded that a mixing ventilation system could reduce the exposure from contaminants in office buildings, depending on the person's position in the room. These results agree with Nielsen et al. (2008), which showed that full mixing of the air can limit the concentration of the pollutants in the breathing zone of the exposed person.

The main objective of the present work is to investigate the effectiveness of the different ventilation methods to remove exhaled contaminants as well as to investigate the influence of these ventilation systems on the airflow pattern generated by a person's exhalation.

The droplet nuclei smaller than 10 μm are the majority generated in the human exhalation flow through the mouth, see Morawska et al. (2009), and they follow the air stream owing to their small size and they are not deposited. The airborne behavior for small droplets has been observed in several studies (Chao et al., 2008; Chen and Zhao, 2010; Lai and Cheng, 2007), while particles larger than 10 μm are more influenced by gravitational effects and they are deposited faster (Chao and Wan, 2007; Chen et al., 2009). Consequently, the exhaled air may be effective in the transportation of organisms, such as viruses that may be carried in these very fine droplets, see Nicas et al. (2005) and Morawska (2006). It is therefore possible to simulate the droplet nuclei using tracer gas because the air distribution of tracer gas is identical to the distribution of droplet nuclei (Tang et al., 2011).

A person's exhalation flow is studied to create a description of the velocity distribution and the concentration distribution around the person. The measurements are taken in a room with three different air distribution systems creating different environments around the person. The exhalation flow of a person is considered as the pollutant to investigate the mechanism of spreading respiratory diseases. Finally, studies are made to show how this exhalation flow can provoke a high exposure to other persons situated in the same room as the source. The level of exposure is measured for the first time for different positions and separation distances between the manikins and for three ventilation strategies: displacement ventilation, mixing ventilation, and nonmechanical ventilation in a room with otherwise similar conditions.

A preliminary report that focused on the displacement ventilation conditions has already been published (Nielsen et al., 2012). Continuing this work, the present paper provides a more thorough analysis, considering three different ventilation modes in further details.

Test room and test equipment

Test room

Figure 1a shows the full-scale room, 4.10 m (length), 3.19 m (width), and 2.68 m (height) where the experiments are carried out. Two different air distribution systems are used: a displacement ventilation system and a mixing ventilation system. For the mixing
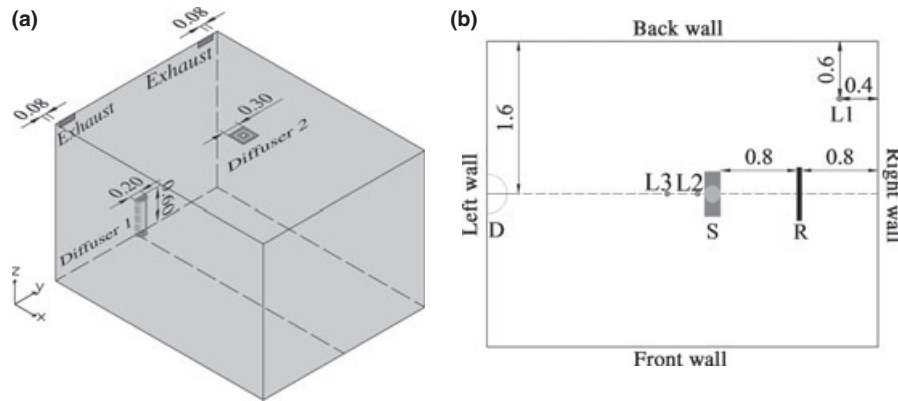
Fig. 1 (a) Sketch of the test chamber and location of the diffusers and exhaust (diffuser 1, wall-mounted displacement diffuser; diffuser 2, square ceiling diffuser), (b) Experimental setup with vertical measuring location 1, 2, and 3 (L1, L2, and L3, respectively). The position of L3 is changed with the separation distances between the manikins, displacement diffuser (D), source manikin (S), and radiator (R). All distances are in meters

ventilation case, a four-way square diffuser is mounted in the center of the ceiling to produce a well-mixed flow field. For the displacement case, a wall-mounted semicircular diffuser is placed in the middle of the left wall. Two return openings, 0.30 m (length) and 0.10 m (width) each, are located in the left wall below the ceiling and used in both cases, see Figure 1a.

The ventilation system provides cold air supply at 16°C, and the air exchange rate is set to 5.6/h. In this way, the mean temperature in the occupied zone is maintained at 22 ± 1°C, and a typical vertical temperature distribution is created in the room in case of displacement ventilation. Before starting each experiment, the steady-state conditions are obtained using at least 5 h to stabilize the temperature in the room.

The experiments for displacement ventilation and mixing ventilation are carried out under steady-state conditions, which mean that the temperature inside the room is monitored and kept at the same level, ±0.5°C. The manikins have a time-dependent breathing function. The exposure in this study is calculated in each test using the average concentration values in the inhalation of the target manikin divided by the exhaust concentration of the room. Using this expression, a higher exposure is equivalent to a higher risk of airborne infection between the contaminated and the exposed person simulated by the source and the target manikins, respectively. The exposure at the chest and above the head of the target manikin is also calculated using the average concentration at these positions, to analyze the contaminant exposure in the microenvironment around the manikin. This expression for the exposure is called 'susceptible exposure index' by Qian and Li (2010).

In addition, an experiment without any air distribution system is carried out. The steady-state conditions are in this case maintained by having an open door between the laboratory and the test room. The temperature in the laboratory is maintained at 22 ± 1°C by a radiator-based heating system. The

volume and size of the laboratory ensure the steady-state conditions during the measuring period.

Breathing thermal manikins and thermal loads

One or two thermal manikins with breathing function are used during the experiments. The manikins are 1.68 m, average-sized women, and the total surface area without clothes is about 1.40 m². The manikins have a human body shape to be able to accurately simulate the thermal plume generated by a person, see Zukowska et al. (2008). For details of body shape, see Bjørn (1999). With regard to the mouth openings, there are slight differences for the two manikins. For the source manikin, the mouth has a 123 mm² opening and a semi-ellipsoid form, and for the target manikin, the mouth consists of a circular opening of diameter of 12 mm. Both manikins exhale the air through the mouth and inhale through the nose. The nose consists of two circular nostrils, with a 6 mm radius each, situated 10 mm above the mouth and facing downwards at a direction of 45º below horizontal plane.

The artificial lungs produce a sinusoidal breathing flow. They can be set to provide a given simulation of the breathing flow with the suitable pulmonary ventilation rate, frequency, gas concentration (in the source manikin), and temperature of the exhaled air.

One of the manikins is used as the source, in which the artificial lung is adjusted to simulate a pulmonary ventilation of 0.57 l per breathing sequence, having 19 breathing cycles per minute. The other manikin is considered the target with a pulmonary ventilation of 0.66 l per breathing sequence, having 15 breathing cycles per minute. The temperature of the exhaled air is kept at 34 ± 0.5°C using two small heaters mounted in the supply air tubes, which simulate human exhaled air saturated with water vapor at 31°C, see Bjørn (1999). This temperature is corrected to compensate for relative humidity in human exhalation. The direction

3

of the exhaled air is to be set horizontally from the mouth using smoke visualization at the beginning of each experiment. It should be mentioned that the direction, as well as different heights of the two manikins, has a large influence on the resulting measurement of the exposure level, but this effect has not been considered in this article.

N_2O is used as tracer gas. It is an invisible and odorless gas, which has a density similar to air. N_2O is mixed into the supply air in front of the air heater to simulate the exhalation of contaminated air from the source manikin. The amount of tracer gas exhaled through the source manikin's mouth is 0.30 l/min.

The velocity and concentration of the exhalation flow are measured at the mouth opening to determine the maximum values, velocity u_0, and maximum concentration c_0 in the breathing. The peak velocity value obtained with the measurements is 4.74 m/s. For the N_2O gas concentration, the maximum mean value obtained during the test is 6687 ppm.

A radiator in the room maintains a constant mean air temperature in the occupied zone. The total heat load in the room for all the cases is 488 W, each manikin responsible for 94 W. The heat load of the radiator is increased or decreased depending on the number of manikins in the room.

Tests with different positions of the manikins are carried out. The layouts of each test are shown in Table 1. Table 2 shows the heat loads used during each test, and the averaged surface temperatures of the manikins are calculated as the average of the measurements of three thermocouples placed at the chest, the hips, and the back of each manikin.

During all the experiments, the manikins are placed along the centerline of the room in the direction of the x axis. For the tests with two manikins, the source manikin is always located at 0.80 m from the radiator, measured from the back, and the target manikin is moved to obtain the different separation distances: 0.35, 0.50, 0.80, and 1.10 m from nose to nose or to the back of the head. Figure 1 shows the centerline where the manikins are positioned during all the tests, the position of the source manikin and the location of the radiator.

For the tests with one manikin, the source is situated at 2.70 m from the right wall facing it. The radiator is placed in the same position as in other experiments. Figure 2 shows the different positions of the manikins in all the experiments.

Test equipment and measurements

The air temperature in the test room is measured during all the tests with thermocouples type K and a data logger. Five thermocouples are located in the vertical measuring line L1, see Figure 1b, at different heights for all the tests carried out to measure the

Table 1 Experimental tests

Test	Manikins	Air ventilation system	Position of the manikins	Distance between the manikins (m)
1	1	Displacement	Standing	–
2	1	Mixing	Standing	–
3	1	Without ventilation	Standing	–
4	2	Displacement	Two manikins standing face to face	0.35
				0.50
				0.80
				1.10
5	2	Displacement	Two manikins standing face to side	0.35
				0.50
				0.80
				1.10
6	2	Displacement	Two manikins standing back to face	0.35[a]
				0.50[a]
				0.80[a]
				1.10[a]
7	2	Displacement	Source sitting and target standing	0.70[b]
				1.10
8	2	Mixing	Two manikins standing face to face	0.35
				0.50
				0.80
				1.10
9	2	Mixing	Source sitting and target standing	0.70
				1.10
10	2	Without ventilation	Standing face to face	0.35
				0.50
				0.80
				1.10

[a]For test 6, the separation distance between the manikin is measured from nose to back of the head.
[b]For the test with the sitting source manikin, the minimum distance between the manikins' mouths is 0.70 m, owing to the geometry of the manikins.

Table 2 Heat loads for the tests

	Manikin heat flux (W)	Averaged Surface Temperature of the manikin (°C)	Radiator heat load (W)
Tests 1–3	94	29.7	394
Tests 4–10	94	29.7	300

temperature gradient in the room, see Figure 4a. The thermocouples are calibrated using an isothermal calibration device (Isocal-6 Venus 2140 B, Isotech North America, Colchester, VT, USA) and a high precision thermometer as a reference. Each thermocouple is calibrated for a temperature range of 10–45°C. The accuracy of the temperature measurements considering the uncertainties of the probe, wire length, and the data acquisition equipment is ± 0.5°C of the reading. The frequency of temperature measurements is 30 s.

The N_2O gas concentration is measured at several locations with a Multi gas Monitor type 1412 and two Multipoint Sampler and Doser type 1303, both
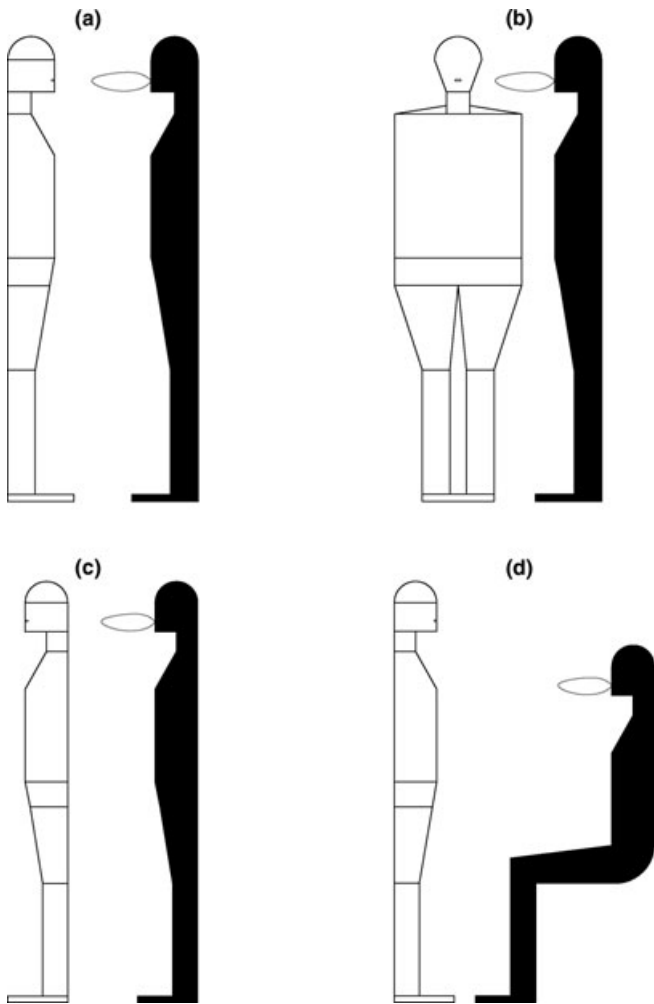
Fig. 2 Positions of the manikins in the room (source in black, target in white) (a) Manikins standing face to face, (b) Manikins standing face to side, (c) Manikins standing face to back, (d) Source manikin seated and target manikin standing

manufactured by Brüel & Kjaer (Skodsborgvej, Naerum, Denmark). The concentration is measured at eleven positions through plastic tubes inside the test room and measured at one position in the laboratory owing to safety reasons. The accuracy of the concentration measurements is ±1%. Velocities are measured with Dantec 54R10 hot sphere anemometers (Dantec

Dynamics, Tonsbakken, Skovlunde, Denmark), which are calibrated in a wind tunnel measuring the voltage and the real velocity value using pressure difference values. The measurements are taken with a precision of ±5% at a frequency of 100 ms.

For the cases with one manikin, only five gas samplers and five anemometers are used to measure the concentration and velocity in the exhalation flow of the breathing. The sensors are situated along the centerline of the exhalation flow to measure the peak centerline values. These five positions are found visualizing the exhalation flow with smoke. Five anemometers are placed along the visualized centerline to measure the instantaneous velocity. After locating the anemometers, smoke is used to confirm that their positions correspond to the centerline of the exhalation airflow previously visualized. This process is repeated until the five positions along the centerline are found to measure the maximum velocities. The locations of thermocouples and concentration tubes in cases with two manikins are shown in Figure 3 and Table 3.

Results and discussion

Temperature and concentration gradients with the three air distribution principles

In the cases with displacement and mixing ventilation, the temperature and concentration level are made dimensionless using T_{in}, T_{out}, and c_R, as shown in the following figures. The measurements of the vertical temperature and concentration gradients are taken in the vertical line L1, see Figure 3.

For each ventilation principle, the vertical temperature profile and concentration profile are measured in all the cases. However, the thermal conditions are kept at the same level when using one or two manikins in the room and are independent of the manikin's position, so only the results of the two manikins facing each other are shown.

It is possible to observe a vertical temperature gradient, which is typical in displacement ventilation when there is a combination of two heat sources, see Figure 4a. It is also quite a common situation to obtain a concentration peak of contaminants in a layer at the
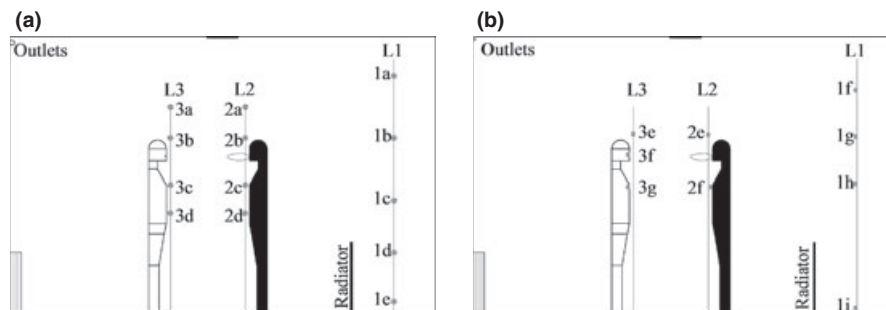
Fig. 3 (a) Locations of the thermocouples, (b) Locations of the gas concentration tubes

Table 3 Positions of thermocouples and concentration tubes for all the tests

Position thermocouples	Height (m)	Position gas tubes	Height (m)
1a	2.30	1f	2.15
1b	1.70	1g	1.70
1c	1.10	1h	1.25
1d	0.60	1i	0.05
1e	0.10	2e, standing/seated	1.76/1.46 (chest)
2a, 3a	2.00	2f, standing/seated	1.40/1.10 (chest)
2b, 3b	1.70	3e	1.70
2c, 3c	1.25	3f	1.53 (nose)
2d, 3d	0.98	3g	1.25

height of the source when this source is not the main heat load in the room, see Bjørn and Nielsen, 2002 and Qian et al., 2006. The contaminant is exhaled by the source manikin at the height of 1.52 m, and this therefore explains the peak concentration value shown in Figure 4b.

Figure 5 shows the vertical temperature and concentration gradients for the mixing ventilation case with values very close to 1.0, which means that the air is fully mixed in the room.

Figure 6 shows the vertical temperature and concentration profile measured during the experiments carried out without a ventilation system in operation. The results show absolute values of temperature and concentration because of the conditions of the experiment, where the supply and return of the air are not controlled by any system. It is noticeable that a small vertical temperature gradient is obtained, see Figure 6a. Furthermore, measurements show an
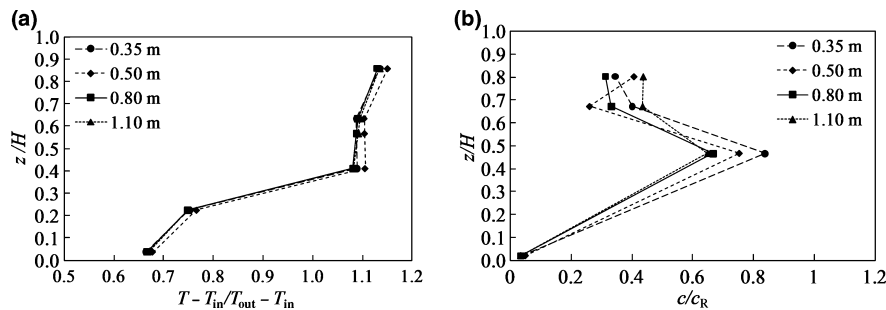
Fig. 4 Vertical gradients in the room with displacement ventilation for the different separation distances: 0.35, 0.50, 0.85, and 1.10 m. (a) Temperature gradient, (b) Concentration gradient
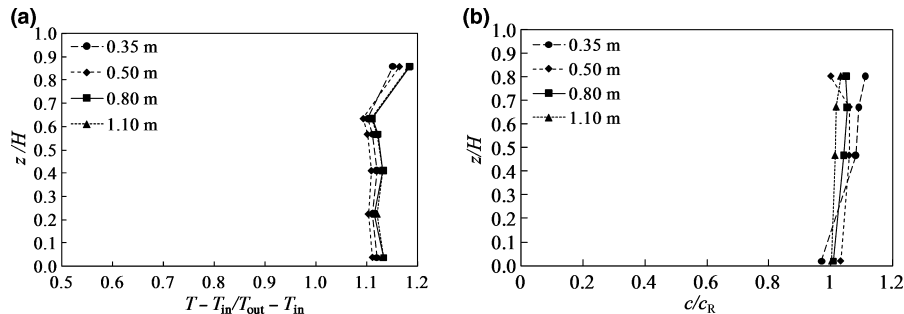
Fig. 5 Vertical gradients in the room with mixing ventilation for the different separation distances: 0.35, 0.50, 0.85, and 1.10 m. (a) Temperature gradient, (b) Concentration gradient
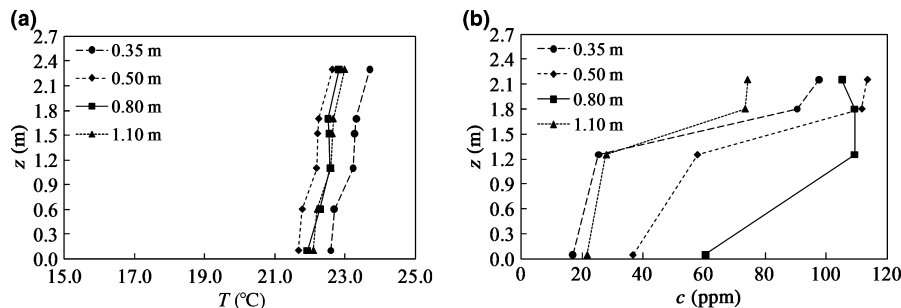
Fig. 6 Vertical gradients in the room without any air distribution system for the different separation distances: 0.35, 0.50, 0.85, and 1.10 m. (a) Temperature gradient, (b) Concentration gradient

evident concentration of contaminants around the breathing area caused by the lack of ventilation, see Figure 6b.

Characteristics of the exhalation from a single manikin

One manikin is used to study the exhalation flow profile with three different ventilation principles: displacement ventilation, mixing ventilation, and without mechanical ventilation, to study the influence of the air distribution design on the human exhalation inside a room.

Human exhalation can be considered partly as a vortex ring and partly as an instantaneous turbulent jet, and it is given as a sinusoidal function of time (Gupta et al., 2010). Nielsen et al. (2009) have shown that peak values for exhalation velocity of the instantaneous human exhalation flow can be described by an expression where the peak velocity is a linear function of the reciprocal horizontal distance from the mouth (Similar to the expression for the centerline velocity in a free jet).

$$\frac{u_x}{u_o} = K_{exp} \cdot \left(\frac{x}{\sqrt{a_o}}\right)^{n_1} \tag{1}$$

K_{exp} is a characteristic constant, a_0 the area of the mouth, x the horizontal distance from the mouth where the measurements are taken, and u_x and u_o are the peak values of the velocity at distance x and in the mouth, respectively. In the same way, peak concentration values of the samples measured during breathing are also related to positions, as shown in the following equation:

$$\frac{c_x - c_s}{c_o - c_s} = K_c \cdot \left(\frac{x}{\sqrt{a_o}}\right)^{n_2} \tag{2}$$

where K_c is a characteristic constant, and c_x, c_0, and c_S are peak concentration values measured at a horizontal distance x from the mouth, in the mouth, and in the surroundings, respectively. The values of c_s are measured at the chest of the manikin. It is important to point out that the measured peak concentration is influenced by the measuring equipment where some averaging takes place.

To find the penetration of the exhalation flow with the three ventilation strategies, five anemometers and five concentration tubes are fixed in the centerline of the exhalation jet, as was explained in the previous section. Figure 7 shows the height and the horizontal distance from the source manikin's mouth to the five positions of maximum concentration and maximum peak velocity for the three ventilation principles.
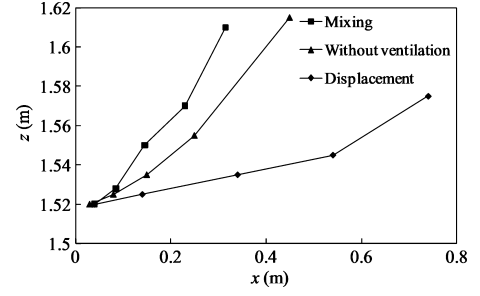
Fig. 7 Location of the exhalation flow from the mouth with respect to peak velocity and concentration. The height of the manikin's mouth is at 1.52 m

The trajectories obtained for the exhalation flows in Figure 7 are in agreement with the theory of the nonisothermal exhalation flow shown by Xie et al. (2007). The penetration of the exhalation flow is not only dependent on the temperature difference between the exhaled and the surrounding air, but it is also dependent on the vertical temperature gradient in the area of the exhalation and therefore on the ventilation and air distribution strategy, see Qian et al. (2006). For all the tests, the average ambient temperature at the head height of the source manikin is calculated as the interpolated temperature at the height of the exhalation between thermocouples in positions 2b and 2c. The temperature of the exhalation flow is maintained constant at 34°C. The temperature difference between the exhalation flow and the ambient temperature in the room, $T_{amb} = 23.6°C$, is $T_0 - T_{amb} = 10.4°C$ for the displacement case. This is the lowest measured value, $T_0 - T_{amb}$, and the exhalation flows a further distance and maintains a more horizontal direction than in case of mixing ventilation or in the case without ventilation. For the nonmechanical ventilation case and for the mixing ventilation case, the ambient temperatures in the room are $T_{amb} = 22.8$ and 22.9°C, respectively, which show the corresponding temperature differences of 11.1 and 11.2°C. In both cases, the directions of the exhaled air show slight variations and the air rises significantly more vertically than in the displacement ventilation case.

The difference in the vertical direction of the exhalation is important with respect to the discussion of personal exposure. The temperature gradient connected to a displacement ventilation system seems to retain the exhalation in head height of surrounding persons, while mixing ventilation allows the exhalation to rise above head height. This effect has also been shown by smoke experiments; see Nielsen et al. (2009).

Equation (1) can be used to describe the human exhalation flow through the mouth with the three air distribution systems considered. Figure 8 is the graphic representation of the Equation (1) for the exhalation flow with the three air distribution principles.
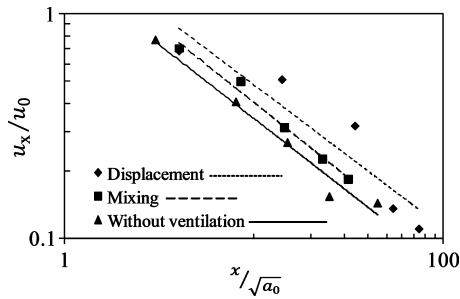
Fig. 8 Log–log graph of the velocity values at certain distances
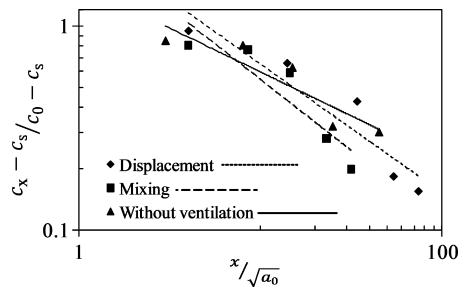
Fig. 9 Log–log graph of the concentration values at certain distances

Table 4 Constants of exposure flow obtained with the three air distribution systems

Air distribution system	K_{exp}	K_c
Displacement ventilation	7.5	10.8
Mixing ventilation	4.5	6.3
Without ventilation	4.5	8.5

The values obtained for the n_1 constants are −0.64, −0.68, and −0.66 for the three cases: displacement ventilation, mixing ventilation, and nonventilation, respectively. Concentration values for the exhalation flow obtained by displacement ventilation, mixing ventilation, and nonventilation are shown in Figure 9.

The maximum mean concentration is measured over a 4 h period in each test. The exponent n_2 is equal to −0.63 and −0.69 for displacement ventilation and mixing ventilation. Under nonventilation, however, the slope, n_2, is −0.43, which differs considerably from the values obtained by displacement and mixing ventilation. The characteristic constants for the three cases are given in Table 4.

The low level of the exponent n_2 for displacement ventilation is probably another important effect of the vertical temperature gradient. It could be explained by the damping effect that the temperature gradient has on the turbulence, and it may have the effect that entrainment into the exhalation flow is decreased and the concentration in the exhalation flow is retained. This effect is also mentioned in the measurements of Nielsen et al. (2009), and it has the consequence that the personal exposure is increased as shown later in Figure 10 and is also shown by Nielsen et al. (2008).

Two manikins in a room with displacement ventilation

Figure 10 shows the results for test 4, where the manikins are facing each other. The exhalation flow follows the line indicated in Figure 10b. A clean area is maintained at the height of the chest in all the cases with an exposure level close to zero, which is typical of displacement ventilation, although the cleanest zone may be lower. The upward flow in the plume around the manikin ensures a concentration value, which is strongly influenced by the concentration in the low zone. This low level of concentration is considered to be the advantage of displacement ventilation in situations where the contaminant sources have a large heat release that carries contaminant to the ceiling level. Displacement ventilation can create a clean low zone, but it will also create a zone with higher concentration of exhaled contaminants because the exhalation is a weak heat source, see Li et al. (2011). This high level of

Fig. 10 (a) Comparison of the exposure concentration values in the inhalation (c_{exp}/c_R), the chest (c_{chest}/c_R), and above the head of the target manikin (c_{10}/c_R) for test 4, (b) Location of the three measured points and breathing flow of a single source manikin in the displacement ventilation case. The two manikins indicate a distance of 0.35 m

concentration is shown in the exposure of the target manikin, reaching a maximum value of 12.0 at a separation distance of 0.35 m. However, this concentration exposure c_{exp}/c_R decreases as the separation distance increases. This result is similar to the data obtained by Bjørn and Nielsen (2002) and Nielsen et al. (2008) for the face-to-face values, and it shows that the contaminated exhalation flow can penetrate the breathing zone of a standing person who faces the manikin and produces an exposure level of several times the return concentration in the room. The high exposure level obtained in Figure 10 indicates that displacement ventilation is an inefficient solution when personal exposure should be minimized as in e.g., hospitals and health care facilities.

The concentration above the head of the target manikin is also high. This effect is provoked by the exhalation flow that rises because of the exhalation temperature and the temperature difference with the surrounding air. The maximum concentration value at this position is for a separation distance of 0.50 m. At the distance of 0.35 m, the value is less; this is

probably because of the direction of the flow at this reduced distance. It is necessary to have a separation distance larger than 0.35 m to have a significant elevation of the flow, as it is shown in Figure 7. For a separation distance of more than 0.50 m, the concentration values in the inhalation and above the head likewise decrease because of the elevation of the exhalation flow and because of the entrainment of the surrounding air.

The measurement results for the two manikins standing in the face-to-side position, test 5, are show in Figure 11. The exposure concentration c_{exp}/c_R is also high, with values very close to 7.0 and 6.0 for the separation distances of 0.35 and 0.50 m, respectively. However, the value is significantly reduced when the distance is more than 0.50 m. It is important to notice that the concentration values above the head of the target manikin are higher than the exposure values. The relative position of the target manikin may cause a different microenvironment and allow the contaminated exhalation flow to move upward above the head of the target manikin. The results close to zero at the

Fig. 11 (a) Comparison of the exposure concentration values in the inhalation (c_{exp}/c_R), the chest (c_{chest}/c_R), and above the head of the target manikin (c_{10}/c_R) for test 5, (b) Location of the three measured points and breathing flow of the source manikin in the displacement ventilation case. The two manikins indicate a distance of 0.35 m

Fig. 12 (a) Comparison of the exposure concentration values in the inhalation (c_{exp}/c_R), the chest (c_{chest}/c_R), and above the head of the target manikin (c_{10}/c_R) for test 6, (b) Location of the three measured points and breathing flow of the source manikin in the displacement ventilation case. The two manikins indicate a distance of 0.35 m
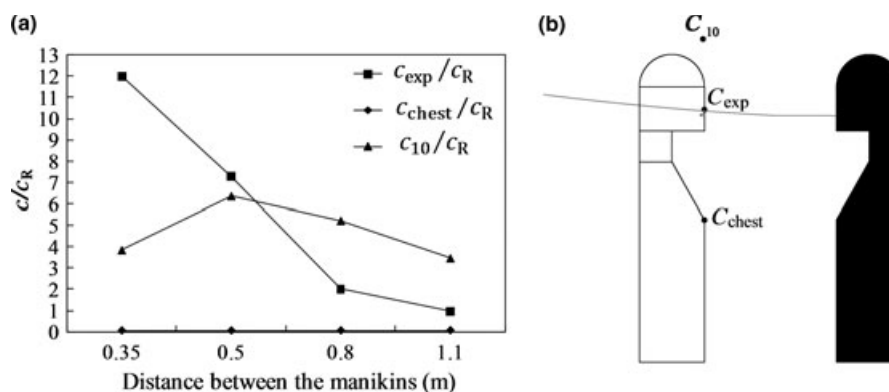
Fig. 13 (a) Comparison of the exposure concentration values in the inhalation (c_{exp}/c_R), the chest (c_{chest}/c_R), and above the head of the target manikin (c_{10}/c_R) test 7, (b) Location of the three measured points and breathing flow profile of the source manikin in the displacement ventilation case (measured on one standing manikin). The two manikins indicate a distance of 0.70 m

chest height are owing to the contaminant stratification as discussed in test 4.

The target manikin has its back to the source, a common situation in a queue, in test 6. The results show that the exposure concentrations at all the separation distances are close to 1.0, which corresponds to a situation of fully mixed air, see Figure 12. The exposure levels, and therefore the infection risk, are reduced significantly. The manikin itself and the surrounding thermal plume protect the breathing zone and the area above the head of the target manikin of direct influence of the exhalation flow. At chest height, similar results are obtained for two previous cases owing to the vertical stratification.

The results for test 7, with the source manikin seated, are shown in Figure 13. With a separation distance of 0.70 and 1.10 m, personal exposure barely varies in the two tests because of the stratification of the contaminant, showing a value close to 4.0. At the chest height, the concentration value is directly influenced by the primary flow from the source manikin, which is exhaling the air at almost the same height as the chest, 1.23 m. When the source manikin is at 0.70 m from the target, the concentration of pollutants c_{chest}/c_R at the chest is almost 10. However, it is possible to see a significant decrease in the concentration value when the separation distance between the two manikins increases to 1.10 m. In this position, the exhaled air from the source manikin moves above chest height before reaching the chest of the target manikin. The effect that the exposure c_{exp}/c_R only has a small variation at different distances from 0.70 to 1.10 m but has a substantial level is very important in connection with cross-infection risk. It indicates, as mentioned earlier, that the exhalation has a tendency both to stratify in a room with the vertical temperature gradient and to generate a layer of exhalation with a possible content of, for example, virus or bacteria. This effect is also seen in Bjørn and Nielsen (2002), Qian et al. (2006), and Nielsen et al. (2008).

The displacement ventilation tests show that the most critical case, in which we have the highest personal exposure of the target manikin, is when the two manikins are facing each other. The face-to-side and back-to-side positions, corresponding to tests 5 and 6, respectively, reduce considerably the personal exposure. Finally, when the source manikin is seated, the concentration exposure shows high values that can be explained by a stratification of the contaminant flow between the manikins and eventually by an upward transportation into the boundary layer of the target manikin. This result shows that the position and also the difference of height between the manikins can influence the concentration field in the surroundings of the target manikin.

Two manikins in a room with mixing ventilation

Figure 14 shows the results of case 8 where the manikins are standing and facing each other. The values of the exposure concentration, and the concentration at the top of the chest of the target manikin, are observed to be around 1.0, which indicates a fully mixed value in the thermal plume around the target manikin and in the inhalation zone. However, although the concentration values above the head of the target manikin are around 1.0 for the largest distances, the pollution level increases when the separation distance is decreased to < 0.80 m. This is owing to a direct influence of the source manikin's exhalation flow in this area, especially when the separation distance is 0.35 m. These results agree with the observed location of the breathing flow profile in the mixing ventilation case, see Figure 8, which shows a similar vertical increase in height of the exhalation flow at 0.35 m from the mouth of the source manikin. It is in this connection important to realize that the personal exposure not only depends on the position of the manikins, but also on the height of the people.
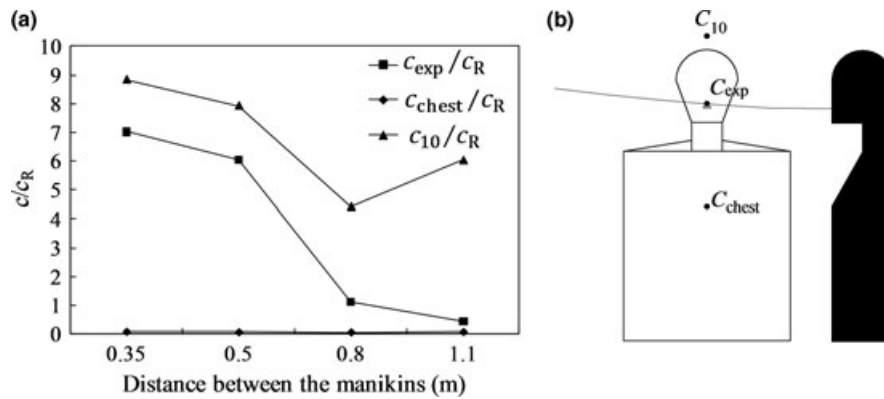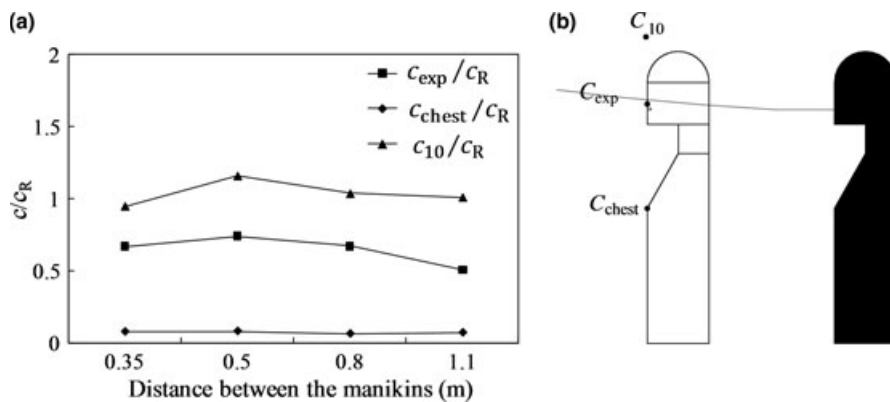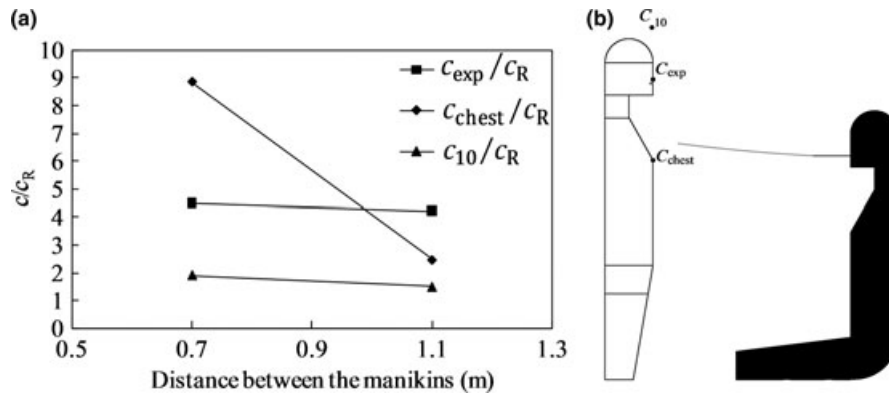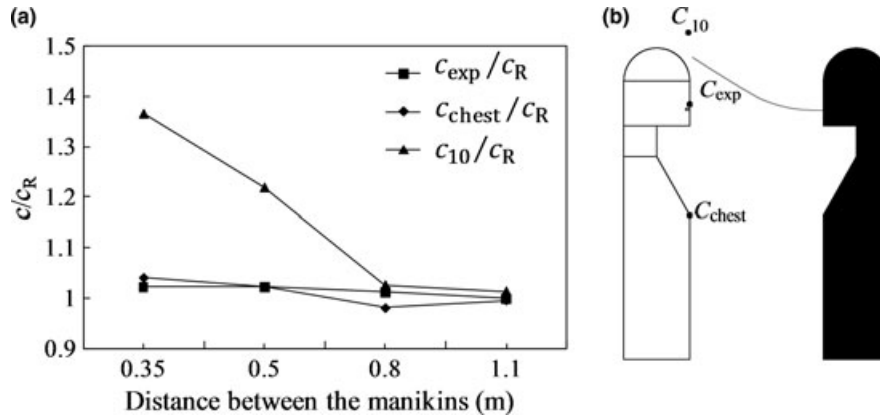
Fig. 14 (a) Comparison of the exposure concentration values in the inhalation (c_{exp}/c_R), the chest (c_{chest}/c_R), and above the head of the target manikin (c_{10}/c_R) for the test 8, (b) Location of the three measured points and breathing flow profile of the source manikin in the mixing ventilation case. The separation distance is 0.35 m

In addition, test 9 is carried out to measure the gas concentration values when the source manikin is sitting and the target manikin is standing. The concentration results are around 1.0 in all the measuring points: the inhalation, the chest, and above the head of the target manikin for the two separation distances, 0.7 and 1.1 m. These results show a situation of fully mixed air that provokes a dilution of the contaminant in the breathing area and around the target manikin.

Two manikins in a room without ventilation

The four different situations with two manikins standing and facing each other are studied in a room without ventilation. During the following tests, the conditions in the room are kept steady by maintaining the same temperature both inside and outside the room and by keeping the door open to the laboratory hall.

As there is no ventilation with return flow, the concentrations in the inhalation area and above the head of the target manikin have been compared to the concentration of the air at the chest of the target manikin. The exposure concentration values c_{exp}/c_{chest} are kept around 1.0, except for the case with the smaller separation distance where the value obtained is 2.2, as it is shown in Figure 15. However, it is possible to see much higher values of gas concentration above the head of the manikin, especially at distances of 0.50 and 0.35 m. The behavior of the airflow in the room is controlled by convective flows and the boundary layers of the manikins. Because of that, a concentration of pollutants from the exhalation flow of the source manikin is built up above the head of the target manikin, and the exhalation flow will influence the measurements when the separation distance is reduced. Also, the results are dependent on the flow which will take place through the open door, and they are therefore not universal as such.
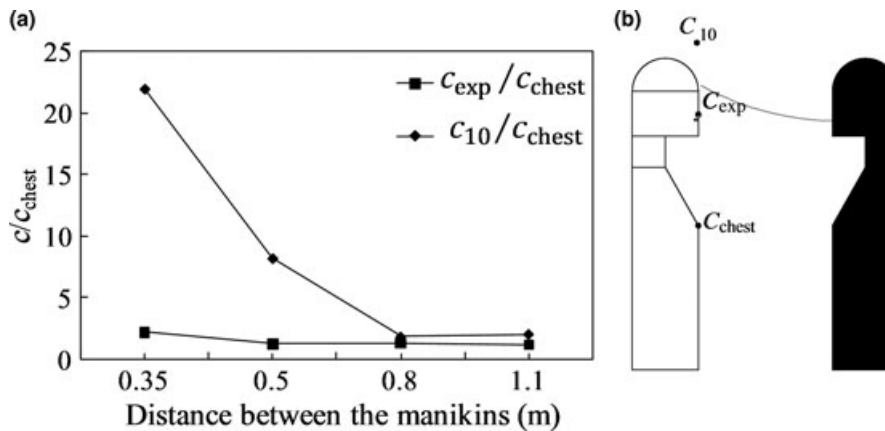

Fig. 15 (a) Comparison of the exposure concentration values in the inhalation (c_{exp}/c_{chest}) and above the head of the target manikin (c_{10}/c_{chest}) for the test 10, (b) Location of the two measured points and breathing flow profile of the source manikin in the case without ventilation. The two manikins indicate a distance of 0.35 m

Olmedo et al.

Conclusions

The flow of the exhalation from a single person is studied in a room with mixing ventilation, displacement ventilation, and without ventilation, respectively. The different air distribution systems create a different microenvironment around the breathing zone, but the air temperature has a level that is typical of comfort. The vertical temperature gradient connected to a displacement ventilation system retains the exhalation at head height of surrounding persons, while mixing ventilation allows the exhalation to rise above head height because of temperature difference between exhalation and the surrounding air. This last effect also takes place in a room without ventilation.

The peak velocity decay and the peak mean concentration decay in the exhalation can be described by simple expressions that show the variables as proportional to the reciprocal horizontal distance from the mouth. The velocity decay and the concentration decay have a smaller value for displacement ventilation with a vertical temperature gradient in the breathing zone than for the two other cases of air distribution. It could be explained by the damping effect that the temperature gradient has on the turbulence, which may cause the entrainment in the exhalation flow to decrease and thus the concentration in the exhalation flow to be retained.

Experiments with cross-infection risk between two persons (source manikin and target manikin) show that

the air distribution systems and especially the microenvironment they create are of importance to the exhalation flow between the manikins. In case of displacement ventilation, one manikin is exposed to the other manikin's exhalation when they are standing face to face. There is also a strong exposure when the manikins are standing face to side. There is no exposure when one manikin is standing face to the back of the other manikin, which may reduce the cross-infection risk. The exposure increases in the two-first cases when the distance between the manikins decreases, and it is up to 12 times the exposure obtained in a fully mixed case at the distance of 0.35 m.

Experiments with two manikins and mixing ventilation, and without ventilation, show almost no exposure of contaminant to the target manikin. Measurements around the manikins show that the relative heights of the manikins are important and that exposure may take place with a specific height difference.

Experiments with a seated source manikin and a standing target manikin in displacement ventilation show that the exposure has a substantial level, which is very important in connection with cross-infection risk. They also show that the variation at different distances from 0.70 to 1.10 m is small. It indicates that the exhalation has a tendency to stratify in a room with the vertical temperature gradient that generates a layer of exhalation with a possible content of, for example, viruses or bacteria.

References

Bjørn, E. (1999) Simulation of human respiration with breathing thermal manikin, *Proceedings of Third International Meeting on Thermal Manikin Testing*, Stockholm, Sweden, National Institute for Working Life, 78–81.

Bjørn, E. and Nielsen, P.V. (2002) Dispersal of exhaled air and personal exposure in displacement ventilated room, *Indoor Air*, **12**, 147–164.

Brohus, H. and Nielsen, P.V. (1996) Personal exposure in displacement ventilated rooms, *Indoor Air*, **6**, 157–167.

Chao, C.Y.H. and Wan, M.P. (2007) Transport characteristics of expiratory droplet nuclei in indoor environments with different ventilation airflow patterns, *J. Biomech. Eng.*, **129**, 341–353.

Chao, C.Y.H., Wan, M.P. and Sze To, G.N. (2008) Transport and removal of expiratory droplets in hospital ward environment, *Aerosol. Sci. Technol.*, **42:5**, 377–394.

Chao, C.Y.H., Wan, M.P., Morawska, L., Johnson, G.R., Ristovski, Z.D., Hargreaves, M., Mengersen, K., Corbett, S., Li, Y., Xie, X. and Katoshevski, D. (2009)

Characterization of expiration air jets and droplet size distributions immediately at the mouth opening, *J. Aerosol Sci.*, **40**, 122–133.

Chen, C. and Zhao, B. (2010) Some questions on dispersion of human exhaled droplets in ventilation room: answers from numerical investigation, *Indoor Air*, **20**, 95–111.

Chen, C., Zhao, B., Cui, W., Dong, L., An, N. and Ouyang, X. (2009) The effectiveness of an air cleaner in controlling droplet/aerosol particle dispersion emitted from a patient's mouth in the indoor environment of dental clinics, *J. R. Soc. Interface*, **7**, 1105–1118.

Cheong, K.W.D. and Phua, S.Y. (2006) Development of ventilation design strategy for effective removal of pollutant in the isolation room of a hospital, *Build. Environ.*, **41**, 1161–1170.

Gupta, J.K., Lin, C. and Chen, Q. (2010) Characterizing exhaled airflow from breathing and talking, *Indoor Air*, **20**, 31–39.

He, G., Yang, X. and Srebric, J. (2005) Removal of contaminants released from

room surfaces by displacement and mixing ventilation: modeling and validation, *Indoor Air*, **15**, 367–380.

Lai, A.C.K. and Cheng, Y.C. (2007) Study of expiratory droplet dispersion and transport using a new Eulerian modeling approach, *Atmos. Environ.*, **41**, 7473–7484.

Lee, E., Khan, J.A., Feigley, C.E., Ahmed, M.R. and Hussey, J.R. (2005) An investigation of air inlet types in mixing ventilation, *Build. Environ.*, **42**, 1089–1098.

Li, Y., Huang, X., Yu, I.T.S., Wong, T.W. and Qian, H. (2005) Role of air distribution in SARS transmission during largest nosocomial outbreak in Hong Kong, *Indoor Air*, **15**, 83–95.

Li, Y., Leung, G.M., Tang, J.W., Yang, X., Chao, C.Y.H., Lin, J.Z., Lu, J.W., Nielsen, P.V., Niu, J., Qian, H., Sleigh, A.C., Su, H.-J.J., Sundell, J., Wong, T.W. and Yuen, P.L. (2007) Role of ventilation in airborne transmission of infectious agents in the built environment – a multidisciplinary systematic review, *Indoor Air*, **17**, 2–18.

Li, Y., Nielsen, P.V. and Sandberg, M. (2011) Displacement ventilation in hospital environments, *ASHRAE J.*, **53**, 86–88.

Morawska, L. (2006) Droplet fate in indoor environments, or can we prevent the spread of infection?, *Indoor Air*, **16**, 335–347.

Morawska, L., Johnson, G.R., Ristovski, Z.D., Hargreaves, M., Mengersen, K., Corbett, S., Chao, C.Y.H., Li, Y. and Katoshevski, D. (2009) Size distribution and sites of origin of droplets expelled from the human respiratory tract during expiratory activities, *J. Aerosol Sci.*, **40**, 256–269.

Nicas, M., Nazaroff, W.W. and Hubbard, A. (2005) Toward understanding the risk of secondary airborne infection: emission of respirable pathogens, *J. Occup. Environ. Hyg.*, **2**, 143–154.

Nielsen, P.V. (2009) Control of airborne infectious diseases in ventilated spaces, *J. R. Soc. Interface*, **6**, 747–755.

Nielsen, P.V., Buus, M., Winther, F.V. and Thilageswaran, M. (2008) Contaminant flow in the microenvironment between people under different ventilation conditions, *ASHRAE Trans.*, **114**, 632–638.

Nielsen, P.V., Jensen, R.L., Litewnicki, M. and Zajas, J. (2009) Experiments on the microenvironment and breathing of a person in isothermal and stratified surroundings, *Proc. 9th Int. Conf. Healthy Buildings*, Syracuse, NY, USA.

Nielsen, P.V., Li, Y., Buus, M. and Winther, F.V. (2010) Risk of cross-infection in a hospital ward with downward ventilation, *Build. Environ.*, **45**, 2008–2014.

Nielsen, P.V., Olmedo, I., Ruiz de Adana, M., Grzelecki, P. and Jensen, R.L. (2012) Airborne Cross-Infection Risk between Two People Standing in Surroundings with a Vertical Temperature Gradient, *Int. J. HVAC and R Res.*, **18**.

Qian, H. and Li, Y. (2010) Removal of exhaled particles by ventilation and deposition in a multibed airborne infection isolation room, *Indoor Air*, **20**, 284–297.

Qian, H., Li, Y., Nielsen, P.V., Hyldgaard, C.E., Wong, T.W. and Chwang, A.T.Y. (2006) Dispersion of exhaled droplet nuclei in a two-bed hospital ward with three different ventilation systems, *Indoor Air*, **16**, 111–128.

Qian, H., Li, Y., Nielsen, P.V. and Hyldgaard, C.E. (2008) Dispersion of exhalation pollutants in a two-bed hospital ward with a downward ventilation system, *Build. Environ.*, **43**, 344–354.

Richmond-Bryant, J., Eisner, A.D., Brixey, L.A. and Wiener, R. (2006) Transport of airborne particles within a room, *Indoor Air*, **16**, 48–55.

Tang, J.W., Noakes, C.J., Nielsen, P.V., Eames, I., Nicolle, A., Li, Y. and Settles, G.S. (2011) Observing and quantifying airflows in the infection control of aerosol- and airborne-transmitted diseases: an overview of approaches, *J. Hosp. Infect.*, **77**, 213–222.

Xie, X., Li, Y., Chwang, A.T.Y., Ho, P.L. and Seto, W.H. (2007) How far droplets can move in indoor environments – revisiting the Wells evaporation-falling curve, *Indoor Air*, **17**, 221–225.

Zukowska, D., Melikov, A. and Popiolek, Z. (2008) Impact of thermal plumes generated by occupant simulators with different complexity of body geometry on airflow pattern in rooms, *Proc. 7th Int. Thermal Manikin and Modeling Meeting*, Coimbra, Portugal.

Appendix G
Risk of airborne cross infection in a room with vertical low-velocity ventilation

Risk of airborne cross-infection in a room with vertical low-velocity ventilation

Abstract

The amount of air that a downward flow ventilation system can move without generating draft is large compared to other systems. This fact makes it one of the most recommended ventilation strategies in order to remove contaminants in rooms and to prevent people from the risk of airborne cross-infection. This study is based on experimental tests carried out in a room with downward flow ventilation. Two breathing thermal manikins are placed in the room face to face. The breathing of one of the manikins is considered the contaminated source in order to simulate a risky situation of airborne cross-infection. The relative position of the manikins respect to the diffuser, the diffuser position in the room as well as the separation distance between the manikins are changed to observe the influence of these factors on the personal exposure of the target manikin. The results show that the downward flow often is unable to penetrate the microenvironment generated by the manikins in the different situations. The results can be an unexpected high level of contaminant exposure to the target manikin especially when the separation distance between the manikins is reduced.

Practical implications

Several guidelines recommend the downward ventilation systems to reduce the risk of cross-infection between people in hospital rooms. This study shows that this recommendation should be taken into consideration carefully. It is important to pay attention on people relative position, relative position to other thermal loads in the room and especially on the separation distance between people if the exposure to exhaled contaminants wants to be reduced.

Nomenclature

a_0 area of the manikin´s mouth, m^2

a_{diff} area of the textile diffusers, m^2

c tracer gas concentration, ppm

c_R tracer gas concentration in the return, ppm

c_{chest} tracer gas concentration at the chest, ppm

c_{exp} tracer gas concentration in the inhalation, ppm

c_{10} tracer gas concentration 0.10 m above the head, ppm

H height of the test room, m

K_{exp} characteristic velocity constant

n_1 characteristic velocity exponent

q_0 volume flow rate in the room, m³/s

T absolute air temperature, K

T_0 exhaled air temperature, K

T_{amb} air temperature at the height of the manikin´s mouth, K

T_{in} supply air temperature, K

T_{out} return air temperature, K

u_0 peak velocity in the manikin´s mouth, m/s

u_x peak velocity at a horizontal distance from the manikin´s mouth, m/s

x horizontal distance, m

z vertical distance, m

Introduction

During the last years there has been a high interest in finding the most efficient ventilation strategy to produce a comfortable indoor climate for people and at the same time that prevents the spreads of contaminants in the air and reduces the risk of cross-infection between people.

Cross-infection of diseases is caused by the transmission of pathogens, such as viruses or bacteria, between people and across environments. When a person is breathing, talking or sneezing, droplets, which may contain biological contaminants, are generated. Depending on the size of the droplets the routes of airborne particle transmission change (Morawska, 2006). While the biggest particles are subjected to heavy gravitational effect (Wan et al., 2007) small droplet nuclei will follow the air stream and be dispersed in the air (Tang et al., 2011) It may cause a risk of cross-infection in a susceptible person situated in the same room, which could inhale the contaminated airborne droplet nuclei.

Li et al. (2007) pointed out several evidences that relate ventilation systems with the airborne transmission of diseases. However, many factors influence the efficiency of the ventilation systems in removing contaminants in a room. Much research including both, experimental and numerical works, have been carried out in order to increase the understanding of the key factors associated with airborne infection (Cheong and Phua, 2006; Mui et al., 2009). Location of the exhaust and supply openings is one of the factors that directly affect the dispersion of contaminants in indoor environments. Some authors (Nielsen, 2009; Chung and Hsu, 2001; Qian et al., 2008; Nielsen et al., 2010;

Lim et al., 2010) determined the influence of these factors in the spread of contaminants in hospital wards. People and thermal loads are also a determinant factor since they can influence the airflow pattern in a room due to the thermal plumes generated by the difference of temperature with the ambient (Woloszyn et al., 2004; Liu et al., 2009) and because of breathing and coughing (Zhu and Kato, 2006; Zhu et al., 2006; Gupta et al., 2010). Therefore their location and relative position to other people or furniture play a determinant role in the risk of cross-infection in rooms (Bjørn and Nielsen, 2002; He et al., 2011).

Recently, ventilation systems that generate a downward parallel flow are recommended to obtain indoor ambient clean of pollutants and to minimize the spread of airborne contaminants (Chow and Yang, 2005; CDC 2005; CDC 2003). These systems are considered one of the most efficient to control the dispersion of contaminants due to the large volume flow of clean air that can apply without draught (Chow and Yang, 2004; Nielsen 2007). However, the ventilation design should be studied carefully. The convective air movement generated by the heat loads may create a mixing flow pattern in the room (Nielsen et al. 2007). In that way, the flow generated in the room and the efficiency of the ventilation system in removing pollutants depend on different factors such as the exhaust opening position, the people and diffuser location, the airflow rate, etc.

The purpose of this paper is to study in detail the dispersion of contaminants exhaled by a person in a position with downward or upward flow, using a ceiling-mounted low velocity air terminal device. The exposure to the contaminants that the human exhalation can provoke to another person placed in the same room is also studied.

In order to carry out the study, two breathing thermal manikins have been used in the experimental measurements. The exhalation flow of one of the manikins is the source of contaminant and the target manikin is the one exposed to the exhaled contaminants.

The simulation of the contaminants has been done by using a tracer gas, in order to simulate the small contaminated droplet nuclei that may cause airborne cross-infection. It has been proved by several studies (Gao and Niu, 2007; Yin et al., 2011) that the use of tracer gas is a valid way to simulate the small droplets generated by the human breathing.

Experimental method

Test room and experimental conditions

The experiments are carried out in a full-scale room, 4.1 m (length), 3.2 m (width) and 2.7 m (height) ventilated by two textile diffusers, 1.2 m (length) and 0.6 m (width) each, placed next to each other in the ceiling of the room, which generate a low-velocity downward flow. One single circular return opening is placed at the height of 2.6 m in the centre of the back wall, see figures 1(a) and 1(b). The recommendation given by Qian and Li (2010) and Nielsen et al. (2010) of locating exhaust openings at high

locations is followed, in order to remove in more efficient way airborne contaminants. The supply air temperature is constant at 16ºC +/- 0.5ºC. During the experiments the air exchange rate is set to 5.6 h^{-1}.

Two breathing thermal manikins, height 1.68 m, are used to simulate two averaged-size people in the room. One of the manikins is considered as the source manikin, who exhaled 0.75 l/exhalation of contaminated air through the mouth, which has an ellipsoid size of 125 mm^2, and the frequency is 14.6 exhalation/min. The volume of exhaled air of the target manikin, which is exposed to the exhalation flow of the source, is 0.66 l/exhalation, and the frequency of 10.0 exhalation/min. The exhalation is taking place through the mouth, which consists of a 100 mm^2 circular opening. The breathing modes and the size of the manikins´ mouth are averaged human values (Gupta et al., 2010). The temperature of both exhalation flows is set to 34ºC +/- 1ºC. Both manikins inhale the air through the nose. The detailed geometry of the manikins can be found in Bjørn (1999).

One radiator, 0.55 m x 0.40 m x 0.05 m size, is also placed in the room. The corresponding power heat loads and surface temperatures of all the heat loads in the room are shown in table 1.

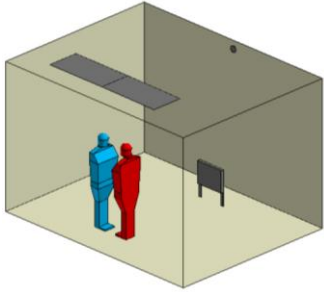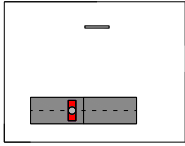<div align="center">Table 1 Heat loads</div>
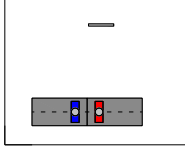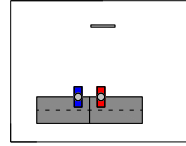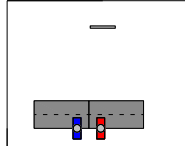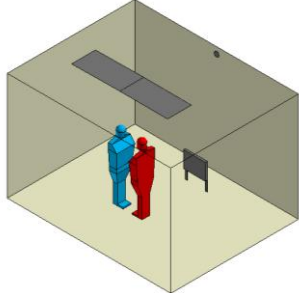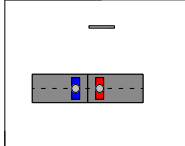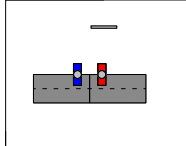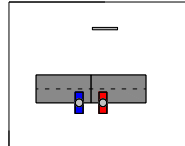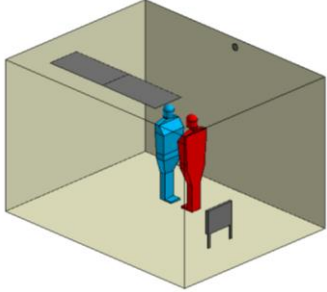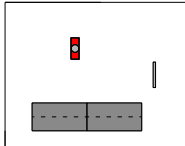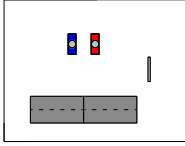
	Temperature (ºC) [a]	Power (W)
Source manikin	29.7	94
Target manikin	29.9	100
Radiator	39.0/42.1	300/390 [b]

[a] The surface temperature of the manikins is obtained as the average temperature at three points: the chest, the back and the head of the manikins. For the radiator the temperature is the average of the temperature at both sides.

[b] Power and temperature of the radiator for the cases with one manikin, *a* and *h*, and with two manikins *b*, *c*, *d*, *e*, *f*, *g* and *i*.

This study consists of nine experimental cases summarized in table 2. The figures in table 2 show the textile diffusers, the circular exhaust opening, the radiator, the source manikin (in red) and the target manikin exposed to the contaminants (in blue). From cases *a* to *g*, the manikins are placed in the downward flow area generated by the textile diffusers. The diffusers are located 0.42 m from the front wall in *Group 1*, while it is 1.02 m for *Group 2*. In the cases with two manikins, the study is made with three relative positions of the manikins with respect to the diffusers: under the center line of the diffuser (tests *b* and *e*) and under the right and left edges (*c*, *f* and *d*, *g* respectively). For *Group 3*, cases *h* and *i*, the manikins are placed in an area with upward flow and the diffuser is placed at 0.42 m from the front wall.

Table 2 Lay out of the experiments

Sketch of the room	Top view configuration of each case			
Group 1				
	a	b	c	d
Group 2				
		e	f	g
Group 3				
	h	i		

In all the cases the two manikins are facing each other and different separation distances are studied: 0.35 m, 0.50 m, 0.80 m (only cases *b* and *i*) and 1.10 m. Every test lasts for 4 hours, in order to obtain a reliable average value of the contaminant concentration.

The cases *a* and *h* with only the source manikin, placed at 1.4 from the left wall (measured from the back of the manikin), in the downward and upward areas, are carried out in order to study the exhalation airflow. In these cases, the exhalation flow is visualized using smoke to find the center line of the exhalation flow jet. The time dependent velocity and the concentration distribution are then measured along this line

to find the maximum peak velocity and the maximum peak concentration values in different distances.

Measurements facilities

A total of 15 thermocouples (type k) are used to make temperature measurements in the room at three vertical poles. Five thermocouples are placed at the height of 0.1 m, 0.6 m, 1.1 m, 1.7 m and 2.0 m from the floor. One vertical line (pole), L1, is placed in a corner of the room, and the other two lines L2 and L3, 0.4 m behind the source and the target manikin respectively, see figure 1(a). The vertical lines are moved together with the manikins when the separation distance is changed. The temperature data are collected with a frequency of 30 s and the results are shown as dimensionless using the inlet temperature of the air, T_{in}, and the temperature in the exhaust opening, T_{out}.

Seven hot sphere anemometers are used to measure the velocity along a horizontal line, L4, placed 0.35 m above the head of the manikins, see figure 1(b). Anemometer 4 is always placed in the center line between the two manikins. The rest of the anemometers change their positions in respect to the center separation line when the distance between the manikins changes as it is shown in table 3. The velocity profile of the diffuser is also measured at twelve points along one horizontal line, L5, placed 0.50 m below the diffuser, see figure 1. The acquisition frequency is of 100 ms with a precision of ± 5%.

(a)   (b)

Figure 1 (a) Horizontal section (Diffusers in grey, source manikin in red, target manikin in blue) position of the radiator for each group (R12 for groups 1 and 2, R3 for group 3), exhaust opening (E) and measuring lines (L1, L2, L3, L4 and L5) (b) Front view of the room, location of the anemometers along the horizontal line L4 and placement location of the concentration tubes: c_R, c_{10}, c_{exp} and c_{chest}. All measurements are in meters

Table 3 Anemometers horizontal positions along L4 for the different separation distances between the manikins

	x (m)						
Separation distance	1	2	3	4	5	6	7
0.35 m, 0.80 m, 1.10 m	-0.9	-0.5	-0.2	0	0.2	0.5	0.9
0.50 m	-0.9	-0.6	-0.3	0	0.3	0.6	0.9

N_2O is used as a tracer gas and applied through the tube which connects the artificial lungs with the mouth of the source manikin. In order to measure this contaminant concentration a photo acoustic multigas monitor (type 1412; Innova Air Tech Instruments) together with two Multipoint Sampler and Doser (type 1303, Brüel & Kjaer) is used to measure N_2O concentration.

For cases *a* and *h*, only a source manikin and the radiator are present in the room, see figure 2. For these tests, five tubes for concentration measurements and five extra anemometers are used to measure the concentration and velocity decay of the center line of the exhalation flow. The center line of the exhalation flow is obtained by observation of the flow with smoke and using the measurements of the maximum velocities at different locations at the center line until the right positions is found. The location of the measuring points, for the velocity and concentration, obtained are shown in table 4.
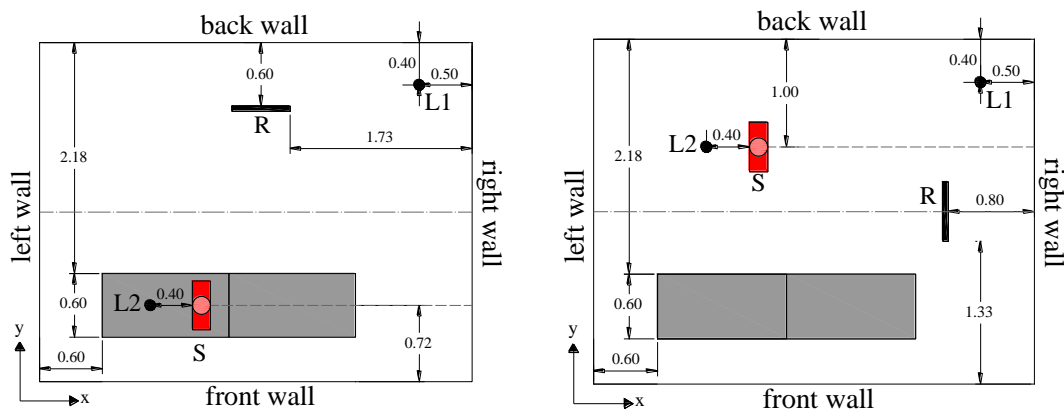

Figure 2 Horizontal section of the room with the position of the manikin (S), the radiator (R) and the measuring lines L1 and L2 (a) in case *a*, (b) in case *h*

Table 4 Position of the anemometers and concentration tubes along the centreline of the exhalation flow

	Case *a* (Downward flow)				
Horizontal distance (m)	0.04	0.16	0.27	0.40	0.65
Height (m)	1.525	1.545	1.56	1.575	1.6
	Case *h* (Upward flow)				
Horizontal distance (m)	0.01	0.095	0.23	0.44	0.65
Height (m)	1.52	1.53	1.537	1.565	1.585

For the tests with two manikins, *b*, *c*, *d*, *e*, *f*, *g* and *i*, three tubes for concentration measurements are used to measure the contaminant concentration in the surroundings of the target manikin and one extra tube in the return opening. The exposure concentrations are the average values obtained at each position. The results are given as normalized values by a division with the concentration at the return opening of the room: c_{chest}/c_R is the exposure at the chest of the target manikin at the height of 1.2 m,

c_{exp}/c_R personal exposure of the target manikin, measured in the inhalation tube, and c_{10}/c_R exposure 0.10 m above the head of the target manikin, 1.8 m from the floor, see figure 1(b).

Results and discussion

A persons breathing profile

The airflow pattern generated by the diffusers and the temperature difference of the exhalation flow with respect to the ambient may produce/give? a significant influence on the direction and movement of the exhalation airflow of a manikin (person). In order to determine this influence the manikin is placed in flow areas where downward (DWF) and upward (UWF) flow in the room. The textile diffuser is placed at 0.42 m from the front wall, tests *a* and *h*. The results of the trajectory flowed by the exhalation flow are shown in figure 3.
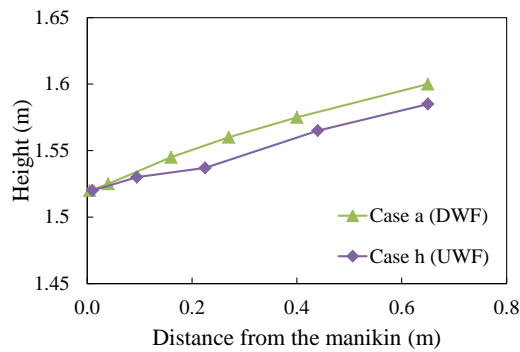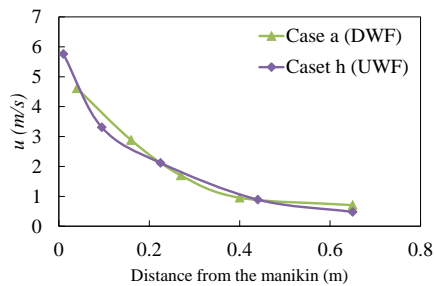

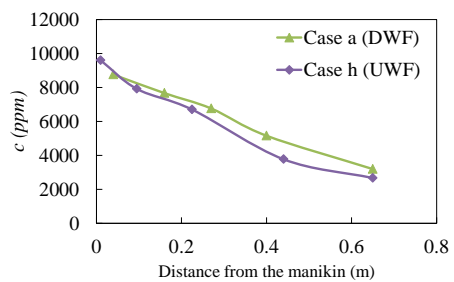Figure 3 Centerline of the exhalation flow obtained for cases *a* and *h*

The peak velocity and peak concentration values along the centerline of the exhalation are measured and the results are shown in figure 4 together with the vertical temperature gradients obtained in the room (L1) and behind the source manikin (L2).

(a)   (b)
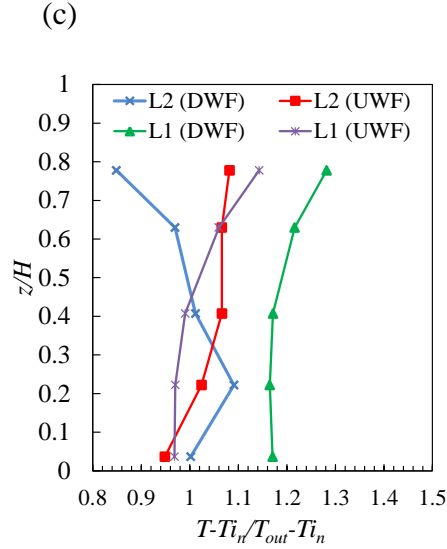
(c)

Figure 4 Maximum values obtained in the centre line of the exhalation (a) velocity, (b) concentration, (c) vertical temperature distributions measured for test *a* and test *h*

A vertical temperature gradient and a local temperature difference may influence the exhalation flow, (Olmedo et al., 2011). In both cases, *a* and *h*, it is possible to observe a slight vertical temperature gradient measured along L1, out of the influence of the manikin. However, the temperature measured close to the manikin, L2, at the height of the breathing, $z/H \sim 0.6$, is lower for case a. It will explain the slight more upward direction of the exhalation flow for case a. However, the difference between the results of the velocity and contaminant concentration along the centerline, for tests *a* and *h*, is small, which means that the airflow pattern generated by the diffuser has no significant influence in the exhalation flow for the two cases studied. Although the exhalation flow may be influenced by other factors in the room, e.g. the thermal loads or relative position of the manikins respect to the diffusers.

Exhalation profile with different ventilation strategies

The exhalation flow velocity profile can be described by an expression similar to describe non-isothermal jets (Xie et al., 2007; Nielsen et al., 2009). The peak velocity values measured in the centerline of the exhalation flow are used to obtain the constants that relate them with the horizontal distance from the jet as an expression of the following type:

$$\frac{u_x}{u_o} = K_{\exp} \cdot \left(\frac{x}{\sqrt{a_o}} \right)^{n1} \tag{1}$$

where K_{exp} is a characteristic constant, a_0 the area of the mouth, x the horizontal distance from the mouth where the measurements are taken, u_x is the peak value of the velocity at distance x from the mouth and u_o is the peak velocity value measured at the mouth of the manikin, 5.74 m/s.

In a non-isothermal free jet the trajectory – and the instantaneous exhalation flow - is directly influenced by the gravity force and momentum flux. The ratio between these two forces can be used to characterize a free jet, and the exhalation flow, and it is represented by the following Archimedes number:

$$Ar = \frac{\beta g \, \Delta T \, \sqrt{a_0}}{u_0^2} \qquad (2)$$

where β, g, a_0, u_0 and ΔT are volume expansion coefficient, gravitational acceleration, mouth opening surface (123 mm^2), maximum velocity of the exhalation flow and temperature difference between the exhalation flow, T_0, and the ambience in the room, T_{amb}. T_{amb} is obtained as the average value of two temperature values given by two thermocouples placed 1.3 m and 1.7 m height at 0.40 m from the manikin.

For cases a and h, the trajectory of the exhalation jet obtained by smoke visualization, together with the local Ar number, as well as the graphic representation of equation (1) are compared with the ones obtained with a displacement ventilation (DV) and a mixing ventilation (MV) systems by Olmedo et al. (2011), see figure 5. The ambient temperature (T_{amb}), the temperature difference between the ambience and exhalation flow (T_{amb}-T_0) and the two constants represented in equation (1) are shown in table 5. The highest temperature difference, T_{amb}-T_0, and Ar number are obtained in the case of mixing ventilation, which makes the exhalation flow to rise to larger height than in the rest of the cases. As this difference becomes lower, the trajectory of the exhalation flow becomes more horizontal, obtaining the more horizontal trajectory for the case of displacement ventilation. This fact is also supported by the temperature gradient generated by the displacement flow. For the mixing ventilation case (MV) (Olmedo et al., 2011), case a (DWF) and case h (UWF) the upward direction of the exhalation flow is a function of Ar, see figure 5(a). The exponent n_1, which correspond to the slope of the log-log graphs, has a similar value for all the cases.
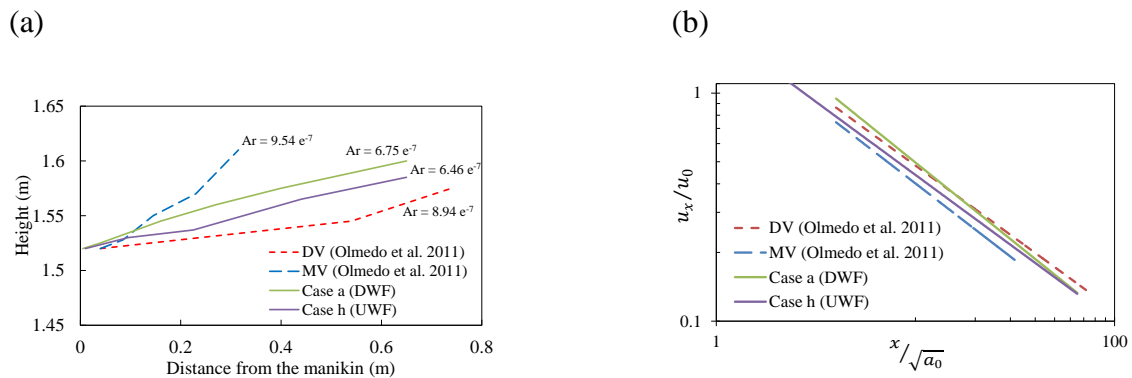
(a)

(b)

Figure 5 Comparison of the four exhalation flows obtained for the four different ventilation systems (a) flow trajectory and Ar number for each case (b) log-log graph of the maximum velocities values

Table 5 Temperature data and constants of exposure flow obtained for the four different ventilation strategies, $T_0 = 34°C$

	T_{amb} (°C)	$T_{amb}-T_0$	K_{exp}	n_1
DV	23.6	10.4	7.5	-0.64
MV	22.9	11.2	4.5	-0.68
DWF	22.4	11.6	6.6	-0.70
UWF	22.9	11.1	5.8	-0.64

Cross infection risk between two persons in downward flow (Group 1)

In these tests the textile diffusers are placed at 0.42 m from the front wall of the room. During the experiments the airflow of the diffusers is visualized using smoke and it shows a tendency to attach to the front wall due to the Coanda effect, see figure 6. Looking at the velocity results obtained along the line L5, for case *a*, shown by figure 7, it is also possible to notice this tendency of the air to flow to the left part of the room. The initial low velocity supplied flow increases in the area close to the left wall due to the low supply temperature compared to the ambient air temperature. The initial velocity of the supply air is 0.038 m/s when it is calculated by dividing the airflow rate (q_0) by the total diffusers area (a_{diff}),

(a)   (b)
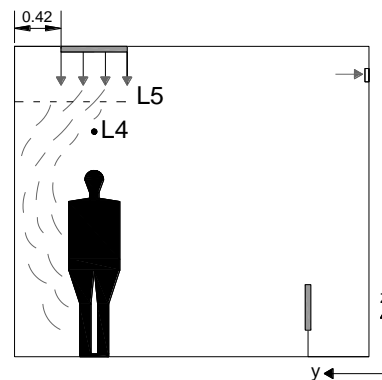

Figure 6 (a) Picture of the airflow generated by the textile diffusers, (b) Sketch of the room with the manikins´ positions of test *b* and placement of the horizontal lines L4 and L5
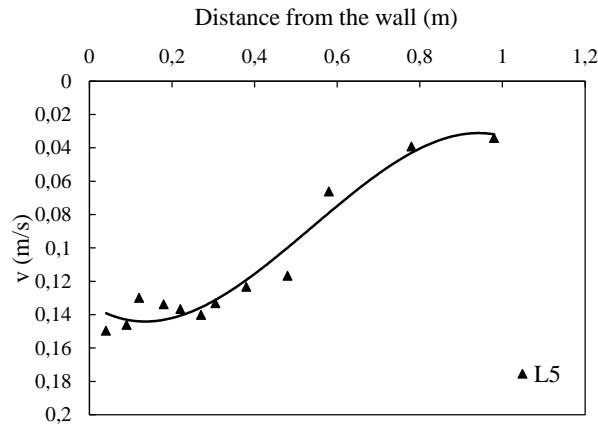
Figure 7 Velocity profile of the textile diffuser along line L5

In order to observe and measure the influence of the manikins´ thermal plumes in the downward flow generated by the diffusers velocity measurements are taken along a horizontal line L4 above the manikins for the case *b*, where the manikins are placed below the centerline of the diffusers, see figures 1(b) and 6(b). Local smoke visualization is also used to determine the direction of the flow at each point of measure. The measurements are made for the distances: 0.35 m, 0.50 m, 0.80 m and 1.10 m between the manikins, maintaining always equidistant from the centerline of the two diffusers, figure 8.
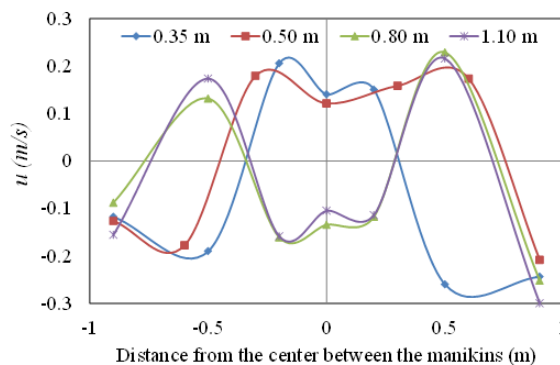

Figure 8 Velocities above the manikins for the four distances between the manikins, *case b*

When the manikins are placed at a separation distance of 0.35 m and 0.50 m, the thermal plumes generated by the manikins generate an upward flow that disturbs the unidirectional downward flow that may be expected in this area. However, for distances larger than 0.50 m to 1.10 m the supply clean air directly enters the breathing zone of the source and target manikins, provoking mixing phenomena and a downward flow between the manikins. This phenomenon could reduce the direct penetration of the contaminated exhalation and therefore the level of personal exposure of the target manikin. It is known that the maximum velocity in the plume is approx. 25 cm/s in a height of 20 cm above a manikin (person) while the velocity in the downward flow is at most equal to 14 cm/s, figure 8. It is thus obvious that the plume above a manikin (person) is stronger than the downward flow from the ceiling inlet in this case and these results are in good agreement with the findings by Nielsen (2009). Also Qian et al.

(2008) show that downward flow from a large ceiling mounted diffuser are deflected by the thermal plume from a lying manikin (patient) with the consequence of a strong mixing effect. The conclusion, that a thermal plume from a person is able to deflect a cold downward flow from a ceiling mounted diffuser with low momentum flow, is important because it shows that the expected downward flow in the CDC recommendation for rooms with patients will not be fulfilled in many practical cases. Figure 9 demonstrates the effect of a local microenvironment which can be created around the manikins in the upward flow from the boundary layers. The figure shows the smoke distribution in an initial phase. The upward flow around the manikins (the microenvironment) is not completely separated from the surroundings because the shear layer in the interface generates a high level of turbulence which gives a mixing with the surroundings. This is obvious from videos of the flow in different cases.
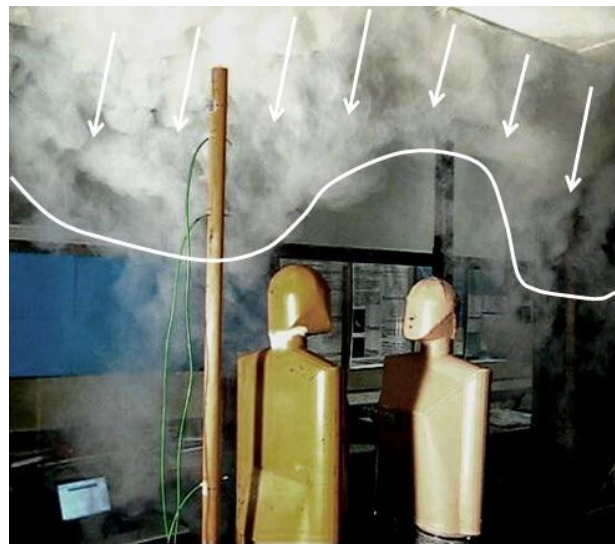

Figure 9 Downward flow from the ceiling mounted diffusers, visualized for case *b* when the separation distance between the manikins is 0.50 m

The three vertical temperature gradients measured along the lines L1, L2 and L3, for the *case b*, are shown in figure 10.
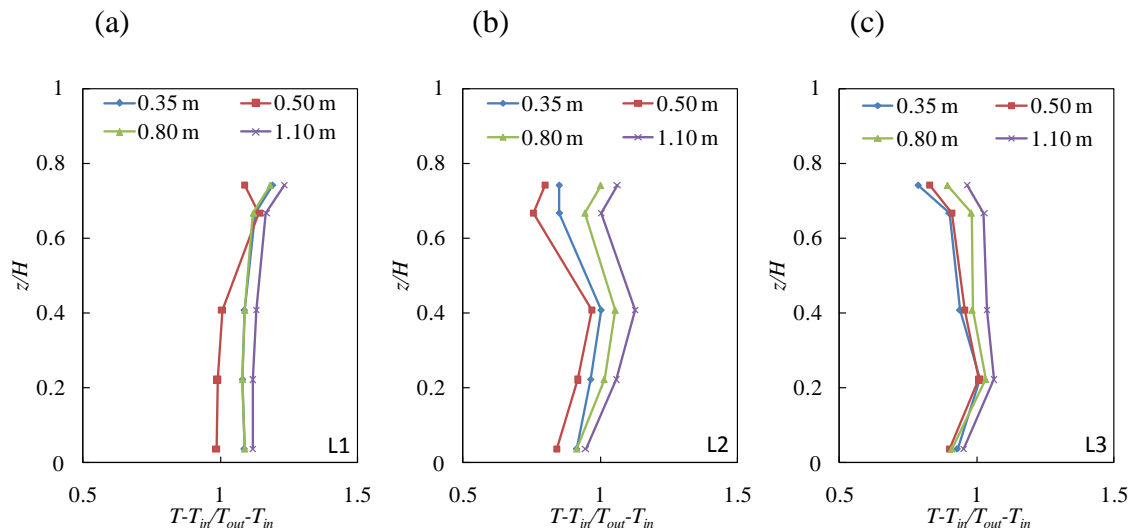
Figure 10 Vertical temperature distributions measured in case *b* (a) in the room (L1), (b) behind the source manikin (L2), (c) behind the target manikin (L3)

The measurements in the room show a slight vertical gradient with the highest temperature close to the ceiling, L1. However, at lines L2 and L3, close to the manikins, the highest temperature is obtained around 1.1 m from the floor, while the temperature of the air close to the ceiling is reduced due to the fresh air coming from the diffusers. For the cases *c* and *d* similar temperature gradients are obtained, so only the results for the case *b* are shown.

During the experiments *b*, *c* and *d*, personal exposure of the target manikin is measured for the three cases at different separation distances between source and target manikin. The exposure is given as c_{exp}/c_R, where c_{exp} is the concentration in the inhalation of the target manikin and c_R is the return concentration. The results are shown in figure 11.
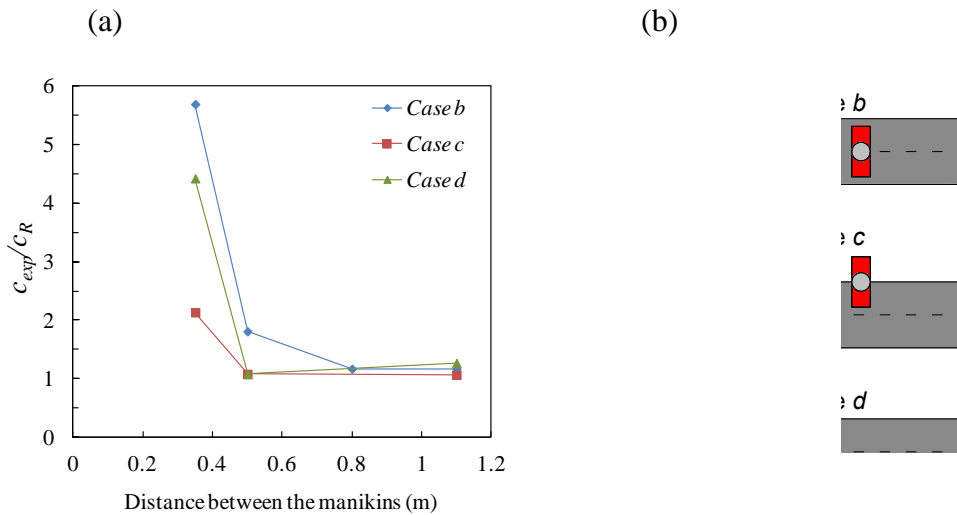

Figure 11 (a) Comparison of the c_{exp}/c_R values obtained for the cases *b*, *c* and *d*, (b) Relative positions of the manikins respect to the textiles diffusers

Case *b*, which corresponds to the test with the manikins placed under the centre line of the diffusers, shows the highest contaminant level. In all the cases, the personal exposure increases significantly as the distance between the manikins' decreases and the maximum value is measured when the target manikin is at 0.35 m from the source. This result is in line with previous investigations using different ventilation strategies to measure the personal exposure (Olmedo et al., 2011). For distances greater than 0.5 m the contaminant concentration is maintained close to 1.0, which corresponds to a case of fully mixed air. This phenomenon of the reduction in the contaminant concentration with the distance can be explained by the measurements of the velocities around the manikins that shows an upward flow between them for a separation distance up to 0.5 m. This fact reduces the mixing process and therefore affects to the direct penetration of the exhalation flow in the breathing area of the target manikin.

For case *d*, the exposure values are slightly lower than in case *b*. It may be due to a Coanda effect provoked by the close wall that is visualized with smoke during the

experiments. The lower exposure values are found in case c, even at a separation distance of 0.35 m that shows a value of 2.14.

N_2O concentration is also measured at the chest and 0.10 m above the head of the target manikin. These concentration results are shown in figure 12(a) and 12(b) respectively.
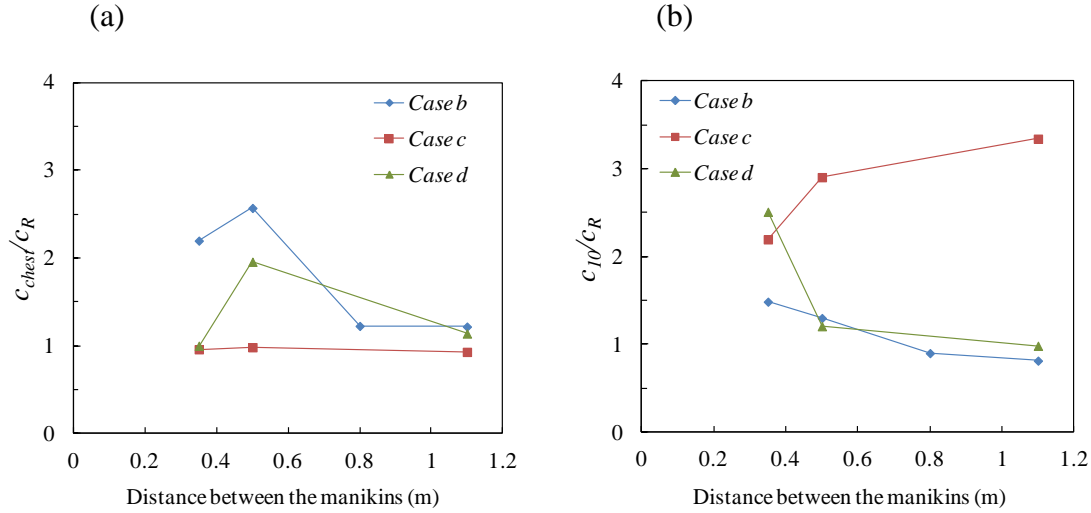
(a)   (b)

Figure 12 Contaminant concentrations at different separation distances for the cases b, c and d (a) c_{chest}/c_R, (b) c_{10}/c_R

Looking at the results of cases b and d, c_{10}/c_R shows values close to 1.0 for all the separation distances except for 0.35 m which shows a higher value. When the manikins are placed under the right edge of the diffusers, case c, the contaminant distribution changes completely compared to cases b and d. The maximum concentration value is obtained above the head of the target manikin, c_{10}/c_R, for all the distances, while c_{exp}/c_R and c_{chest}/c_R are lower. It may be due to the upward flow provoked by the hot plumes generated by the manikins and by the limited influence of the supplied air above the head of the manikins. The Coanda effect produce by the front wall can also make the clean supplied air stay closer to the wall instead of mixing with the manikins' microenvironment directly from above, which allow the contaminants to rise up to the ceiling maintaining cleaner the breathing and chest area of the target manikin.

Cross infection risk between two persons in downward flow (Group 2)

For these tests the diffusers were moved to 1.02 m from the front wall. It was observed by smoke visualization no tendency of the air to move to any side of the room. The separation distances between the manikins and the relative positions respect to the diffusers are the same than in the *Group 1*, see figure 13.
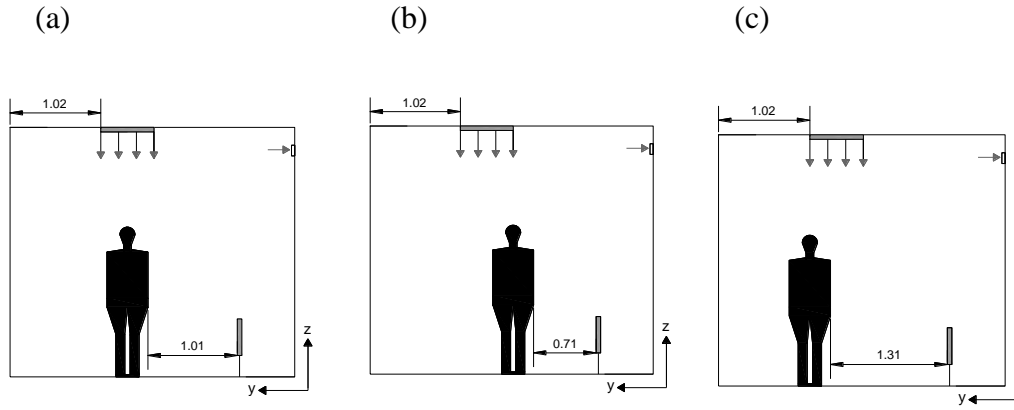
(a)   (b)   (c)

Figure 13 Sketch of the room with the relative position of the manikins respect to the diffuser (a) case *e,* (b) case *f,* (c) case *g*

Figure 14 shows the results of the vertical temperature gradients measured at the vertical lines L1, L2 and L3 for case *e.*
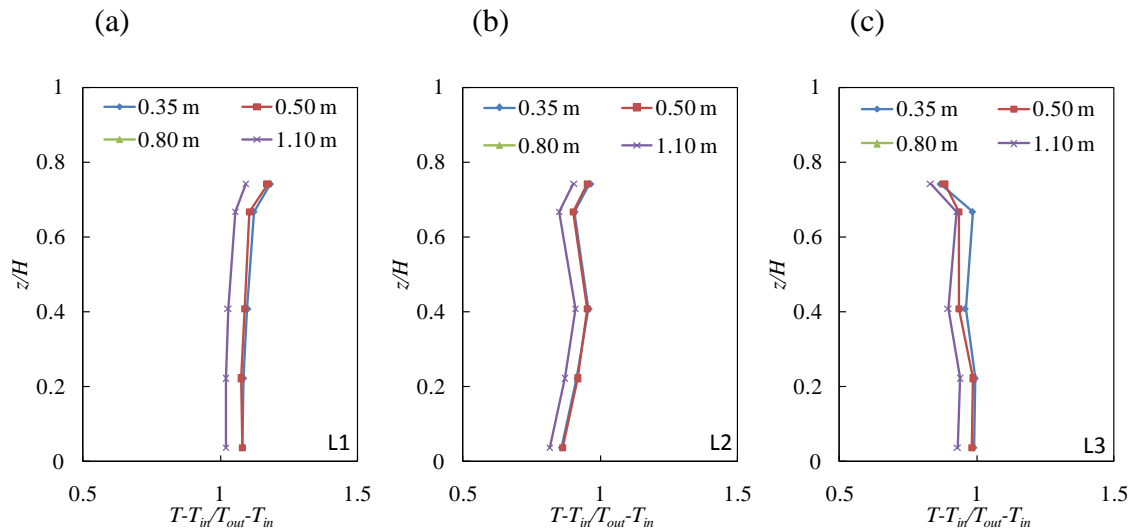

(a)   (b)   (c)

Figure 14 Vertical temperature distributions for case *e,* measured (a) in the room (L1), (b) behind the source manikin (L2), (c) behind the target manikin (L3)

The results indicate almost no vertical temperature gradient in any of the cases of *Group 2* at any position in the room. The dimensionless temperature values are close to 1.0, which corresponds to a case of fully mixing.

In the cases *e*, *f* and *g*, the personal exposure is significantly high when the separation distance is 0.35 m, see figure 15. The exhalation flow penetrates directly the inhalation area of the target manikin increasing the contaminant concentration and giving a high value of the personal exposure, for each case. Moreover, these values are larger than the contaminant concentration values in the inhalation area of the target manikin obtained in the cases *b*, *c* and *d* (*Group 1*). The exposure to the contaminants of the target manikin decreases as the distance between the manikins increases.

The personal exposure is high at the two distances of 0.35 and 0.50 m which means that there is not a protection from vertical downward flow close to the manikins at those

distances. Olmedo et al. (2011) show that traditional mixing gives a protection for cross infection in those distances between the manikins. A theory could be that the downward flow will have some influence on the plume flow around the manikins and increase the concentration in the microenvironment while the exhalation will move above the target manikin in the case of mixing ventilation.
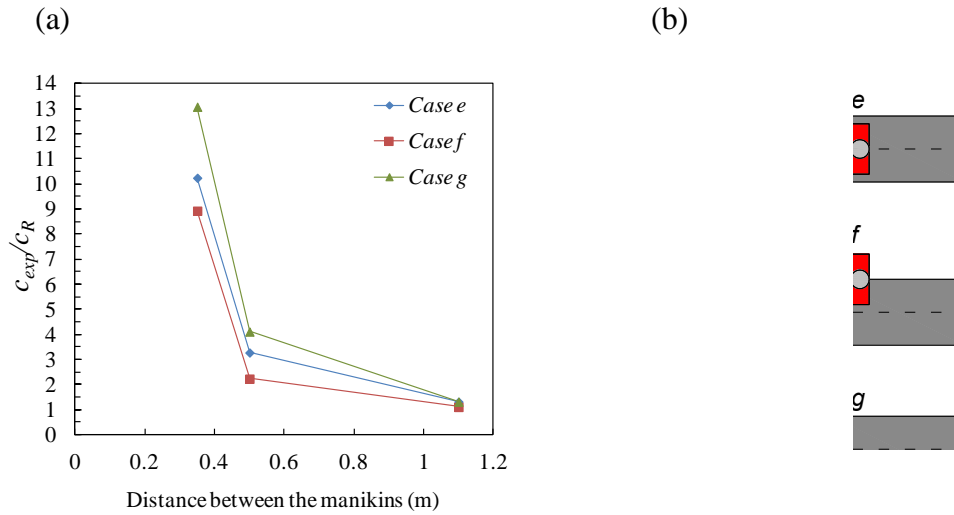
(a)

(b)

Figure 15 (a) Comparison of the c_{exp}/c_R values obtained for the cases e, f and g (b) Relative positions of the manikins respect to the textile diffusers (see also figure 13)

The contaminant profiles at the chest, c_{chest}/c_R, and above the head of the target manikin, c_{10}/c_R, for the cases e, f and g are represented in figure 16. For a distance of 1.10 m the contaminant concentrations, c_{chest}/c_R and c_{10}/c_R, are almost the same and close to 1.0 in all the cases. For the rest of distances c_{10}/c_R shows high contaminants values for the cases e and f.
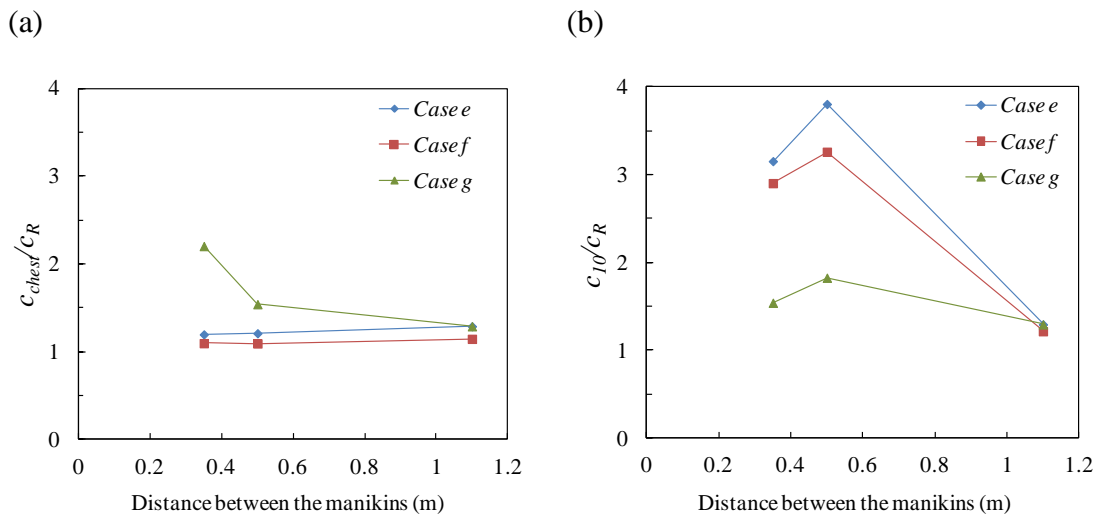
(a)

(b)

Figure 16 Contaminant concentration at different separation distances for the cases e, f and g (a) c_{chest}/c_R (b) c_{10}/c_R

Cross infection risk between two persons in upward flow (Group 3)

For the case with the manikins placed in the upward flow area of the room, case i, the velocity measurements along the horizontal line, L4, are shown in figure 17. For all the separation distances an upward airflow pattern is generated above the manikins. This upward flow generated by the air distribution pattern, the heat load and by the thermal plumes of the manikins moves the contaminants up to the ceiling region of the room. It is seen that the plumes from the manikins do not merge to one plume when the distance is 0.35 and 0.5 m as they will do when the manikins are located in a downward flow below the diffuser. This is a special effect generated by the direction of the surrounding flow.
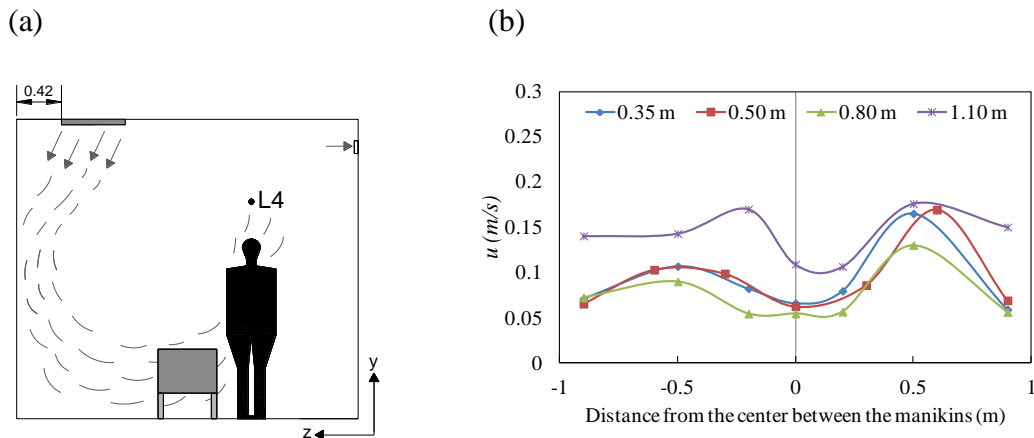
(a)   (b)

Figure 17 (a) Sketch of the room for case i (b) Vertical velocities along L4 for case i, considering the four separation distances between the manikins. The direction of the flow is determined by smoke visualization

For case i, it is possible to observe a slight vertical temperature gradient at the three vertical lines, L1, L2 and L3, see figure 18. The maximum temperature value is obtained close to the ceiling, for the three lines, due to the upward flow generated.
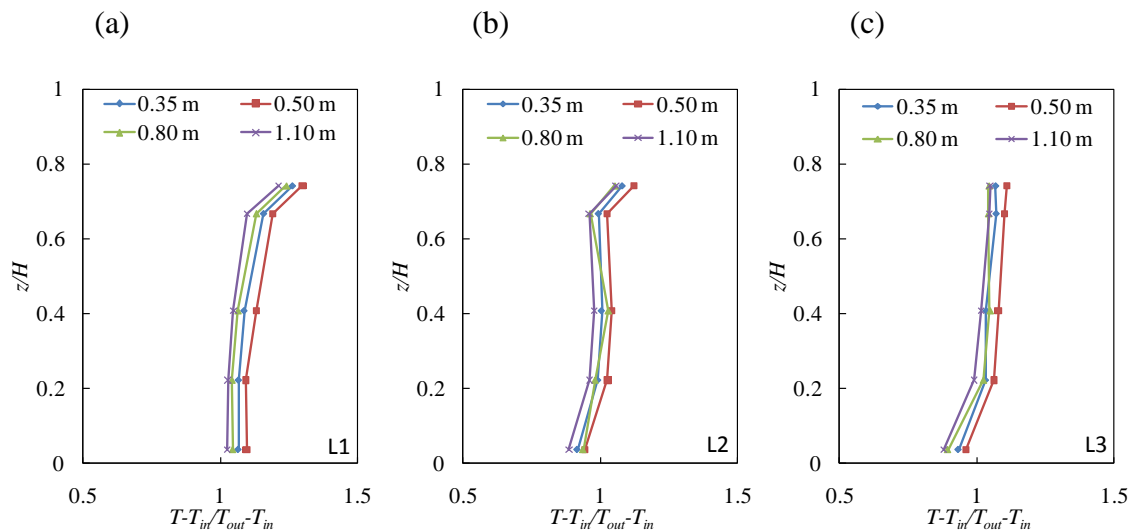
(a)   (b)   (c)

Figure 18 Vertical temperature distributions for the test i, measured (a) in the room (L1), (b) behind the source manikin (L2), (c) behind the target manikin (L3)

Figure 19 shows the contaminant concentration measured at the same three points that in the other cases: the chest, the inhalation and above the head of the target manikin.
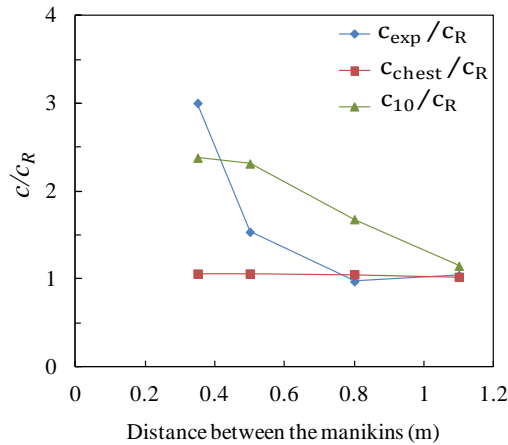

Figure 19 Comparison of the concentration values obtained for the case i at different separation distances

The results show that c_{chest}/c_R is kept close to 1.0 at all the separation distances. The personal exposure, c_{exp}/c_R, is also kept close to 1 when the manikins are separated 0.80 m and 1.10 m. However, this value increases significantly for 0.50 m and reaches a maximum value of 3.0 for 0.35 m. This maximum value is due, like in the rest of the cases, to the direct influence of the source exhalation flow that penetrates into in the breathing area of the target manikin at this short distance, increasing the level of contaminants, even when the dominating airflow is upward. It is especially surprising that the protection from cross infection is larger in this area outside the ceiling mounted diffuser area. The measurements support the theory that upward flow in the manikin's micro environment has a strong influence on the exposure of the target manikin and it might be a question on the direction of the exhalation and an influence of the temperature difference. Experiments with manikins of different height show a similar problem, namely the importance of the target manikin location in the exhalation flow of the source manikin, Liu et al. (2010).

Measurements above the head of the target manikin, c_{10}/c_R, reaches a maximum value, close to 2.5 at the distance of 0.35 m. The high values produced at this location may be because of the upward flow generated by the room air flow and the exhalation flow. Contaminant rises to the upper part of the room, keeping the chest and breathing area free of contaminants.

Comparison of the cross-infection risk with the situation in other ventilation strategies

Vertical downward ventilation is considered to be an efficient air distribution system for minimizing the cross infection risk (CDC, 2003; ASHRAE, 2003). The room air movement connected to vertical downward ventilation will have a low draught level, Nielsen (2007), which allows a high air change rate and therefore a low level of airborne contaminant from people's exhalation. Figure 20 shows, as another aspect,

how the personal exposure c_{exp}/c_R varies with the distance between persons in the different ventilation systems. It is possible to see that displacement ventilation is a system where the cross infection between two people has a high risk (see also Liu et al., 2010, and Li et al., 2011). Mixing ventilation seems to minimize the cross infection risk between two people standing close to each other.
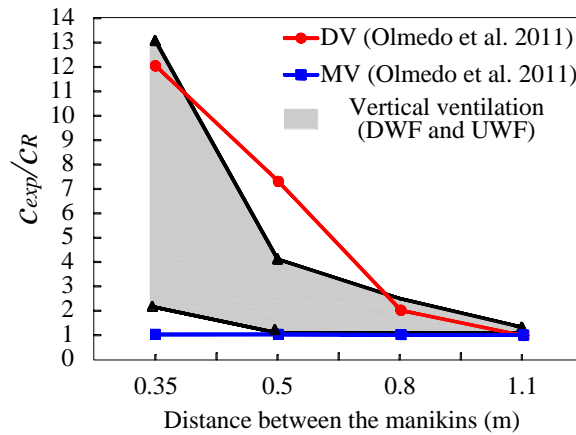

Figure 20 Comparison of the personal exposure concentration values for the different ventilation systems: displacement (DV), mixing (MV) and vertical ventilation (grey area)

Figure 20 shows that there is an increased cross infection risk for small distances as 35 cm with a personal exposure up to 14 when the diffuser is located close to the side wall. This is a serious situation which shows that vertical ventilation is not always the best solution for hospital wards and isolation rooms when the question is a protection from cross infection risk in the micro environment between two people standing close to each other.

Conclusions

The downward flow ventilation system is considered to be an efficient system to use in rooms where the cross infection risk must be minimized. The room air movement connected to vertical downward ventilation will have a low draught level which allows a high air change rate and therefore a low level of airborne contaminant from people's exhalation. The cross infection risk between two people standing far away and close to each other is analyzed. The exposure is given as the concentration in the inhalation of the target manikin divided by the return concentration.

The exposure of a target manikin, standing in a distance of more than 0.8 to 1 m from a source manikin, has a level corresponding to a fully mixed flow. The downward flow is not able to create any special protection in that case. The entrainment in the downward flow from the ceiling diffuser seems to create a mixing of the room air.

The measurements show that the exposure is high when the source and target manikin are close to each other. The exposure increases when the distance between the manikins (persons) are closer to each other than 0.5 m. The exposure can be as high as 2 to 13

times the fully mixed value in a distance of 0.35 m between the source and target. Breathing through the mouth is considered in all the cases.

It is shown that the downward cold flow from a low momentum diffuser in the ceiling is unable to penetrate the thermal boundary layer around people. The expected downward flow indicated in the CDC recommendation for rooms with patients will therefore not be fulfilled in many practical cases.

The experiments show that the direction of the downward flow can be influenced by a near wall Coanda effect. The clean air supplied from the diffusers tends to follow the wall.

A deeper study is recommended to extent the knowledge of other factors in the airflow pattern and dispersion of contaminants such as location of the supply and return openings, air change rate, furniture distribution, manikins' height, activity level, number of people in the room, room size or others.

References

ASHRAE (2003) *HVAC design manual for hospitals and clinics*, Atlanta GA, American Society of Heating, Refrigerating and Air-Conditioning Engineers.

Bjørn, E. (1999) Simulation of human respiration with breathing thermal manikin, *Proceedings of Third International Meeting on Thermal Manikin Testing*, Stockholm, Sweden, National Institute for Working Life, 78–81.

Bjørn, E. and Nielsen, P.V. (2002) Dispersal of exhaled air and personal exposure in displacement ventilated room, *Indoor Air*, **12**, 147-164.

CDC (2003) *Guidelines for Environmental Infection Control in Health-Care facilities*, USA, U.S. Department of health and human services centers for disease control and prevention (CDC).

CDC (2005) *Guidelines for preventing the transmission of Mycobacterium tuberculosis in Health-Care Settings*, USA, U.S. Department of health and human services centers for disease control and prevention (CDC).

Cheong, K.W.D. and Phua, S.Y. (2006) Development of ventilation design strategy for effective removal of pollutant in the isolation room of a hospital, *Build. Environ.*, **41**, 1161–1170.

Chow, T.T. and Yang, X.Y. (2004) Ventilation performance in operating theatres against airborne infection: review of research activities and practical guidance, *J. Hosp. Infect.*, **56**, 85–92.

Chow, T.T. and Yang, X.Y. (2005) Ventilation performance in operating theatres against airborne infection: numerical study on an ultra-clean system, *J. Hosp. Infect.*, **59**, 138–147.

Chung, K.C. and Hsu, S.P. (2001) Effect of ventilation pattern on room air and contaminant distribution, *Build. Environ.*, **36(9)**, 989-998.

Gao, N.P. and Niu, J.L. (2007) Modeling particle dispersion and deposition in indoor environments, *Build. Environ.*, **41**, 3862–3876.

Gupta, J.K., Lin, C. and Chen, Q. (2010) Characterizing exhaled airflow from breathing and talking, *Indoor Air*, **20**, 31–39.

He, Q., Niu, J., Gao, N., Zhu, T. and Wu, J. (2011) CFD study of exhaled droplet transmission between occupants under different ventilation strategies in a typical office room, *Build. Environ.*, **46 (2)**, 397-408.

Li, Y., Leung, G.M., Tang, J.W., Yang, X., Chao, C.Y.H., Lin, J.Z, Lu, J.W., Nielsen, P.V., Niu, J., Qian, H., Sleigh, A.C., Su, H.J.J., Sundell, J., Wong, T.W. and Yuen, P.L. (2007) Role of ventilation in airborne transmission of infectious agents in the built environment - a multidisciplinary systematic review, *Indoor Air*, **17**, 2-18.

Li, Y., Nielsen, P.V., Sandberg, M. (2011) Displacement ventilation in hospital environments, *Ashrae J.*, **53:6**, 86-88.

Lim, T., Cho, J. and Kim, B.S. (2010) The predictions of infection risk of indoor airborne transmission of diseases in high-rise hospitals: Tracer gas simulation, *Energ. Buildings,* **42**, 1172–1181.

Liu, J., Wan, H. and Wen, W. (2009) Numerical simulation on a horizontal airflow for airborne particles control in hospital operating room, *Build. Environ.*, **44**, 2284–2289.

Liu, L., Li, Y., Nielsen, P.V. and Jensen, R.L. (2010) An Experimental Study of Exhaled Substance Exposure between Two Standing Manikins , *Proceedings of 16th ASHRAE IAQ Conference,* Kuala Lumpur, Malaysia.

Morawska, L. (2006) Droplet fate in indoor environments, or can we prevent the spread of infection?, *Indoor Air*, **16(5)**, 335–347.

Mui, K.W., Wong, L.T., Wu, C.L. and Lai, A.C.K. (2009) Numerical modeling of exhaled droplet nuclei dispersion and mixing in indoor environments, *J. Hazard. Mater.*, **167**, 736–744.

Nielsen, P.V. (2007) Analysis and Design of Room Air Distribution Systems. *HVAC and R Research*, **13:6**, 987-997.

Nielsen, P.V., Hyldgaard, C.E., Melikov, A., Andersen, H. and Soennichsen, M. (2007) Personal exposure between people in a room ventilated by textile terminals: with and without personalized ventilation, *HVAC and R Research*, **13**, 635-643.

Nielsen, P.V. (2009) Control of airborne infectious diseases in ventilated spaces, *J.R. Soc. Interface*, **6**, 747-755.

Nielsen, P.V., Jensen, R.L., Litewnicki, M. and Zajas, J. (2009) Experiments on the microenvironment and breathing of a person in isothermal and stratified surroundings, *Proceedings of 9th Int. Conf. Healthy Buildings*, Syracuse, NY, USA.

Nielsen, P.V., Li, Y., Buus, M. and Winther, F.V. (2010) Risk of cross-infection in a hospital ward with downward ventilation, *Build. Environ.*, **45**, 2008–2014.

Olmedo, I., Nielsen, P.V., Ruiz de Adana, M., Jensen, R.L. and Grzelecki, P. (2011) Distribution of exhaled contaminants and personal exposure in a room using three different air distribution strategies, *Indoor Air*, *doi: 10.1111/j.1600-0668.2011.00736.x.*

Qian, H., Li, Y., Nielsen, P.V. and Hyldgaard, C.E. (2008) Dispersion of exhalation pollutants in a two-bed hospital ward with a downward ventilation system, *Build. Environ.*, **43**: 344–354.

Qian, H. and Li, Y. (2010) Removal of exhaled particles by ventilation and deposition in a multibed airborne infection isolation room, *Indoor Air*, **20**, 284–297.

Tang, J.W., Noakes, C.J., Nielsen, P.V., Eames, I., Nicolle, A., Li, Y. and Settles, G.S. (2011) Observing and quantifying airflows in the infection control of aerosol- and airborne-transmitted diseases: an overview of approaches *J. Hosp. Infect.,* **77**, 213-222.

Wan, M.P., Chao, C.Y.H., Ng, Y.D., Sze To, G.N. and Yu, W.C. (2007) Dispersion of expiratory droplets in a general hospital ward with ceiling mixing type mechanical ventilation system, *J. Aerosol Sci.*, **41**, 244–258.

Woloszyn, M., Virgone, J. and Mélen, S. (2004) Diagonal air distribution system for openings rooms: experiment and modeling, *Build. Environ.*, **39**, 1171–1178.

Xie, X., Li, Y., Chwang, A.T.Y., Ho, P.L. and Seto, W.H. (2007) How far droplets can move in indoor environments – revisiting the Wells evaporation-falling curve, *Indoor Air*, **17**, 221–225.

Yin, Y., Gupta, J.K., Zhang, X., Liu, J. and Chen, Q. (2011) Distributions of respiratory contaminants from a patient with different postures and exhaling modes in a single-bed inpatient room, *Build. Environ.*, **46**, 75–81.

Zhu, K. and Kato, S. (2006) Investigating how viruses are transmitted by coughing, *ASHRAE IAQ Applications*, **7**, 1-5.

Zhu, K., Kato, S. and Yang, J. (2006) Investigation into airborne transport characteristics of airflow due to coughing in a stagnant indoor environment, *ASHRAE Trans.*, **112: 2**, 123-133

Appendix H
Analysis of the IEA 2D test. 2D, 3D steady or unsteady airflow?

Analysis of the IEA 2D test. 2D, 3D, steady or unsteady airflow?

Inés Olmedo
Peter V. Nielsen

Aalborg University
Department of Civil Engineering
Division of Architectural Engineering

DCE Technical Report No. 106

Analysis of the IEA 2D test. 2D, 3D, steady or unsteady airflow?

by

Inés Olmedo
Peter V. Nielsen

September 2010

Scientific Publications at the Department of Civil Engineering

Technical Reports are published for timely dissemination of research results and scientific work carried out at the Department of Civil Engineering (DCE) at Aalborg University. This medium allows publication of more detailed explanations and results than typically allowed in scientific journals.

Technical Memoranda are produced to enable the preliminary dissemination of scientific work by the personnel of the DCE where such release is deemed to be appropriate. Documents of this kind may be incomplete or temporary versions of papers—or part of continuing work. This should be kept in mind when references are given to publications of this kind.

Contract Reports are produced to report scientific work carried out under contract. Publications of this kind contain confidential matter and are reserved for the sponsors and the DCE. Therefore, Contract Reports are generally not available for public circulation.

Lecture Notes contain material produced by the lecturers at the DCE for educational purposes. This may be scientific notes, lecture books, example problems or manuals for laboratory work, or computer programs developed at the DCE.

Theses are monograms or collections of papers published to report the scientific work carried out at the DCE to obtain a degree as either PhD or Doctor of Technology. The thesis is publicly available after the defence of the degree.

Latest News is published to enable rapid communication of information about scientific work carried out at the DCE. This includes the status of research projects, developments in the laboratories, information about collaborative work and recent research results.

1. Introduction

The "IEA Annex 20 two-dimensional test case" was defined by Nielsen (1990) and was originally considered two-dimensional and steady flow [1]. However, some recent works [2, 3] considering the case as three dimensional have shown different solutions from the 2D case as well as different solutions depending on the turbulence model used in CFD simulations.

The aim of the simulations is to investigate the two dimensional or three dimensional nature of the test, as well as to analyze the results obtained considering the case as steady or unsteady.

The sizes of the Annex 20 room are specified as:

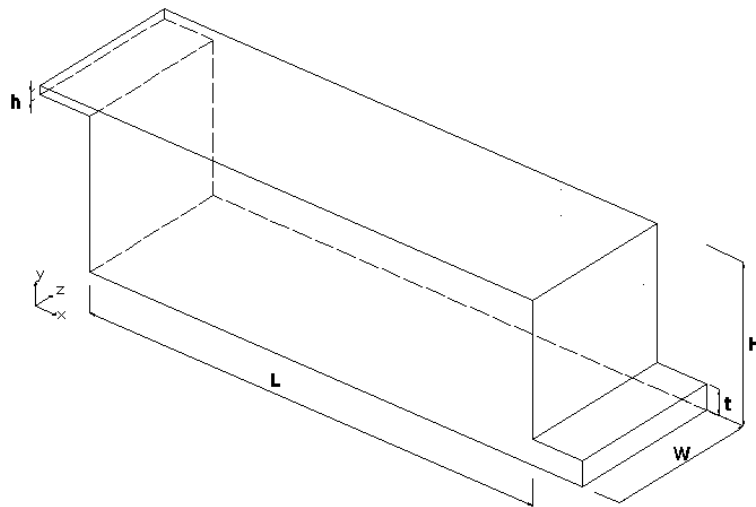L=9m, H=3m, W/H=1, h=0.168 m, t=0.48m.

Figure 1 Sketch of the benchmark test

The air is supplied in the room by a slot inlet in the left top of the room with the velocity of 0.455 m/s which corresponds with a Reynolds number of 5000. The exhaust is situated in the right bottom.

In this study a commercial CFD program (FLUENT 6.0) was used with mesh generation from the Gambit 2.6. For the simulations, the k-epsilon turbulence model was used since it produces good quality predictions in indoor airflows.

2. Description of the simulation tests

The isothermal two-dimensional case has been solved numerically as a steady state case. The grid used for the calculation contained 3,586 control volumes.

After looking at the results obtained in the two-dimensional simulations a three-dimensional case was considered in order to study the real nature of the airflow.

The three dimensional simulations were carried out under steady and unsteady conditions. The same grid distribution as in the two-dimensional case was used in the X-Y plane, plus a 60 grid cells division in Z direction. The resulted grid is formed by 215,160 control volumes. The solutions were considered converged when the sum of absolute normalized residuals for all cells in the flow domain becomes less than 10^{-5}.

3. Results and discussion

3.1. Airflow patterns and velocity contours

Figure 2 shows the contours lines of the stream for the three tests simulated. For the three dimensional tests the stream lines are calculated at the plane z/W=0.5 which corresponds with the middle plane of the test room.
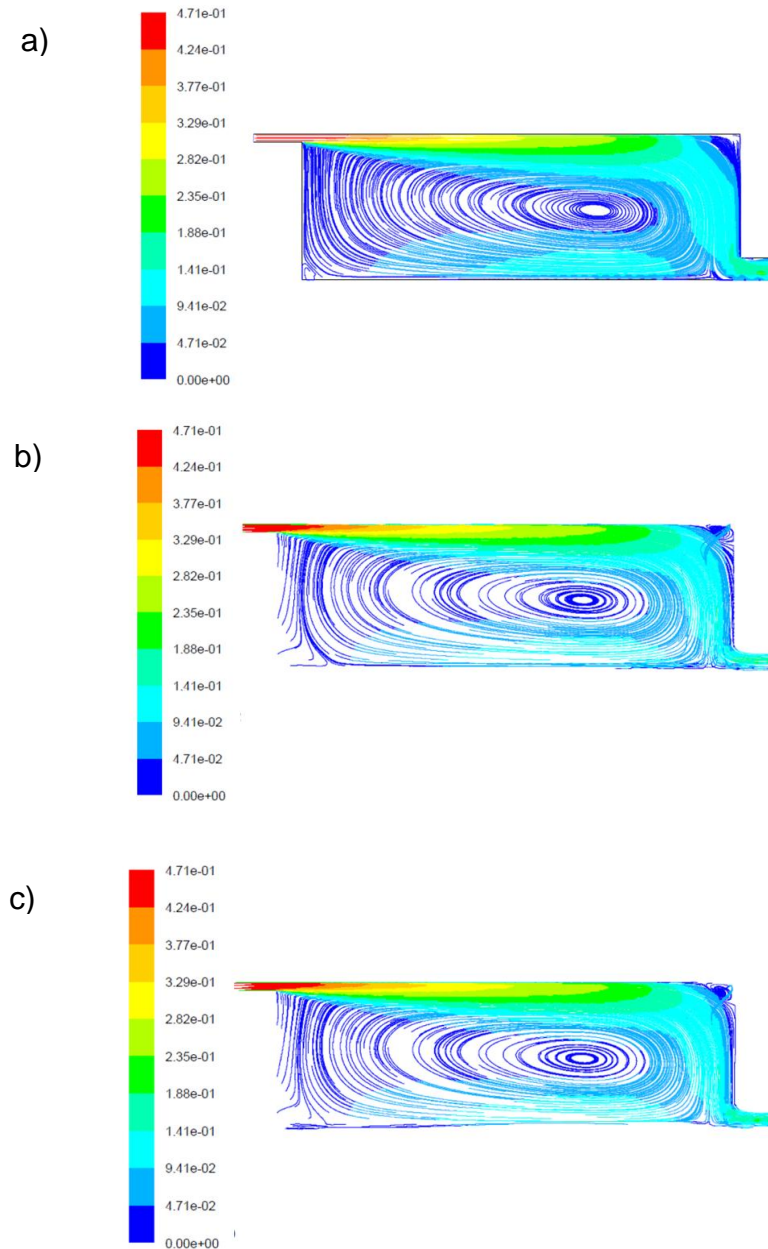

Figure 2 Streamlines calculated using the standard k-ε model for the plane z/W=0.5. a) two dimensional simulation, b) three dimensional steady simulation, c) three dimensional unsteady simulation.

For the three cases considered, the flow is completely developed in the upper part of the room where it is not possible to see larger difference between the cases. However there is an area around x/L= 1 in the lower part of the room when the measurements show large turbulence with both positive and negative instantaneous velocities. In this area is possible to see a slight difference between the path lines in the three predictions.

The x-velocity contours are obtained at the position y=0.028H, in the low part of the room, in order to find any difference in the velocity distribution, see figure 3.

a)
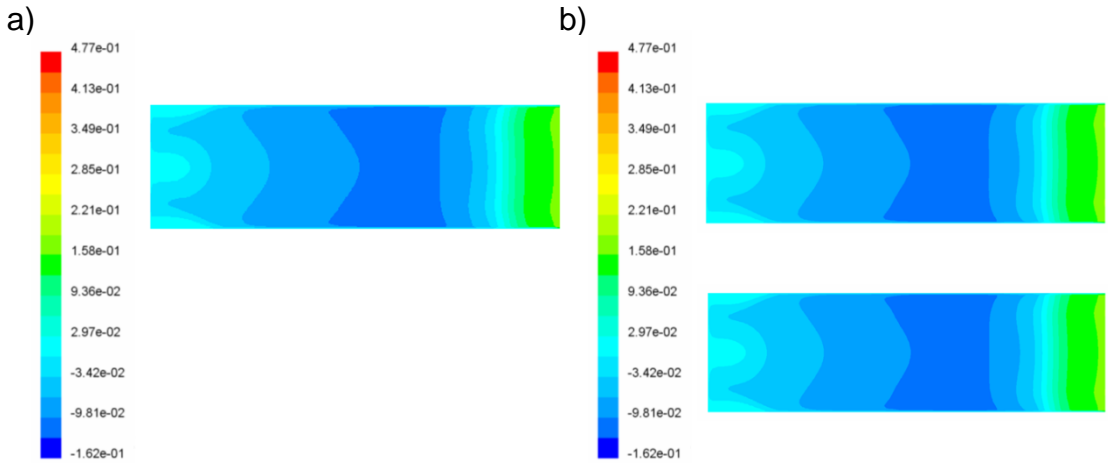
b)

Figure 3 X-velocity contours calculated using the standard k-ε model for the plane y=0.028H. a) three dimensional steady simulation, b) three dimensional unsteady simulation at different instants of time.

As looking figure 3(b) is not possible to see any evidence that indicate an time dependent nature of the test since the velocity profiles are the same in two different instant of time. Moreover, it should be noticed that no different patterns have been observed compared to the three dimensional steady case.

3.2. Turbulent intensity

The profiles of the turbulent kinetic energy for the three cases at the position x=H and x=2H are shown in figure 4, where is possible to find slight differences comparing the two dimensional case to the three dimensional cases. However, the same level of turbulence is shown for the steady and unsteady three dimensional simulations.
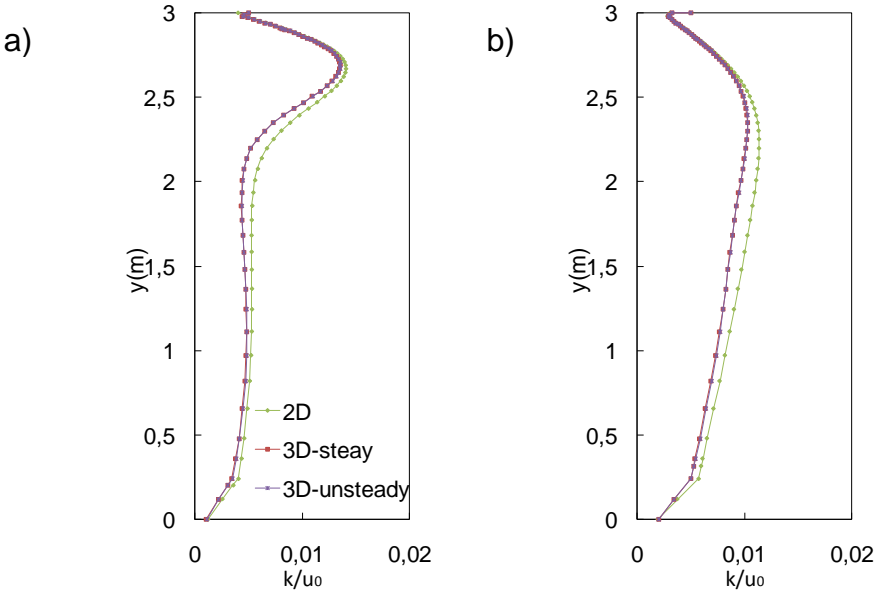
a)

b)

Figure 4 Dimensionless turbulent kinetic energy profiles for x=H and x=2H.

3.3. Velocity comparison

The velocities profiles calculated with the standard k-ε model for four positions of the room, in the middle plane are shown in figure 5.

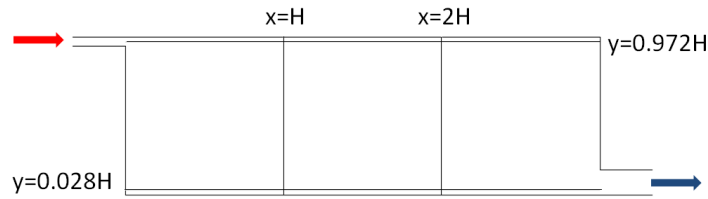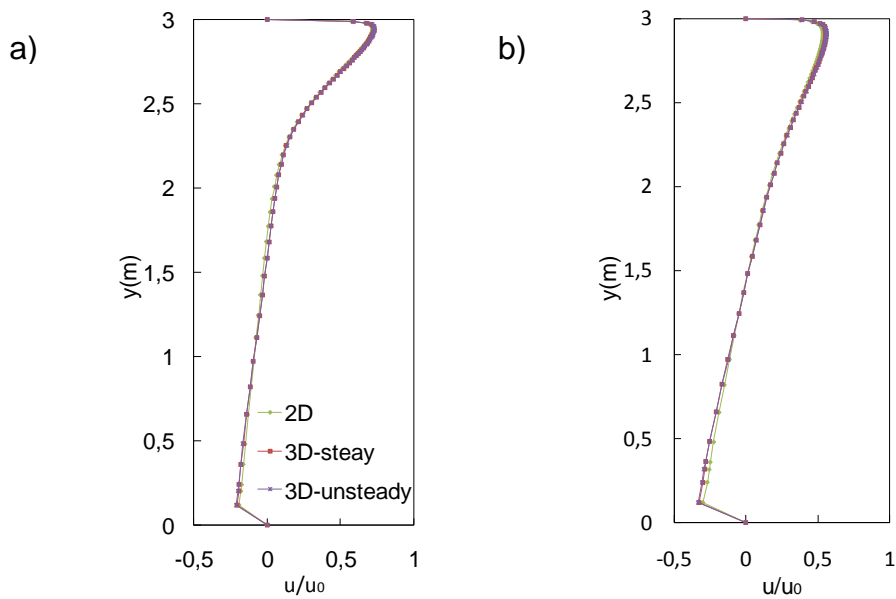Figure 5 Sketch of the vertical and horizontal lines where the results are shown.

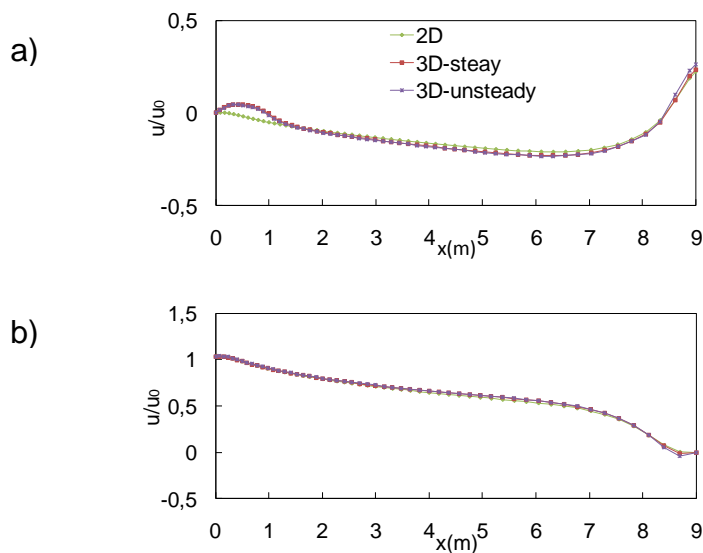Figure 6 Dimensionless x velocity profiles predicted at a) x=H and b) x=2H.

Figure 7 Dimensionless x velocity profiles predicted at a) y=0.028H and b) y=0.972H.

4. Conclusions and suggestions

It has been shown that the IEA Annex 20 case solved with time dependent equations and k-epsilon model gives a solution similar to the solution obtained with steady state three dimensional and the two dimensional equations.
By analyzing the results of the three tests it has been observed that the streamlines are the same in the major part of the domain, which means the flow may in practice be considered two-dimensional.
Moreover, the predictions show no evidence of unsteady nature of the flow. Time dependent equations give the same solution as steady state equations.
In general the most significant differences between the cases were obtained in the level of turbulence comparing the two dimensional case to the three dimensional cases. However, the test can be considered as a steady two dimensional case in the major part of the domain since it is no possible to find huge differences with the three dimensional, steady or unsteady, cases.

5. References

[1] www.cfd-benchmarks.com, IEA Annex 20 2D test case.

[2] Peter V. Nielsen, Li Rong and Inés Olmedo, The IEA Annex 20 Two-Dimensional Benchmark Test for CFD Predictions, Clima 2010, Turkey, 2010.

[3] Roberto Mathias Susin, Guilherme Anrain Lindner, Viviana Cocco Mariani and Kátia Codeiro Mendoza. (2009) Evaluating the influence of the width of inlet slot on the prediction of indoor airflow: Comparison with experimental data, *Building and Environment*, 44, 971-986.

TÍTULO DE LA TESIS:
INDOOR AIRFLOW PATTERNS, DISPERSION OF HUMAN EXHALATION FLOW
AND RISK OF AIRBORNE CROSS-INFECTION BETWEEN PEOPLE IN A ROOM

DOCTORANDA: Inés Olmedo Cortés

INFORME RAZONADO DE LOS DIRECTORES DE LA TESIS

La doctoranda Inés Olmedo Cortés ha realizado bajo la dirección de los profesores Peter. V. Nielsen de la Universidad de Aalborg y el profesor Manuel Ruiz de Adana Santiago de la Universidad de Córdoba la tesis doctoral titulada "*Indoor airflow patterns, dispersion of human exhalation flow and risk of airborne cross-infection between people in a room*".

Inés Olmedo Cortés inició su doctorado en la Universidad de Córdoba en octubre 2007 y alcanzó exitosamente la suficiencia investigadora en junio 2009. En el trascurso del trabajo de investigación ha realizado tres estancias predoctorales en la Universidad de Aalborg, donde ha realizado gran parte del trabajo experimental necesario para alcanzar los objetivos planteados.

Los resultados han generado distintas publicaciones entre las que cabe destacar: un report interno de la Universidad de Aalborg, una publicación en congreso nacional, tres publicaciones en congresos internacionales así como tres publicaciones en revistas de impacto, de las cuales dos están aceptadas y la última está enviada. Se trata por tanto de una tesis doctoral cuya metodología, calidad científica y resultados se valoran de forma muy favorable.

De la doctoranda cabe destacar su actitud personal, capacidad de trabajo y disciplina, valores fundamentales sobre los que se ha desarrollado el trabajo de investigación.

Por todo ello, se autoriza la presentación de la tesis doctoral.

Córdoba, 13 de diciembre de 2011

Firma de los directores

Fdo: Peter Nielsen   Fdo.: Manuel Ruiz de Adana Santiago

TÍTULO DE LA TESIS:
INDOOR AIRFLOW PATTERNS, DISPERSION OF HUMAN EXHALATION FLOW
AND RISK OF AIRBORNE CROSS-INFECTION BETWEEN PEOPLE IN A ROOM

DOCTORANDO/A: Inés Olmedo Cortés

INFORME RAZONADO DEL/DE LOS DIRECTOR/ES DE LA TESIS
(se hará mención a la evolución y desarrollo de la tesis, así como a trabajos y publicaciones derivados de la misma).

This PhD project is a study of the airflow patterns generated by different air distribution systems and the influence in the spread of human contaminants in the room. The PhD project is based on full-scale experiments in test rooms in Cordoba University and Aalborg University using thermal manikins with breathing function for the simulation of people in the room.

Different air distribution systems as mixing ventilation, displacement ventilation and vertical ventilation has been studied with respect to comfort around standing people and the microenvironment generated around the people. Location of people and location of supply openings in the ceiling have has been studied in the case of vertical ventilation.

There has been a special focus on the different systems ability to protect people from cross infection risk. This work has also been extended to the situation in a room without ventilation.

The work is a strong support to the new findings that although displacement ventilation is a good system in rooms with warm sources, it is a bad system in connection with cross infection risk between people in a room.

The work is a co-operation between Cordoba University and Aalborg University. Ines Olmedo has, during her studies, made three visits to Aalborg University where she worked with the full-scale room and made CFD predictions of the air distribution in rooms.

The candidate, Ines Olmedo, works efficiently in the laboratory and the results have a high level of scientific quality.

The PhD project has resulted in the following publications:

Olmedo, I., Nielsen, P.V., Ruiz de Adana, M., Grzelecki, P. and Jensen, R.L. (2010) Study of the human breathing flow profile in a room with three different ventilation strategies. Proceedings of the 16th ASHRAE IAQ Conference "Airborne Infection Control - Ventilation, IAQ & Energy", Kuala Lumpur/Malaysia 10-12 November 2010.

Nielsen, P.V., Olmedo, I., Ruiz de Adana, M., Grzelecki, P. and Jensen, R.L. (2010) Airborne Cross-Infection Risk between Two People Standing in Surroundings with a Vertical Temperature Gradient. HVAC&Research.

Olmedo, I., Nielsen, P.V., Ruiz de Adana, M. and Jensen, R.L. (2010) Airflow pattern generated by three air diffusers: Experimental and visual analysis. Proceedings of the 6th Mediterranean Congress of Climatization, Madrid/Spain 2-3 June 2010.

Olmedo, I., Nielsen, P.V., Ruiz de Adana, M., Grzelecki, P. and Jensen, R.L. (2010) Experimental study about how the thermal plume affects the air quality a person breathes. Proceedings of the 12th International Conference on Air Distribution, Trondheim/Norway 19-22 June 2011.

Olmedo, I., Nielsen, P.V., Ruiz de Adana, M., Grzelecki, P. and Jensen, R.L. (2011) Distribution of exhaled contaminants and personal exposure in a room using three different air distribution strategies. Indoor Air doi: 10.1111/j.1600-0668.2011.00736.x.
Paper VI Olmedo, I., Nielsen, P.V., Ruiz de Adana, M. and Jensen, R.L. (2011) Risk of airborne cross-infection in a room with vertical low-velocity ventilation. Submitted for Indoor Air.

Olmedo, I. and Nielsen, P.V. (2010) Analysis of the IEA 2D test. 2D, 3D, steady or unsteady airflow? Technical report. Series number 106, Department of Civil Engineering, Aalborg University.

Por todo ello, se autoriza la presentación de la tesis doctoral.

Córdoba, 19 de Diciembre de 2011

Firma del/de los director/es

Fdo.: Peter V. Nielsen